AD-A117 451 SOUTHWEST RESEARCH INST SAN ANTONIO TX F/G 11/6
RESEARCH ON MULTI-ION INTERACTIONS AND DEFECTS IN METALS.(U)
JUL 82 R E BEISSNER DAAG29-79-C-0099
UNCLASSIFIED ARO-16387.4-PH ARO-10993.3-PH NL

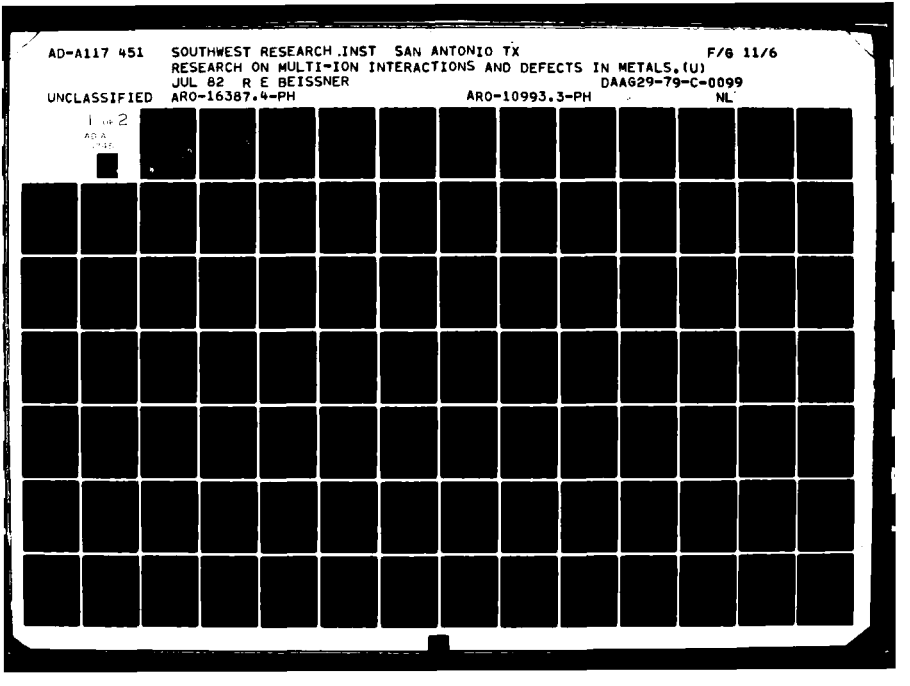

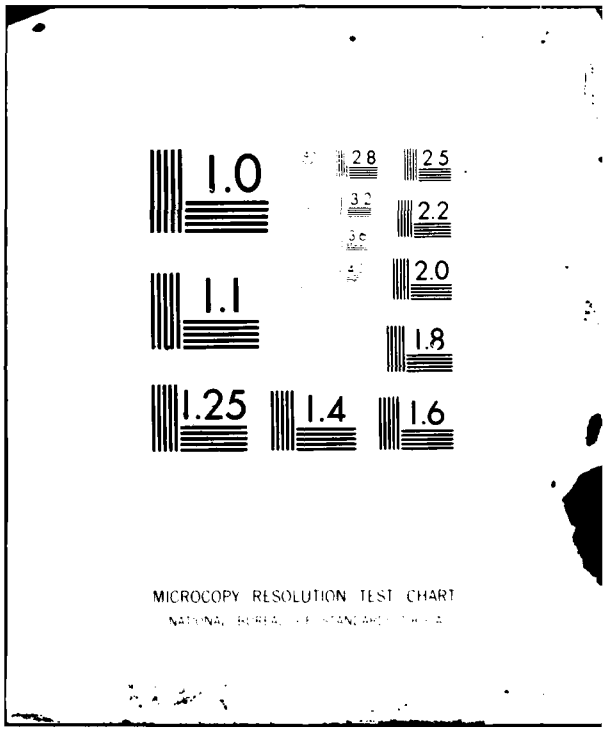
1.0
2.8
2.5
3.2
2.2
3.6
2.0
1.1
1.8
1.25
1.4
1.6
MICROCOPY RESOLUTION TEST CHART

(12)

RESEARCH ON MULTI-ION INTERACTIONS IN NONTRANSITION METALS

by
R. E. BEISSNER

FINAL REPORT
SwRI Project 15-5676
Contract No. DAAG29-79-C0099
ARO Proposal No. 16387-P

Prepared for
U.S. Army Research Office
P.O. Box 12211
Research Triangle Park, North Carolina 27709

July, 1982

Approved for public release; distribution unlimited

SOUTHWEST RESEARCH INSTITUTE
SAN ANTONIO HOUSTON

Unclassified

SECURITY CLASSIFICATION OF THIS PAGE (When Data Entered) ARO 10993.3-PH; 13061.3-PH; 16387.4-PH

REPORT DOCUMENTATION PAGE	READ INSTRUCTIONS BEFORE COMPLETING FORM
1. REPORT NUMBER	2. GOVT ACCESSION NO. AD-A117451	3. RECIPIENT'S CATALOG NUMBER
4. TITLE (and Subtitle) Research on Multi-Ion Interactions and Defects in Metals	5. TYPE OF REPORT & PERIOD COVERED Final Report 15 March 1973 - 9 May 1982
	6. PERFORMING ORG. REPORT NUMBER None
7. AUTHOR(s) R. E. Beissner	8. CONTRACT OR GRANT NUMBER(s) DAAG29-79-C-0099 DAAG29-76-C-0031 DAHC04-73-C-0022
9. PERFORMING ORGANIZATION NAME AND ADDRESS Southwest Research Institute P.O. Drawer 28510 San Antonio, TX 78284	10. PROGRAM ELEMENT, PROJECT, TASK AREA & WORK UNIT NUMBERS
11. CONTROLLING OFFICE NAME AND ADDRESS U. S. Army Research Office P.O. Box 12211 Research Triangle Park, NC 27709	12. REPORT DATE 9 July 1982
	13. NUMBER OF PAGES 107
14. MONITORING AGENCY NAME & ADDRESS(if different from Controlling Office)	15. SECURITY CLASS. (of this report) Unclassified
	15a. DECLASSIFICATION/DOWNGRADING SCHEDULE

16. DISTRIBUTION STATEMENT (of this Report)

Approved for public release; distribution unlimited

17. DISTRIBUTION STATEMENT (of the abstract entered in Block 20, if different from Report)

18. SUPPLEMENTARY NOTES

The view, opinions, and/or findings contained in this report are those of the author(s) and should not be construed as an official Department of the Army position, policy, or decision, unless so designated by other documentation.

19. KEY WORDS (Continue on reverse side if necessary and identify by block number)

Interionic potentials, Defects in crystals, Nontransition metals

20. ABSTRACT (Continue on reverse side if necessary and identify by block number)

A summary of research on multi-ion interactions is presented. Emphasis is placed on point defects in nontransition metals and the calculation of screening charge densities, electric field gradients and lattice distortion. Multi-ion interactions in transition metals are also treated, as are calculations of stacking-fault energies in both transition and nontransition metals.

DD FORM 1 JAN 73 1473 EDITION OF 1 NOV 65 IS OBSOLETE

Unclassified

SECURITY CLASSIFICATION OF THIS PAGE (When Data Entered)

TABLE OF CONTENTS

I. INTRODUCTION

It is well known that interatomic interactions play a crucial role in the determination of macroscopic phenomena such as plastic flow, fracture and diffusion-controlled processes like void or precipitate formation. In many cases, metallurgical properties of practical concern are controlled by interactions involving defects, often point defects such as vacancies or impurity ions. A theory of the properties of defects in terms of interatomic interactions is therefore vital to a fundamental understanding of important metallurgical processes.

Almost all studies of the structures and properties of defects in metals are based on the assumption that interatomic forces are derived from central, pairwise interatomic potentials. This assumption specifically excludes the possibility of multi-ion interactions, i.e., interactions that involve three or more ions and that are not simply a sum of pairwise interactions. Although theory shows that multi-ion interactions do indeed exist, calculations of the interaction energies are difficult, and, as a result, not much was known about their importance until recently. Now, however, there is a growing body of evidence that tells us that three-ion interactions can be quite strong, and that ignoring them can lead to spurious, sometimes unphysical results. This is particularly true of certain calculations involving defects, where recent results indicate that one must include at least three-ion interactions, in addition to pairwise interactions, to obtain accurate predictions of some properties.

Accordingly, the objectives of the work reported here were to (1) assess the relative importance of two- and three-ion interactions involving defects in metals, (2) develop and test methods for calculating three-ion interaction energies, and (3) develop simplified, approximate models of multi-ion

interactions for use in computer simulation studies of defects. Emphasis was placed on calculations of the properties of point defects in aluminum because three-ion interactions are known to play an important role in the determination of some point defect properties, and because ample experimental data are available for testing the results of the calculations.

Section II of this report contains a brief review of the basic ideas in multi-ion interaction theory and a summary of progress toward meeting our objectives. Additional technical information is reported in reprints and preprints, which are included as Appendices.

II. TECHNICAL DISCUSSION

A. Background

This section contains a brief review of pseudopotential/perturbation theory as applied to simple nontransition metals. The principal purpose here is to establish terminology and notation; comprehensive reviews are available elsewhere (Ref. 1, 2).*

We visualize a system of N ions with fixed core states embedded in a valence election gas of density ρ_o. The average energy per ion can be expressed as the sum of a direct ion-ion interaction energy E_i and an electronic energy E_e. Thus

$$E = E_i + E_e \tag{1}$$

The electronic energy is expressed as a perturbation expansion in the electron-ion pseudopotential W

$$E_e = E_o + E_1 + E_2 + E_3 + \ldots \tag{2}$$

where E_n contains terms of n'th order in W. The crystal pseudopotential is the sum of two terms

$$W = W_{ion} + W_v \tag{3}$$

*References cited in the text are listed at the end of this report.

where W_{ion} is, in general, a nonlocal potential (an operator), while W_v is the self-consistent local potential energy of a valence electron in the presence of all other valence electrons. Self-consistency means that the plane wave matrix elements of W_v satisfy the modified Poisson equation (in Rydbergs)

$$W_v(\vec{q}) = \frac{8\pi}{q^2}[1-G(q)]\rho_v(\vec{q}) \tag{4}$$

where $\rho_v(\vec{q})$ is the Fourier transform of the valence electron density and G(q) is a correction for exchange and correlation interactions among electrons.

The electron density may also be written as a perturbation expansion

$$\rho_v(\vec{q}) = \delta_{\vec{q}o}\rho_o + \rho_1(\vec{q}) + \rho_2(\vec{q}) + \cdots \tag{5}$$

where the linear term $\rho_1(\vec{q})$ is a sum of two terms, one containing a matrix element of W_{ion} and the other proportional to $W_v(\vec{q})$. The second order term involves an integral over products of these matrix elements, the third order term involves double integrals, etc. To calculate the self consistent pseudopotential to order n, one must truncate (5) at the n'th term, substitute in (4) and solve for $W_v(\vec{q})$; for $n > 2$ this means solving an integral equation.

It is easily shown that, to calculate E_e to order n, one needs $W_v(\vec{q})$ to order n-1 (Ref. 1, 2). A second order calculation of the energy therefore involves a linear screening approximation to the self consistent solution of (4) and (5). The well known result is

$$\langle\vec{k}+\vec{q}|W|\vec{k}\rangle \sim \langle\vec{k}+\vec{q}|W_{ion}|\vec{k}\rangle/\varepsilon(q) \tag{6}$$

where ε, the dielectric function, depends on the average electron density as well as on the momentum change q.

After rearranging terms, the average energy per ion, to second order in W, can be written

$$E_2 = V_o + \frac{1}{2n} \sum_i \sum_{i \neq j} V_{ij}(R_{ij}) \tag{7}$$

where V_o is independent of the arrangement of ions, R_{ij} is the distance between ions at $\vec{R}_i$ and $\vec{R}_j$, and V_{ij} is the effective interaction between ions, or the interatomic potential. We include the subscript ij to account for the possibility that different types of ions may be present. For a homogeneous system, the function V(R) is the same for all ion pairs and can be expressed as the direct ion-ion potential plus the Fourier transform of a function, $F_n(q)$, called the energy wavenumber characteristic of the material.

In a higher order approximation, one does not obtain a central, pairwise interatomic potential. The energy can be written in a form similar to (7), (Ref. 3,4)

$$E = \tilde{V}_o + \frac{1}{2n} \sum_i \sum_{i \neq j} V_{ij}(\vec{R}_i, \vec{R}_j) \tag{8}$$

but now the effective potential is a pairwise term plus a sum of multi-ion interactions. If all ions are identical (Ref. 3,4) we have

$$V_{ij}(\vec{R}_i, \vec{R}_j) = \tilde{V}(R_{ij}) + \frac{1}{3} \sum_{\substack{k \neq j \\ k \neq i}} V_3(\vec{R}_i, \vec{R}_j, \vec{R}_k) + \ldots \tag{9}$$

The second term is a three-ion interaction energy that results from carrying the calculation of E to third order; the next term would be a fourth order, four ion term, etc.

It is possible to develop formal expressions for higher order energies in terms of matrix elements of nonlocal pseudopotentials, and thus determine the corresponding formulas for V_3, V_4, etc. However, even in third order, the result is too complicated to be of use in practical computations (Ref. 5). It is therefore necessary to make local approximation in third and higher order terms, which amounts to taking

$$\begin{aligned} \langle \vec{k}+\vec{q}|W|\vec{k}\rangle &= NS(\vec{q})\langle \vec{k}+\vec{q}|\omega|\vec{k}\rangle \\ &\sim S(\vec{q})\omega(q) \end{aligned} \tag{10}$$

Here $S(\vec{q})$ is the structure factor,

$$S(\vec{q}) = \frac{1}{N}\sum_i e^{-i\vec{q}\cdot\vec{R}_i} \tag{11}$$

ω is the nonlocal pseudopotential operator for a single ion (all ions are assumed identical), and $\omega(q)$ is a local approximation to $N\langle \vec{k}+\vec{q}|\omega|\vec{k}\rangle$. This leads to the following expression for the third order energy (Ref. 6,7).

$$E_3 = \Omega_0 \sum_{\vec{q}_1}\sum_{\vec{q}_3} g(q_1,q_2,q_3)\omega(q_1)\omega(q_2)\omega(q_3)S(\vec{q}_1)S(\vec{q}_2)S(\vec{q}_3) \tag{12}$$

where Ω_0 is the average volume per ion, $\vec{q}_2 = -(\vec{q}_1+\vec{q}_3)$, and $g(q_1,q_2,q_3)$ is the function defined by Lloyd and Sholl (Ref. 6). If, for convenience, we also use the local approximation in the second order term (it is not necessary to make this approximation) then the effective potential in (8) becomes

$$V(\vec{R}_i,\vec{R}_j) \sim \frac{\Omega_0}{N} \sum_{\vec{q}} \frac{q^2}{8\pi} \frac{1-\varepsilon(q)}{1-G(q)} \varepsilon(q)\omega^2(q)e^{-i\vec{q}\cdot\vec{R}_{ij}}$$

$$+ \frac{6\Omega_0}{N^2} \sum_{\vec{q}_1} \omega(q_1)e^{-i\vec{q}_1\cdot\vec{R}_{ij}} \sum_{\vec{q}_3} g(q_1,q_2,q_3)\omega(q_2)\omega(q_3)$$

$$+ \frac{2\Omega_0}{N^2} \sum_{\vec{q}_1} \omega(q_1)e^{-i\vec{q}_1\cdot\vec{R}_{ij}} \sum_{\vec{q}_3} g(q_1,q_2,q_3)\omega(q_2)\omega(q_3) \sum_{\substack{k\neq i\\ k\neq j}} e^{-i\vec{q}_3\cdot\vec{R}_{kj}} \quad (13)$$

Expressions similar to (12) and (13) can be derived for the case where all ions are not the same by using, in place of (10),

$$\langle\vec{k}+\vec{q}|\,\omega|\vec{k}\rangle \sim S(\vec{q})\omega_k(q) + \frac{1}{N}\sum_i \Delta\omega_i(q)e^{-i\vec{q}\cdot\vec{R}_i} \quad (14)$$

where ω_k is the host ion form factor and $\Delta\omega_i$ is change in form factor caused by an impurity at site $\vec{R}_i$.

The first term in (13) is a local approximation to the pairwise potential obtained from second order theory. The second term is a third order correction which is also pairwise, and the third term is a sum over all three-ion interactions involving sites i and j. It is the presence of this last term that makes V dependent on the arrangement of neighboring ions. That is, because of the three-ion term, the effective potential is not only a function of the distance R_{ij} or even the vector displacement $\vec{R}_{ij}$, it depends also on the positions $\vec{R}_i$ and $\vec{R}_j$ relative to neighboring ions. As we shall se in the next section, this has important implications regarding interatomic forces in the vicinity of defects.

B. Applications to Defect Calculations

In a perfect crystal the structure factor vanishes unless $\vec{q}$ equals a recpirocal lattice vector $\vec{K}$, and all form factors in (12) are evaluated at $q = K$, where they are quite weak for most nontransition metals. This is why a second order treatment is often adequate for the calculation of perfect crystal properties, though significant third order effects have been noted in calculations of phonon spectra (Ref. 5) and cohesive energies (Ref. 8) if polyvalent metals.

The structure factor is usually nonvanishing at all q in imperfect crystals and at most q in partially ordered systems such as liquid metals, and this brings larger, long wavelength values of $\omega(q)$ into play. Because the perturbation is now stronger, one expects the series (2) to converge more slowly, meaning that higher-order, multi-ion terms in (9) become more important. In liquid sodium and potassium, for example, Hasegawa (Ref. 9) found that three-ion interactions result in strong, short range attractive forces, while our own calculations (to be described in Section C) indicate that similar effects occur in aluminum. In their calculations of vacancy formation energies for sodium, magnesium and aluminum, So and Woo (Ref. 10) found that, although third order terms are small, indicating reasonably good convergence even in this strong perturbation case, the third order contribution to the formation energy is important because other terms nearly cancel. For aluminum, in particular, third order terms are essential to obtaining a positive formation energy. Though agreement with experiment is poor, the calculations still serve as convincing evidence that third order, multi-ion effects are important in defect calculations.

More such evidence is presented by Jacucci, et al (Ref. 11) who also calculated the vacancy formation energy as well as the phonon spectrum, liquid

structure factor and vacancy migration energy for aluminum. Their calculations were molecular dynamics simulations based on a pairwise interatomic potential derived by Rasolt and Taylor (RT) (Ref. 12). The RT potential was obtained from a density functional calculation for an aluminum ion in jellium, and therefore contains, in effect, all of the pairwise corrections appearing in the perturbation expansion of V_{ij} in (9); it specifically excludes multi-ion interactions involving three or more ion sites. Jacucci, et al, show that this potential leads to good agreement with all properties except the vacancy formation energy, and argue that the failure of this calculation is caused by the exclusion of three-ion interactions involving the vacancy. They conclude that one cannot use a simple pairwise potential derived from bulk crystal data, such as phonon spectra, to predict certain defect properties, because localized, multi-ion interactions involving the defect are not accounted for in bulk crystal data. Conversely, if one uses experimental point defect data to derive a pairwise potential, this potential should not be used to calculate bulk crystal properties because it does include the effects of localized multi-ion interactions at the defect site.

This, we think, is an extremely important point. It confirms an assertion we made in our proposals to ARO, and has been the underlying motivation for our work on multi-ion interactions. It is important in a basic sense because the demonstrated importance of multi-ion interactions involving defects refutes the idea that there exists a universal, central pairwise potential. It is also important technologically, because the central potential assumption underlies almost all studies of defect properties by the molecular dynamics method, the lattice statics method and other techniques for predicting the structures and interacitons of crystalline defects. If one cannot use the same potential in a defect-free region as one uses near a defect, then there is

serious reason to question the validity of such defect studies.

Our research has been concerned with simple defects in aluminum. We have chosen aluminum because it is amenable to a pseudopotential/perturbation treatment, its perfect crystal characteristics are well understood, and because experimental data on its defect properties are readily available. Also, because aluminum is a polyvalent metal, we expect third order effects to be more prominent than they would be, for example, in the alkali metals (Ref. 8,10).

We have been concerned mostly with third order effects, though some of our earlier work dealt with second order calculations (Ref. 3) and with a t-matrix version of the multi-ion expansion (Ref. 4) for use with strong scatterers. We are interested in determining the circumstances under which a third order treatment is sufficient, and in exploring some of the properties of third order forces. Because a nonlocal third order calculation is not feasible, we have also studied the use of various local approximations to model potential form factors for use in third order terms. More recently, we completed a third-order lattice statics calculation of the lattice displacement field around point defects following the theory of Solt and Werner (Ref. 14). This work is summarized in the next section.

C. Summary of Progress

1. Early Work

Our first defect studies were second order calculations of stacking fault energies for various nontransition metals (Ref. 13, Appendix A). This is a situation where a second order treatment should suffice because structure factors for stacking faults are such that the large values of atomic form factors at small q do not enter the calculation (Ref. 1,2). Agreement with experiment was reasonable considering the uncertainties in pseudopotentials, screening fucntions and experimental data that existed at that time.

In considering applications to other defects and to transition metals, however, it was clear that the strong perturbations encountered in such cases required a higher order treatment. We therefore developed a t-matrix generalization of Harrison's multi-ion theory (Ref. 3), and demonstrated that three-ion interaction energies are indeed quite large for transition metals (Ref. 4, Appendix B).

An application to stacking faults in transition metals followed (Ref. 15, Appendix C). We used an approximate version of the third order t-matrix theory and obtained reasonable agreement with experimentally determined stacking fault energies. Predictions of the relative stabilities of close-packed structure were obtained from these calculations and agreement with observed stable structurs was obtained in almost all cases. A somewhat surprising result was that resonant scattering of d-electrons made three-ion interactions dominant in transition metals, these energies being about ten times as large as pairwise contributions to the stacking fault energy.

We then returned to the study of defects in nontransition metals and attempted to formulate a third order treatment of defect scattering in terms of the electron Green function for the perfect crystal. We used a first order, degenerate perturbation theory calculation of the Green function, because we were concerned about the influence of discontinuities at Brillioun zone boundaries on defect screening charge distributions. Although the results are quite complicated, we were successful in developing a spherical harmonics expansion of this Green function for use in a partial wave treatment of point defect scattering. Unfortunately, the large number of terms (as many as 50) needed in the expansion made such a calculation impractical, and the idea of performing a full calculation was abandoned. Instead we applied the Green function to an idealized delta function scatterer and calculated the resulting screening charge

density, and host-ion defect interaction energy. The results, which were not published, indicated that host crystal scattering is important and that it leads to strong anisotropy in both the screening charge density and the host-ion defect interaction energy.

To permit the use of more realistic defect potentials, we then turned to a third-order, nondegenerate perturbation treatment, as given by Lloyd and Sholl (Ref. 6), and Brovman and Kagan (Ref. 7,16). We chose to concentrate on second-order calculations of the point defect screening charge density because such calculations are formally similar to third order calculations of the effective interatomic potential, and both calculations involve the same physical assumption, namely, that second order screening is adequate.

Another reason for concentrating on screening charge densities for point defects is that, according to Kohn and Vosko (Ref. 17) and Blandin and Friedel (Ref. 18), the electric field gradient (EFG) at a host ion site a distance R from an impurity ion is given by

$$q(R) = -\frac{8\pi e}{3}\,\alpha\,\delta\rho_s(R) \qquad (15)$$

where e is the electronic charge, $\delta\rho_s(R)$ is the change in the smooth part of the valence wave function (that part determined by pseudopotential/perturbation theory) and α is a dimensionless constant that corrects for the effect of the oscillatory part of the valence electron density inside the host ion core. The EFG, which can be determined from nuclear magnetic resonance experiments, is therefore proportinal to $\delta\rho_s$, which is calculated quantity, thus providing a basis for verifying screening charge calculations. The fact that our preliminary calculations indicated a strong host crystal scattering effect on $\delta\rho_s$ made such comparisons all the more interesting, because experimental data on the

EFG's at second neighbor sites in aluminum alloys are unusually small, a fact that had been attributed to some unknown influence of the host crystal (Ref. 19). Thus, the idea was that a second order calculation of $\delta\rho_s$ that includes host crystal scattering might serve to explain the second neighbor EFG anomaly in aluminum.

Preliminary second order calculations were performed for five impurities using damped Ashcroft potentials (Ref. 20) with parameters adjusted to obtain rough agreement with the energy-wavenumber data of Appapillai and Williams (Ref. 21). The results once again showed strong anisotropy in $\delta\rho_s$ with a tendency for first and second order terms to cancel at the second site. While this aspect of the calculation was encouraging, overall agreement with experiment was quite poor.

This led us to consider several possible improvements in the calculations. The first, and most seriuos question raised by the results concerned the adequacy of a second-order treatment. The fact that second order terms were large seemed to say that third and possibly even higher order corrections are also important. On the other hand, the pseudopotentials used were rather crudely constructed, and we could not be sure that they were realistic. Also, because were were concentrating on anisotropic effects involving scattering by the defect and host crystal, we did not include the isotropic second order term corresponding to double scattering at the defect site. Another possible source of error was that lattice distortion effects were completely ignored. Finally, from the derivation of (15) it is clear that if one carries the calculation of $\delta\rho_s$ to second order, then the formula for the core enhancement factor should be modified accoridngly, and this was not done in our calculations. Attempts to incorporate these improvements in the calculations are described below.

2. Nonlinear Screening of Point Defects

a. Jellium Model

As a first test of a second order theory, screening charge densities were calculated for the proton, an isolated aluminum ion, and for substitutional magnesium and zinc in a neutral, uniform medium (jellium) with electron density equal to that in the aluminum crystal (Appendix F). To calculate the density to second order we use the following expressions, which are derived in Appendix F:

$$\delta\rho_s(q) = \frac{q^2}{8\pi}\left[\frac{1-\varepsilon(q)}{1-G(q)}\right]\left[\omega_\ell(q) + \frac{\omega(q)-\omega_\ell(q)}{1-\varepsilon(q)}\right] \tag{16}$$

where $\omega(q)$, the form factor self consistent to second order, satisfies,

$$\omega(q) = \omega_\ell(q) + \frac{24\pi}{q^2}\left[\frac{1-G(q)}{\varepsilon(q)}\right]\frac{1}{N}\sum_{\vec{p}} g(q,p,r)\,\omega(p)\,\omega(r) \tag{17}$$

where $\omega_\ell(q) = \omega_{ion}(q)/\varepsilon(q)$ is the linear screening form factor and $\vec{r} = -(\vec{q}+\vec{p})$. An approximate solution for $\omega(q)$, which is accurate through third order in $\omega_\ell(q)$ (Appendix E), is obtained by substituting $\omega_\ell(q)$ for $\omega(q)$ inside the sum; successively better approximations can then be generated by repeated substitutions. Self consistent numerical results obtained by this iterative method, by the approximate solution for $\omega(q)$, and by linear screening theory are presented in Appendix F.

For a substitutional defect, the perturbation is taken as the difference between the impurity and aluminum potentials, and is therefore much weaker than an isolated ion potential. The results show that for substitutional defects second order effects are small, and that the screening charge density obtained by iteration to full self consistency differs very little from that obtained with the approximate solution for $\omega(q)$. As one might expect, the stronger perturbation associated with the aluminum ion potential (or, with a

change of sign, the aluminum vacancy potential) produces somewhat greater second order effects and is more dependent on approximations to self consistency, while the strongest scatterer, the proton, shows very large second order effects and still greater dependence on self consistency.

Comparison of the proton calculations with exact density functional results (Ref. 22) shows that adding second order terms gives much better results but does not fully account for nonlinear screening effects. For the aluminum ion there is some disagreement between published density calculations (Ref. 23,24) and comparisons of second order calculations with these results is therefore inconclusive. However, it is encouraging to note that the disagreement between second order and density functional results is no greater than the disagreement among the density functional calculations themselves. For substitutional impurities, the fact that nonlinear screening corrections are small suggests that a second order theory of the screening charge density is adequate for such defects.

b. Host Crystal Effects

When host ion scattering is added to the jellium model, the Fourier transform of the screening charge density is still given by (16), but with anisotropic $\omega(\vec{q})$ and $\delta\rho_s(\vec{q})$. We have not attempted a fully self consistent treatment in this case because of the computational difficulty it presents. Instead we calculated the self consistent spherical average of $\omega(\vec{q})$, which satisfies

$$\omega(q) = \omega^o(q) + \frac{48\pi}{q^2}\left[\frac{1-G(q)}{\varepsilon(q)}\right] \sum_{\vec{k}\neq o} \omega_k^h \frac{1}{4\pi} \int g(q,K,p)\omega(p)d\Omega_p \qquad (18)$$

with

$$\omega^o(q) = \omega_\ell(q) + \frac{24\pi}{q^2}\left[\frac{1-G(q)}{\varepsilon(q)}\right] \frac{1}{N} \sum_{\vec{\rho}} g(q,p,r)\omega(p)\omega(r) \qquad (19)$$

where ω_k^h is the host crystal form factor at $q = K$.

The screening charge density is then

$$\delta\rho_s(\vec{q}) = \frac{q^2}{8\pi}\left[\frac{1-\varepsilon(q)}{1-G(q)}\right]\left[\omega_\ell(q) + \frac{\omega^o(q)-\omega k(q)}{1-\varepsilon(q)}\right]$$
$$+ \frac{6}{\varepsilon(q)} \sum_{k\neq 0} g(q,K,p)\omega_k^h\omega(p) \qquad (20)$$

Typical results for substitutional magnesium are presented in Appendix G, in this case for average local potentials based on damped Heine-Abarenkov model potentials for magnesium and aluminum. These data show, once again, that anisotropic contributions to the screening charge density are important, though they are not as pronounced as our earlier calculation with delta function potentials would indicate. As it turns out, however, second order corrections to the EFG are much smaller than one would expect, and for this reason, calculations of anisotropic screening were not carried beyond this point. The role of higher order terms in the EFG formula is discussed below.

3. Electric Field Gradient Calculations

a. Second Order Effects

If we let $\delta\rho(\vec{r})$ be the total change in valence electron density (including host ion oscillations) then the radial component of the valence effect EFG (the EFG in the absence of lattice distortion) is given by (Ref. 25)

$$q_v(\vec{R}) = -\frac{2e\Delta z}{R^3} + \frac{4\pi e}{3}\delta\rho(\vec{R}) + 2e\int\frac{P_2(\hat{r}\cdot\hat{R})\delta\rho(R+r)}{r^3}d^3r$$
$$= -\frac{2e\Delta z}{R^3} + \frac{4\pi e}{3}\delta\rho(\vec{R}) - \frac{8\pi e}{3N}\sum_{\vec{q}}\delta\rho(\vec{q})P_2(\hat{q}\cdot\hat{R})e^{i\vec{q}\cdot\vec{R}} \qquad (21)$$

where $P_2(\hat{r}\cdot\hat{R})$ is a Lengendre polynominal, and Δz is the impurity valence minus the host valence.

Following Kohn and Vosko (Ref. 17) we might now assume that $\delta\rho(\vec{q})$ can be replaced by $\alpha\delta\rho_s(\vec{q})$ where α is the core enhancement factor. However, as we show in Ref. 26 (Appendex E), if we include anisotropic second order terms in $\delta\rho_s(\vec{q})$, then such terms should also be included in the calculation of α. This, it turns out, leads to anisotropic corrections to α of the order of 20%.

We might also assume that R is large and that the only important $\vec{q}$ directions are therefore those that are nearly parallel to $\vec{R}$, in which case $P_2(\hat{q}\cdot\hat{R})\sim 1$, and the last term, as well as the second term, becomes proportional to $\delta\rho_s$. However, in our calculations we chose to avoid this particular asymptotic approximation because numerical evaluation of the $\vec{q}$ integral is required in any case.

Typical results are reported in Appendix G. The two principal points to be noted here are (1) the linear screening part of the last term in (21) is the dominant contribution at R of interest, and (2) this term is not proportional to $\delta\rho_s(\vec{R})$, contrary to the Kohn-Vosko formula.

This totally unexpected result tells us that the long standing disagreement between calculated and measured EFG's is caused not so much by inaccuracies in the calculation of $\delta\rho_s$ or α, as by the failure of the Kohn-Vosko formula itself. In particular, the asymptotic argument that leads to $P_2(\hat{q}\cdot\hat{R})\sim 1$ produces serious errors at all R of interest.

This being the case, we were led to question the validity of the core enhancement approximation, $\delta\rho(\vec{R}) \sim \alpha\delta\rho_s(\vec{R})$, because this approximation is also based on a large R assumption. For this reason we decided to abandon the Kohn-Vosko formula, return to the original EFG expression (21), and recalculate the EFG without invoking an asymptotic approximation. These calculations, which are reported in Appendix G, were done in the linear screening approximation

because Table I of Appendix G shows that second-order effects are very small.

b. A Correction to the Kohn-Vosko Formula

As reported in Appendix G, we used the core state projection operator technique (Ref. 1) to calculate the impurity-induced change in the oscillatory part of the valence wave function in host ion cores. This result was then used in (21) to calculate the core enhancement part of the EFG. Not surprisingly, the numerical results show that core enhancement effects cannot be accounted for by a simple core enhancement factor that is a property of the host crystal alone.

On the other hand, we also show in Appendix G that the Kohn-Vosko EFG formula results if we make the approximation

$$j_2(qR) \sim j_0(qR) \tag{22}$$

which holds for large qR, and also assume that certain core state matrix elements that appear inside the q integral can be approximated by their values at the singular point $q = 2_{kF}$. This, as we said, leads to the Kohn-Vosko approximation and gives $\alpha = 6.8$, in reasonable agreement with more elaborate calculations (Ref. 27).

The reason this approximation fails is that (22) is not valid at small q and, when $\Delta z \neq 0$, the small q part of the EFG integrand is quite important. To demonstrate this we calculated a correction term to account for the error in (22) and found that when $\Delta z \neq 0$, this new term dominates at all R. Finally, returning to the large R assumption, we found the following corrected version of (15):

$$q_v(R) \sim \frac{2eF(q=0)\Delta z}{R^3} - \frac{8\pi e}{3}\alpha\delta\rho_s(R) \tag{23}$$

where the first term is the correction for small q (long wavelength) effects and F(q) is a function of core state matrix elements. Data presented in Appendix G

show that the new asymptotic formula gives EFG predictions in good agreement with a full numerical treatment even at nearest neighbor sites.

4. Lattice Distortion Calculations

In Section B we cited reasons why we believe a point defect/lattice distortion calculation should be carried to third order. To repeat, we agree with Jacucci, et al (Ref. 11), that their calculations demonstrate that three-ion interactions are important in point defect studies such as theirs, and that some such interactions are not accounted for when one uses a semiempirical interatomic potential derived from bulk crystal data. Furthermore, according to Solt (Ref. 28), the asymptotic expression for the displacement field, as calculated by lattice statics (Refs. 29,30) is incorrect unless one includes third order terms.

Therefore, encouraged by the results of our second order calculations of defect screening charge densities (Appendix F), we undertook a third order, lattice statics calculation of the ion displacement field caused by a vacancy in aluminum. The expression we used for the third order force was that given by Solt & Werner (Ref. 14), while the perfect crystal dynamical matrix was calculated to second order using the empirical model potential of Sen, et al (Ref. 31).

The results are reported in Appendix H. They show that, in second order, our calculated displacements are significantly smaller than those obtained by Singhal in an earlier calculation (Ref. 32). This is not particularly surprising in view of the fact that Singhal's model potential differs from that of Sen, et al. However, when third order forces were added, the displacements became still smaller, in some cases even changing sign, which indicates that second and third order forces are of the same order of magnitude.

This raises some serious questions concerning the use of third order perturbation theory in the calculation of defect properties. In particular, if we are to believe that third order forces are as strong as our calculation shows, then we might expect that higher order multi-ion interactions are also strong and cannot be ignored. On the other hand, perhaps our use of the local approximation tends to exaggerate third order forces thus leading to unreasonably large third order displacements. In either case, our results tend to cast doubt on the validity of a local, third order theory of interionic forces involving defects.

D. Conclusions

For the most part, our research has focused on the calculation of screening charge densities around defects in nontransition metals. This is because changes in the screening charge distribution induced by defects are of fundamental importance in determinig interionic forces among neighboring ions.

Our calculations indicate that a pseudopotential/perturbation calculation carried to second order is adequate for the calculation of charge densities around weak scatterers, such as substitutional impurities with small valence difference. In fact, in such cases we find that a linear screening (first order) treatment should suffice for most purposes. Even for strong scatterers like the vacancy in aluminum, the theory is in reasonable agreement with more accurate density functional calculations.

Comparisons with experimental data on electric field gradients (EFG), around point defects, which are determined in part by the charge density distribution, are inconclusive. This is because the calculations are, in a sense, incomplete in that an accurate treatment of the lattice distortion contribution to the EFG is still lacking. Still, from the calculations themselves we can draw two important conclusions regarding EFG theory. These are the following: (1) a first order calculation of the screening charge density is sufficient for

EFG predictions, and (2) the approximate Kohn-Vosko formula, which relates the EFG to the screening charge density, misses an important contribution to the EFG in cases where the host and impurity valences differ. An approximate expression for this missing contribution was derived and is reported in Appendix G.

We conclude, therefore, that second order perturbation theory gives a good account of defect screening in all but a few cases where the defect pseudopotential is extremely strong. In fact, from the opinions expressed in the literature on defect screening, we would say that the theory is much better than expected.

The theory of interionic forces is, however, another matter. Our calculation of the effect of three-ion forces on lattice distortion around a vacancy produced third order displacements that are, in our opinion, much too large. It is unclear at present whether this was caused by the omission of higher order forces or by the local potential used in our third order term. Because both the calculation of higher order terms and the calculation of nonlocal effects in third order are extremely difficult, it seems unlikely that this question can be easily answered.

We are left, then, with a strong indication that the path we have been pursuing, i.e., a low order, local peturbation theory of interionic forces, no longer appears promising. This leaves only density functional methods, which are so far restricted to spherically symmetric systems, and self-consistent cluster tyupe calculations as candidate methods for calculating interionic forces. Unfortunately, neither of these approaches is well-suited to a force calculation where defects are involved, and it is therefore difficult to recommend a direction for further research. At present, our personal choice would be to use density functional theory to derive accurate pairwise potentials and then look for approximate ways to correct these potentials for multi-ion interactions associated with the presence of neighboring ions.

III. LIST OF PUBLICATIONS

1. R. E. Beissner, "Model Potential Calculations of Stacking-Fault Energies", Phys. Rev. B. 8, 5432 (1973).

2. R. E. Beissner, "Multi-Ion Interactions in Transition Metals", Phys. Rev. B 9, 5108 (1974).

3. R. E. Beissner, "Role of Multi-Ion Interactions in the Stacking-Fault Energies of Transition Metals", Phys. Rev. B 13, 5131 (1976).

4. R. E. Beissner, "Self Consistency in the Third-Order Perturbation Theory of Simple Metals", Phys. Lett. 67A, 155 (1978).

5. R. E. Beissner, "An Anisotropic Screening Effect in the Theory of Electric Field Gradients in Dilute Alloys of Simple Metals", Phys. Lett. 71A, 109 (1979).

6. R. E. Beissner, "Self-Consistent, Second-Order Screening of Point Defects in Aluminum", submitted to Phys. Rev. B.

7. R. E. Beissner, "New Contribution to the Valence Effect Electric Field Gradient in Simple Metal Alloys", submitted to Phys. Rev. B.

8. R. E. Beissner, "Third-Order Calculation of Lattice Distortion for a Vacancy in Aluminum", in preparation.

APPENDIX A

Model-Potential Calculations of Stacking-Fault Energies

PHYSICAL REVIEW B VOLUME 8, NUMBER 12 15 DECEMBER 1973

Model-Potential Calculations of Stacking-Fault Energies

R. E. Beissner
Southwest Research Institute, San Antonio, Texas 78284
(Received 16 July 1973)

Calculations of stacking-fault energies in aluminum, magnesium, beryllium, copper, silver, and gold are reported. For the polyvalent metals it is shown, by means of comparisons of numerical results based on several different energy–wave-number characteristics, that exchange and correlation corrections are not as significant in the present context as they are in most other defect calculations. Nonlocal effects are quite important but can be approximately accounted for by empirical adjustments of the form factors based on simpler local models. Although stabilities against faulting and the relative magnitudes of stacking-fault energies are correctly predicted, quantitative agreement with experiment is not obtained. Possible reasons for this discrepancy are discussed. Results for the noble metals indicate a severe sensitivity to the detailed curvature of the energy–wave-number characteristic in the vicinity of the smallest reciprocal-lattice vector. Failure to obtain agreement with experiment in these cases may therefore be due to minor inaccuracies in the energy–wave-number characteristics for noble metals.

I. INTRODUCTION

Applications of the pseudopotential theory of metals to analyses of the energetics of most crystalline defects are made difficult by a number of factors. Among these are the questionable validity of a first-order perturbation treatment,[1] the sensitivity of interionic potentials to exchange and correlation corrections,[2,3] and the need to properly account for the nonlocal nature of the pseudopotential itself.[4] However, the calculation of stacking-fault energies in close-packed crystals is one class of problems that apparently does not suffer from the first mentioned difficulty, owing essentially, to the fact that close packing is preserved across the fault plane.[1] There is also reason to expect that stacking-fault-energy predictions are less sensitive than other defect calculations to uncertainties in exchange and correlation effects. This is because effective interionic potentials, which are always used at least implicitly in defect-energy calculations, are most sensitive to such many-body corrections at small interionic distances (or the order of the nearest neighbor distance),[3] while the smallest distance involved in a stacking-fault-energy calculation is twice the distance between close-packed planes.[5] The effects of nonlocality, however, are more difficult to estimate because such effects persist, in the form of a reduction in magnitude of the oscillations in the interatomic potential, at large interatomic distances.[4] On the other hand, fully nonlocal treatments do exist,[2,6–8] so that it is now possible to avoid this difficulty altogether. Thus, if our suggestion that the stacking-fault energy is insensitive to many-body corrections is valid, it should be possible to proceed with reasonable confidence in the prediction of stacking-fault energies for at least a few close-packed metals.

In the present paper we examine the effects of both many-body corrections and nonlocality by means of comparisons of calculated stacking-fault energies. Our principal purpose in undertaking this work was to test the sensitivity of the result to such effects and thus to investigate the usefulness of the more rigorous models, and simple local potentials as well, for predicting trends in stacking-fault energies. A secondary objective was to explore possible advantages of the calculational method of Blandin, Friedel, and Saada,[5] in which the stacking-fault is expressed as a real-space sum, as opposed to the usual reciprocal-space formulation,[9] involving the effective interaction between close-packed planes.

A review of the method of calculation and a description of the scope of the work are presented in Secs. II and III. In Sec. IV we present numerical results for the interplanar potential in aluminum and gold, these results being typical of polyvalent and noble metals, respectively. Topics discussed here include the effects of nonlocality and many-body corrections in polyvalent metals, the asymptotic approximations of Blandin *et al.*,[5] the sensitivity of the gold potential to minor features of the energy–wave-number characteristic, and implications of this sensitivity as regards the relative stabilities of the two close-packed structures for noble metals. Section V contains the results of stacking-fault-energy calculations, comparisons with experiment, and an analysis based on the discussion in Secs. III and IV.

II. METHOD OF CALCULATION

The stacking-fault energy, which will be denoted by γ, is defined as the difference in energy per unit fault area between the faulted and perfect crystals. In the usual pseudopotential-perturbation approximation, the expression for γ is a sum over

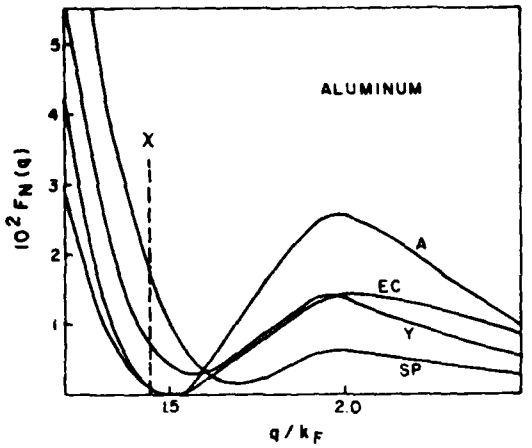

FIG. 1. Normalized energy–wave-number characteristics for aluminum. Stacking-fault energy calculations involve only those data for which q is greater than the smallest reciprocal-lattice vector, indicated here by the line labeled χ. Sources are as follows: A, Animalu (Ref. 12); Y, Yamamoto (Ref. 8); SP, Shaw and Pynn (Ref. 7); and EC, the empty-core model discussed in the text. The energy–wave-number characteristics of Shaw (Ref. 6) and Shyu *et al.* (Ref. 2) differ only slightly from the Shaw–Pynn curve.

wave-vector space of a factor that depends only on q, the electron wave number, multiplied by the difference in the absolute squares of the faulted- and perfect-crystal structure factors.[9] Blandin *et al.*,[5] have shown that this expression can be reduced to the simple form

$$\gamma = \sum_{n=2}^{\infty} N(n)\,\Delta\varphi(nh) \ , \tag{1}$$

where h is the distance between close-packed planes, $N(n)$ is a set of integral weights corresponding to a particular fault configuration, and $\Delta\varphi(nh)$ is an interplanar potential difference defined as follows: If the stacking sequence of close-packed planes is denoted in the usual way by a sequence of symbols (e.g., *ABABAB*... for the hcp structure), then $\Delta\varphi(nh)$ is the interaction energy of a pair of planes in nonequivalent (e.g., *A-B*) positions minus the energy of a pair of planes in equivalent (e.g., *A-A* or *B-B*) positions, the interplanar distance in both cases being nh. The reason that the sum in Eq. (1) begins with $n = 2$ is that in all of the stacking sequences considered here, nearest-neighbor planes are in nonequivalent positions in both the perfect and faulted crystals and their interaction energy therefore cancels in calculating the energy change due to faulting.

The function $\Delta\varphi(nh)$ is given by

$$\Delta\varphi(nh) = \frac{16z^2}{3k_F a^4} \sum_{\vec{g}} (\cos\vec{g}\cdot\vec{d} - 1) J(g, nh) \ , \tag{2}$$

where z is the effective valence,[1] k_F is the Fermi wave number, a is the lattice constant for the close-packed plane, $\vec{g}$ is a reciprocal lattice vector for the close-packed plane, $g = |\vec{g}|$, and $\pm\vec{d}$ is the parallel displacement of one plane relative to a second plane in a nonequivalent position.[1] The dimensionless function $J(g, nh)$ is the integral

$$J(g, nh) = \int_0^{\infty} \left[\frac{1 - F_N([\eta^2 - \chi^2]^{1/2})}{\eta^2 + \chi^2} \right] \cos k_F nh\eta \, d\eta \ , \tag{3}$$

where $\chi = g/k_F$ and $F_N(q/k_F)$ is the normalized energy–wave-number characteristic.[4] In practice the only significant terms in Eq. (2) are those for the smallest nonvanishing value of g. (By actual numerical test, higher-order terms contribute less than 1% to $\Delta\varphi$.) In all subsequent discussions we will therefore use

$$\Delta\varphi(nh) \approx -\frac{48z^2}{k_F a^4} J(nh) \ , \tag{4}$$

which is obtained by summing over the six smallest $\vec{g}$ vectors. The integral $J(nh)$, which is proportional to the interplanar potential, is, of course, given by the right side of Eq. (3) with χ equal to its minimum value. Actually, as the development of Eq. (2) reveals,[1] the interplanar potential is proportional to $+J(nh)$ for planes in equivalent positions and $-J(nh)$ for planes in nonequivalent positions.

From Eq. (3) it is evident that the only values of the argument of F_N that enter the calculation are those for which $q/k_F > \chi$. In Figs. 1 and 2 we show the location of χ with respect to the peaks and valleys in the energy–wave-number characteristics

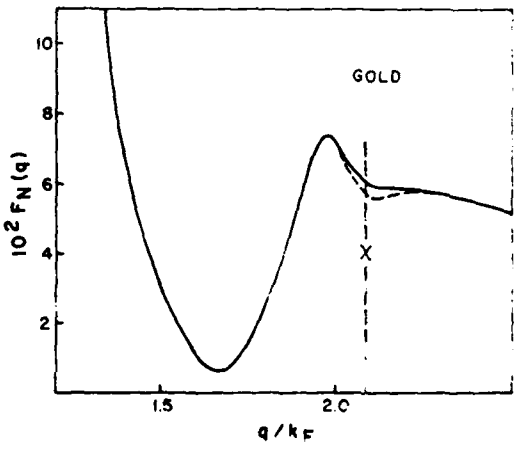

FIG. 2. Normalized energy–wave-number characteristics for gold. The line marked χ has the same significance as in Fig. 1. The solid curve is based on the tabulation of Moriarty (Ref. 16) and the dashed curve is an arbitrary alteration of that data as described in the text.

for aluminum and gold; these data are typical of polyvalent and noble metals, respectively. Since χ is of the order of, or greater than, the position of the first minimum in F_N, the large matrix elements of the pseudopotential that occur near $q/k_F = 0$ do not enter the calculation. Thus, as Heine and Weaire[1] point out, the first-order perturbation approximation on which the formalism is based is more likely to be valid for stacking-fault calculations than it is for other defect studies that do involve values of q/k_F near zero.

If $\chi < 2$, so that the integrand in Eq. (3) contains the logarithmic singularity at the point $q = 2k_F$ (i.e., $\eta^2 + \chi^2 = 4$), we can expect $J(nh)$ to exhibit a long-range oscillatory behavior similar to that of interionic potentials.[9] Blandin *et al.*,[5] showed that, in this case, the asymptotic form for $J(nh)$ is (with the usual assumption of a local pseudopotential)

$$J(nh) \approx -\frac{3a^4k_F\,\nu[w(2k_F)]^2}{128\,\pi^2 z^2}\,\frac{\sin(2k_F\nu nh)}{n^2}\,, \qquad (5)$$

where

$$\nu = [1-(\chi/2)^2]^{1/2} \qquad (6)$$

and $w(2k_F)$ is the screened-pseudopotential form factor evaluated at $q = 2k_F$. They also found that if this asymptotic approximation is used to calculate $\Delta\varphi(nh)$, the stacking-fault-energy sum given by Eq. (1) can be evaluated exactly for intrinsic, extrinsic, and twin faults in both fcc and hcp crystals. For $\chi > 2$ the poles in Eq. (3) occur at imaginary η and the resulting asymptotic form is a decaying exponential. In this case the sum in Eq. (1) converges quite rapidly.

In the present case, for $\chi < 2$, we used the asymptotic formulas of Blandin *et al.*, with numerically computed corrections to $\Delta\varphi(nh)$ for small n. Thus, if we let γ_A and $\Delta\varphi_A(nh)$ denote the asymptotic approximations described above, then the formula used in place of Eq. (1) is

$$\gamma = \gamma_A + \sum_{n=2}^{M} N(n)\,[\Delta\varphi(nh) - \Delta\varphi_A(nh)]\,, \qquad (7)$$

where M is a number large enough that the difference between $\Delta\varphi(Mh)$ and $\Delta\varphi_A(Mh)$ is small.

As it turned out, the most serious difficulty we encountered in applying Eq. (7) was in the numerical evaluation of the integral $J(nh)$ for large nh. Since preliminary tests showed that the mesh-point spacing in tabulated values of F_N is too coarse for the application of standard numerical-integration methods, it was necessary to interpolate the data to obtain estimates of F_N at intermediate values of q/k_F. After experimenting with various interpolation and integration schemes we finally settled on the Aitken interpolation method[10] for obtaining values of F_N at ten points within each tabulated interval. The integration over each subinterval was then done by fitting the quantity in brackets in Eq. (3) with a single exponential in η and evaluating the resulting integral exactly.

In an attempt to minimize the inevitable inaccuracy of interpolated values near the logarithmic singularity at $q = 2k_F$, we performed the interpolation on the function $\epsilon(q)F_N(q/k_F)/[\epsilon(q)-1]$, where $\epsilon(q)$ is the Hartree dielectric function. The idea here was that in the local approximation with Hartree screening this function is smooth and, therefore, more easily interpolated than F_N itself. Even so, when we tested the method by applying it to such approximate functions we were not able to consistently reproduce the asymptotic oscillations in $J(nh)$ for n greater than about 4. This is illustrated in Fig. 3, where we show the asymptotic form of $J(nh)$, the curve obtained by evaluating F_N exactly at each mesh point, and the data obtained with an interpolated function. For the test shown here we used an exponentially damped, empty-core-model potential,[11] with parameters chosen to obtain an approximate fit to tabulated F_N data for magnesium. The lengths of the vertical lines drawn at integral values of n are proportional to the weights $-N(n)$ for an intrinsic fault in an hcp crystal. [From Eqs. (1) and (3) it follows that γ is proportional to the sum of the products $-N(n) \times J(nh)$.]

From the erratic behavior obtained with the interpolated F_N at large values of n, it is evident that when n is large the numerical integration is too sensitive to interpolation errors to be reliable. It is also evident that the interpolation procedure leads to some error for small n, as evidenced by results for n between 2 and 3. These errors, however, are not as important because the weights used in computing γ [the $N(n)$ in Eq. (7)] are greater

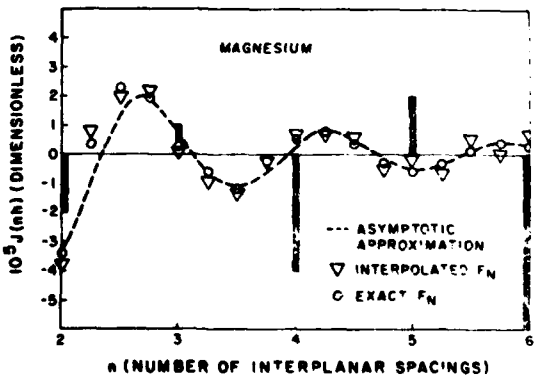

FIG. 3. Interplanar potential function for magnesium based on the local empty-core model described in the text. The lengths of the vertical bars are proportional to the weights involved in Eq. (1) in the calculation of the intrinsic fault energy in an hcp crystal.

for large n. Thus, if we use the data shown in Fig. 3 to compute the energy of an intrinsic fault in the hcp structure, we obtain 11.5 erg/cm^2 with the computed F_N and 13.2 erg/cm^2 with the interpolated function, if the sum in Eq. (7) is terminated at $M = 4$. With $M = 6$, however, we obtain 11.9 and 7.7 erg/cm^2 using the computed and interpolated functions, respectively. Similar results were obtained with empty-core models for aluminum and beryllium, although the errors in γ for these data were much smaller.

Since interpolation difficulties of this type undoubtedly exist with tabulated nonlocal F_N, the sum in Eq. (7) was terminated at $M = 4$ in all of the calculations reported here. Fortunately, this caused no serious problem in most of the computations because the agreement between computed and asymptotic approximations to J was generally quite good at $n = 4$. With some of the data for beryllium, however, the difference between the computed and asymptotic J was still significant at $n = 4$ and the fact that we could not handle larger interplanar distances prevented us from obtaining reliable results.

III. SCOPE OF THE CALCULATIONS

The remaining sections of this paper are concerned with the results of calculations for aluminum, magnesium, beryllium, copper, silver, and gold. In all cases stacking-fault energies were computed for intrinsic, extrinsic, and twin faults in both the fcc and hcp structures, thus providing tests of the ability of the method to predict stability against faulting and the relative energies of different fault configurations.

The energy–wave-number data used in calculations for the polyvalent metals are indicated in Table I. In comparing the results of such calculations it is important to recall that there is an inherent arbitrariness in the construction of a model potential and that this arbitrariness leads, in a truncated perturbation expansion, to some unknown, model-sensitive error. Thus, as far as tests of sensitivity to many-body corrections are concerned, the most meaningful comparisons we can make are those involving the first three sets of data listed in Table I. All three sets were derived from the same ionic-model potentials and differ only in the treatment of electron exchange and correlation energies. Similarly, because they differ only in the way nonlocality is handled, the

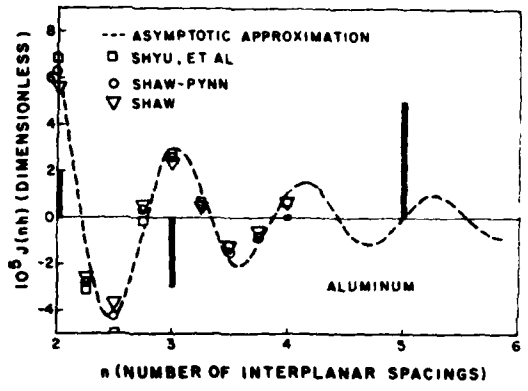

FIG. 4. Interplanar potential functions for aluminum based on the optimized model potential. The vertical bars correspond to weights for an fcc intrinsic fault.

TABLE I. Energy–wave-number characteristics used in calculations for polyvalent metals.

Data source	Model potential	Screening approximation	F_N calculation
Shaw–Pynn (Ref. 7)	Optimized[a]	Shaw–Pynn (Ref. 7)	*nonlocal*
Shaw (Ref. 6)	Optimized	Hartree	nonlocal
Shyu *et al.* (Ref. 2)	Optimized	SSTL[c]	nonlocal
Animalu (Ref. 12)	Heine–Abarenkov[b]	Hubbard–Sham[d]	semilocal
Yamamoto (Ref. 8)	Heine–Abarenkov	Hubbard–Sham	nonlocal
Empty-core model	Exponentially damped empty core	Hartree	local

[a]R. W. Shaw, Jr. and W. A. Harrison, Phys. Rev. 163, 604 (1967).
[b]References 13–15.
[c]K. S. Singwi, A. Sjölander, M. P. Tosi, and R. H. Land, Phys. Rev. B 1, 1044 (1970).
[d]L. J. Sham, Proc. R. Soc. Lond. A 283, 33 (1965).

next two sets of data, those based on the Heine–Abarenkov-model potential, provide a basis for investigating the importance of nonlocal effects. The primary reason for including calculations based on the empty-core model was to determine, through comparisons with results based on the more refined models, to what extent the simpler theory might be useful for estimating trends in stacking-fault energies.

The only nonlocal energy–wave-number characteristics available for the noble metals are those reported by Moriarty.[16] Although comparisons with results based on simpler local models could have been made, we did not do this because such models are obviously unrealistic for the noble metals, where the energy–wave-number characteristic is dominated by the highly nonlocal effects of resonant scattering. Our analysis for the noble metals is therefore limited to comparisons with experiment and a numerical test of the sensitivities of the interplanar potential and stacking-fault energies to minor alterations of the energy–wave-number characteristic.

IV. INTERPLANAR POTENTIALS

The interplanar potential function $J(nh)$ for aluminum, as determined from the energy–wave-number tabulations of Shaw[6] (Hartree approximation), Shaw and Pynn,[7] and Shyu *et al.*,[2] is plotted in Fig. 4 along with the asymptotic approximation based on the Shaw–Pynn form factor. The lengths of the vertical lines shown here are proportional to the negative of the weight factors for an intrinsic fault in an fcc crystal. Figure 5 is a similar plot, the tabulated F_N in this case being those of Animalu[12] and Yamamoto,[8] while the corresponding asymptotic curve was computed for the Heine–Abarenkov form factor.[13–15] The points and asymptotic curve for the empty-core model correspond to the energy–wave-number characteristic shown in Fig. 1. Potential functions for magnesium and beryllium were also computed but are not shown here because the main features we wish to consider are similar for all three polyvalent metals.

The first thing we should note regarding Fig. 4 is that it is very easy to see, from a plot such as this, how the interactions between various pairs of planes contribute to the stacking-fault energy. At the second nearest interplanar distance ($n = 2$) in aluminum, for example, J is positive and the weight $-N(2)$ is also positive. This indicates, according to Eqs. (1) and (4), that the interaction between second-nearest-neighbor planes is such as to oppose the formation of an intrinsic fault; i.e., this particular interaction leads to a positive contribution to the stacking-fault energy. At the next interplanar distance, however, the contribution is negative because J and $-N(3)$ are of opposite sign. The fourth- and fifth-neighbor planes are not important because $N(4) \approx 0$ and $J(5h) \approx 0$. Thus, neglecting possible contributions from larger n (which turns out to be valid in this case), we can see that the reason aluminum has a positive intrinsic fault energy, or equivalently, the reason that the fcc structure is stable against faulting, is because the positive contributions of second-nearest-neighbor planes outweigh the negative contributions of third-nearest-neighbor planes. The same kind of analysis can, of course, be applied to the magnesium plot shown in Fig. 3. Here the fact that the hcp structure is stable tells us that the positive stacking-fault-energy contributions from second- and third-nearest-neighbor planes must be greater than the negative contribution from more distant pairs.

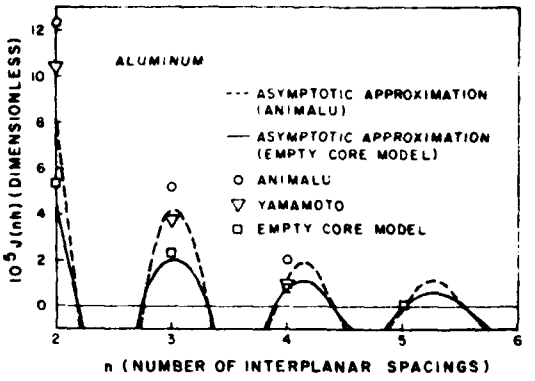

FIG. 5. Interplanar potential functions for aluminum based on the Heine–Abarenkov and empty-core-model potentials.

Another point illustrated in Fig. 4 is that at the interplanar distances of importance here, it makes very little difference whether we use the data of Shaw, Shaw and Pynn, or Shyu *et al.* in the calculation of J. Since the only difference among these three sets of data is the way in which exchange and correlation effects are handled in the screening calculation, the comparison shown here indicates that such effects are of little consequence in the present context. In fact, the good agreement of the results obtained with the other two characteristics with the result based on Shaw's data, which was calculated in the Hartree approximation, suggests that exchange and correlation corrections can safely be ignored in calculations of stacking-fault energies. The reason is, as we indicated earlier, that the effects of such corrections are observed at interplanar or interatomic distances somewhat shorter than those involved in the calculation of stacking-fault energies.

Figure 4 also illustrates the generally good

agreement experienced between the numerically computed value of J and the value obtained from the asymptotic approximation of Blandin *et al.* at separation distances of about four interplanar spacings. Further examples are provided by the Yamamoto and empty-core results shown in Fig. 5. Thus, as we indicated in Sec. III, it was possible to terminate the numerical-integration computations at $n = 4$ and, in effect, use the asymptotic curve for larger n without introducing serious errors in most applications.

An exception is illustrated in Fig. 5, where it is evident that computed values based on Animalu's semilocal energy-wave-number characteristic are significantly greater than the corresponding asymptotic curve. This difficulty was also observed with the Animalu calculation for magnesium and, to a much greater extent, with the beryllium calculation. In fact, with beryllium, the disagreement was so serious that we were not able to obtain even a reasonable estimate of the stacking-fault energy based on the Animalu data. Some difficulty was also experienced with the beryllium potentials based on the data of Shaw, Shaw-Pynn, and Shyu *et al.*, but not to such an extent as to completely invalidate the corresponding estimates of γ.

We can get some idea of the influence of nonlocality through a comparison of the Animalu and Yamamoto results shown in Fig. 5, since Yamamoto's data were obtained from a fully nonlocal treatment of the same model potential used in Animalu's calculations. The principal result is just what one would expect from Shaw's[4] investigation of similar effects on interionic potentials, namely, that a fully nonlocal treatment tends to diminish the amplitude while preserving the frequency and phase of the long-range oscillations of the potential function. It should be noted, however, that Animalu's energy-wave-number characteristic is semilocal, in the sense that he made use of certain simplifying approximations, usually invoked in the local theory, in performing the final integration to obtain F_N.[12] If a truly local approximation had been employed, Shaw's[4] studies indicate that the amplitude of the oscillations in J would be even greater than that obtained with the Animalu approximation. We conclude, therefore, in agreement with Shaw, that nonlocality must be accounted for in any accurate first-principles predictions of interionic or interplanar potentials.

This is not to say, however, that we cannot use simpler, empirically adjusted local models for the prediction of trends or even for obtaining rough estimates of the values of the stacking-fault energy itself, provided that we have some prior knowledge of the general features of the nonlocal energy-wave-number characteristic. This is illustrated by the fact that the empty-core calculations shown in Fig. 5 actually agree rather well with the more sophisticated first-principles results shown in Fig. 4. The energy-wave-number characteristic used here was of the usual form,[11]

$$F_N(q/k_F) = \{[\epsilon(q) - 1]/\epsilon(q)\}M^2(q/k_F), \tag{8}$$

where $\epsilon(q)$ is the Hartree dielectric function and

$$M(x) = \cos(\pi x/2x_0)e^{-Dx^2}. \tag{9}$$

The parameter x_0 was fixed by requiring that the first zero in F_N coincide with that in Animalu's tabulation, and the damping parameter D was chosen to bring the peak near $q = 2k_F$ down into rough agreement with tabulated nonlocal functions. The value used for all three polyvalent metals was $D = 0.12$, which is somewhat larger than the damping parameters usually employed in local-empirical-pseudopotential studies.[11] This value did, however, lead to rather good agreement with the nonlocal energy wavenumber characteristics and interplanar potential functions for all three polyvalent metals, the results shown in Figs. 1, 4 and 5 being typical.

Turning now to the noble metals we show a representative result in Fig. 6. This is the interplanar potential function for gold, as determined from Moriarty's energy-wave-number characteristic,[16] along with the corresponding asymptotic approximation. The second set of points shown here was obtained with the altered energy-wave-number characteristic shown in Fig. 2; the significance of these data will be discussed shortly. Again, the vertical lines are proportional to the weights $-N(n)$ for an intrinsic fault in an fcc crystal.

From these results, and those for copper and silver as well, it is evident that there is serious disagreement between the interplanar potential func-

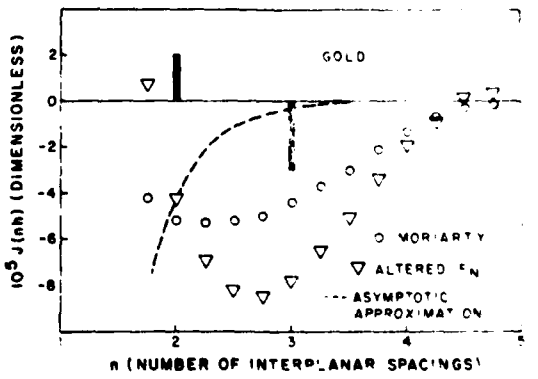

FIG. 6. Interplanar potential functions for gold. The corresponding energy-wave-number characteristics are shown in Fig. 2.

tion predicted by the asymptotic theory and that obtained by direct numerical integration. This is not surprising in view of the fact that the asymptotic approximation is based on the assumption that, as far as the long-range behavior of J is concerned, the logarithmic singularity at $q = 2k_F$ is the dominant feature of the energy-wave-number characteristic. Thus, when the asymptotic form resulting from this assumption turns out to be a rapidly decaying exponential, as it does here, there emerges the possibility that other features of F_N may dominate at large values of nh. Our results show that this is in fact the case for the noble metals and suggest that similar results might be expected for other monovalent metals as well.

One encouraging consequence of the radical departure of the numerically computed J from the asymptotic approximation is that the computed values lead to positive energies for fcc faults while the asymptotic theory incorrectly predicts negative fault energies.[5] As is evident from Fig. 6, this happens because the positive contribution from third-nearest-neighbor planes is strong enough to offset the negative contribution from $n = 2$ interactions. Thus, the strong negative dip in J between $n = 2$ and 3 seems to be essential to the correct prediction that the fcc noble metals are stable against faulting.

Unfortunately, the dip in J is not strong enough. In Sec. V we will present predictions of γ that show that although positive energies are obtained for fcc faults, these energies are low by about an order of magnitude for gold and silver. Furthermore, our calculations also indicate that noble-metal fault energies for the unstable hcp crystals, which one would expect to be negative, turn out to be positive and quite large. This indicates, of course, that the hcp structure is more stable than the fcc structure, an incorrect prediction that agrees with Moriarty's total-energy calculation.[16] The trouble is obviously due to some inaccuracy in the Moriarty F_N data, probably, as he suggests, to his neglect of the subtle effects of crystal field splitting on s-d hybridization.[16] However, whatever the basic reason may be, it is of interest to note that the correct interplanar potential function must have a more pronounced minimum than that obtained from the Moriarty data. This would produce a greater difference between the positive ($n = 3$) and the negative ($n = 2$) contributions to the fcc intrinsic-fault energy, while at the same time reducing the predicted values of fault energies in the hypothetical hcp structure.

An interplanar potential function having the desired characteristic is shown in Fig. 6. This curve was generated from the altered F_N data shown in Fig. 2. We wish to emphasize that this alteration is entirely arbitrary; it was obtained by trial-and-error manipulations of the data in the neighborhood of $q/k_F = \chi$, since J seems to be most sensitive to the detailed curvature of F_N in this region. We think the result is of interest, however, because it shows that for the noble metals at least, seemingly insignificant changes in the energy-wave-number characteristic can lead to major changes in the interplanar potential (Figs. 2 and 6) and in the predicted stacking-fault energy (the alteration shown here increased the fcc intrinsic-fault energy by about a factor of 7). Unfortunately this extreme sensitivity to detailed structure in the energy-wave-number characteristic also suggests that, in contrast to the situation for polyvalent metals, there is little hope for making useful estimates on the basis of simple models for the noble metals.

V. STACKING-FAULT ENERGIES

Table II is a listing of intrinsic-stacking-fault energies for the stable structures of aluminum, magnesium, and beryllium. Calculations were also performed for extrinsic and twin faults and, with few exceptions, the approximate relations for hcp crystals[10] $\gamma_{ext} \approx \frac{3}{2}\gamma_{ist} \approx 3\gamma_{twin}$, were found to hold within about 10%. The exceptions were the twin-fault energies in magnesium, as determined from the energy-wave-number characteristics of Shaw and Pynn, Shaw, and Shyu *et al.*, where we

TABLE II. Intrinsic-stacking-fault energies in erg/cm^2 for aluminum (fcc), magnesium (hcp), and beryllium (hcp).

Data source	Al	Mg	Be
Shaw–Pynn	57.9	13.9	439
Shaw	52.1	8.54	390
Shyu *et al.*	69.2	16.6	468
Animalu	104	33.4	···
Yamamoto	110	37.7	305
Empty-core model	43.1	11.5	128
Other calculations	195[a] 62[b] 142[c]	8.7[f] 30[g] 50[g]	225[f]
Experimental estimates	135[d] 135–280[e]	60–93[h] 100–150[d]	190[i]

[a]Reference 17; based on Animalu data.
[b]Reference 18; based on Shaw data.
[c]Reference 18; based on Animalu data.
[d]Reference 20.
[e]P. C. J. Gallagher, Met. Trans. 1, 2429 (1970).
[f]Reference 19; based on Shaw data.
[g]Reference 9; based on Harrison's pseudopotential.
[h]D. H. Sastry, Y. V. R. K. Prasad, and K. I. Vasu, Scripta Met. 3, 927 (1969).
[i]H. Conrad, Air Force Materials Laboratory Report No. AFML-IR-65-310 (1965) (unpublished).

TABLE III. Intrinsic-stacking-fault energies in erg/cm^2 for fcc copper, silver, and gold. Calculated values are based on the energy–wave-number characteristics of Moriarty (Ref. 16).

	Cu	Ag	Au
Calculated	44.8	1.7	4.8
Average experimental estimate[a]	55	21.7	50

[a]P. C. J. Gallagher, Met. Trans. 1, 2429 (1970).

found $\gamma_{ext} \approx 2.3\gamma_{twin}$. With fcc aluminum we obtained, to within about 25%, $\gamma_{ext} \approx \gamma_{int} \approx 2\gamma_{twin}$. For the unstable close-packed structures (hcp aluminum and fcc magnesium and beryllium) we obtained negative energies for all three types of fault, thus correctly indicating the instability of these structures against faulting.

Intrinsic-fault energies for fcc copper, silver, and gold, as determined from Moriarty's energy–wave-number data, are shown in Table III. As was noted in the Sec. IV, the hcp fault energies for these metals, rather than being negative as they should be, were calculated to be positive and quite large (γ = 26, 15, and 25 erg/cm^2 for the hcp intrinsic-fault energies in copper, silver, and gold, respectively). The good agreement with experiment obtained for the fcc intrinsic-fault energy in copper is therefore probably fortuitous.

When the energy–wave-number characteristic for gold was altered as shown in Fig. 2, we obtained 37 and 20 erg/cm^2 for the fcc and hcp intrinsic faults, respectively. We wish to emphasize again, however, that although this change is in the right direction, the alteration of F_N shown in Fig. 2 is entirely arbitrary, and serves only to illustrate the sensitivity of noble-metal results to rather minor features in the energy–wave-number characteristics. This being the case, there is not much more we can say about the noble metals except to note that the calculation of stacking-fault energies appears to be a very demanding test of the accuracy of the energy–wave-number characteristic in the vicinity of the smallest reciprocal-lattice spacing.

Returning now to the polyvalent metals we can see, as anticipated from the plots of the interplanar potential function shown in Fig. 4, that exchange and correlation effects are not particularly significant since little change was experienced in going from the Hartree approximation (Shaw) to calculations with such many-body corrections included (Shaw and Pynn and Shyu *et al.*). The only appreciable effect was that shown for magnesium, where there is roughly a factor of 2 spread in predicted intrinsic-fault energies.

Results based on the energy–wave-number data of Animalu and Yamamoto indicate that, in two cases at least, differences between fully nonlocal and semilocal calculations are not as great as one might expect from the data shown in Fig. 6. Apparently what has happened in aluminum is that the large differences between the Animalu and Yamamoto calculation of J at second- and third-nearest-neighbor planes are approximately canceled in performing the sum in Eq. (7) (recall that the second-nearest-neighbor plane gives a positive contribution to γ while the third-nearest-neighbor plane yields a negative contribution). A similar situation exists for magnesium, the cancellation in this case being between the positive contributions of the second- and third-neighbor pairs and the negative contribution of fourth-nearest-neighbor planes. For beryllium, however, the effect was quite marked because the Animalu data gave correction terms [those in the sum on the right side of Eq. (7)] that were about an order of magnitude greater than the corresponding values obtained with Yamamoto's data. As was mentioned previously, it is this large deviation of the numerically integrated J from the asymptotic approximation that prevented us from obtaining a meaningful estimate of γ for beryllium from Animalu's data. One should, of course, expect to encounter difficulties with the local or semilocal approximation for beryllium because the absence of p states in the core leads to a strongly nonlocal pseudopotential.[11]

It would appear, however, from results such as those illustrated in Figs. 1, 4, and 5, that in the present context the principal effect of a fully nonlocal treatment is the suppression of the peak in F_N near $q = 2k_F$ and the resulting reduction in the interplanar potential function J. Thus, given some prior knowledge of the magnitude of the peak in the nonlocal F_N, it should be possible to use empirically adjusted local-model potentials, even for such strongly nonlocal elements as beryllium, to obtain rough estimates of γ. To test this idea, we used the modified empty-core model described in the Sec. IV to compute the intrinsic-fault energies shown in Table II. Considering the fact that the model is extremely simple and that the same damping-factor adjustment was used for all three metals, the agreement with other predictions of γ is surprisingly good. Although improved agreement could probably be obtained by further adjustments of the model-potential parameters, we see little reason for doing so, particularly since there is still considerable uncertainty as to what one should assume for the correct value of γ. In any case, even if γ were known more accurately, the real merit of such simplified models lies in their ability to predict trends in relative magnitudes and

perhaps, obtain rough estimates of γ itself, with minimum requirement for prior adjustment of the model-potential parameters. In this sense, then, the rough agreement shown here is actually quite encouraging.

As far as the more rigorous models are concerned, comparisons of our computations with those performed by other methods met with mixed results. With aluminum, for example, our value of 104 erg/cm^2 based on Animalu's data is significantly lower than Hodges[17] value of 195 erg/cm^2, which was computed from the same energy-wave-number characteristic using the reciprocal-space formulation. It is also lower than the value of 142 erg/cm^2 obtained by Wilkes and Sargent,[18] who used the same data in a real-space treatment involving the sums of interionic potentials over a large number of pairs of ions in the faulted and perfect structures. There is, unfortunately, reason to question the accuracy of both the Wilkes-Sargent result and our own. The Wilkes-Sargent calculation did not make use of the asymptotic theory of Blandin *et al.* and, therefore, suffers from a convergence difficulty typical of pairwise sums over the direct lattice. Our calculation in this case is also subject to a convergence uncertainty because, as we noted earlier, with the Animalu data it was not possible to carry the calculation out to distances large enough to obtain agreement with the asymptotic potential. We can be less certain of possible sources of error in Hodges result, although the fact that he had to perform a number of rather sensitive computations by hand could have resulted in some inaccuracy. The only other comparison we can make for aluminum is our value of 52 erg/cm^2, obtained from Shaw's data, with the Wilkes-Sargent value of 62 erg/cm^2. In view of the convergence difficulty experienced by Wilkes and Sargent this ageement is probably as good as can be expected.

For magnesium, our results based on the Shaw and Animalu energy-wave-number data are in excellent agreement with the values reported by Ducharme[19] (8.7 erg/cm^2 with Shaw's data) and Hodges[17] (30 erg/cm^2 with Animalu's data). Harrison's calculation of 50 erg/cm^2 was based on a different energy-wave-number characteristic[9] and is included here only as a further illustration of the rather significant differences that can result from the use of different potentials. The only comparison we can make for beryllium is our calculation of the fault energy with that of Ducharme,[19] both of which made use of Shaw's energy-wave-number characteristics. Here again, however, we experienced some convergence difficulty, which could account for the discrepancy.

Agreement with experimental results is generally rather poor. We are not particularly concerned that our results for beryllium seem to be too high, because of the convergence problem discussed earlier. The poor agreement for magnesium and aluminum, however, deserves further comment.

First we should point out that it is quite possible that the experimental values for these metals are too high, since experimental difficulties are usually encountered when γ is greater than about 20 erg/cm^2.[20] The source of this difficulty is that fault widths are roughly proportional to the inverse of the stacking-fault energy and are therefore too small for direct observation when γ is large. One must then resort to indirect methods, such as the observation of dislocation-loop annealing rates,[20] to obtain estimates of γ. Interpretations of such data necessarily involve the assumption of physical models and subsequent calculations to extract γ from the direct experimental results. The present situation is therefore one of considerable uncertainty, as evidenced by the spread in experimental data referenced in Table I. For this reason we are inclined to regard comparisons with experiment primarily as tests of the ability to predict trends, placing less emphasis on the achievement of absolute numerical agreement.

As for why the calculations might be inadequate, if indeed it is the calculations that are at fault, we cannot offer a completely satisfactory explanation. While it is certainly possible that the numerical problems discussed in Sec. II led to significant errors in the predictions, agreement with calculations performed by other methods seems to indicate that this is not the case. Nor does it seem likely that uncertainties in exchange and correlation corrections are responsible, because we can totally ignore such effects and still obtain about the same answers. Nonlocal effects can be ruled out because they are fully accounted for in some of the energy-wave-number characteristics of concern here. Although magnesium and aluminum are generally considered "simple" metals, in the sense that the matrix elements of their pseudopotentials are small, we cannot ignore the possibility that higher-order terms in the perturbation expansion, which would be structure dependent and therefore different in the faulted and perfect crystals, may have a greater effect in stacking-fault-energy calculations than they do in calculations of other properties. Still, if agreement with presently available experimental data is our goal, we are looking for a factor of about 2 or 3 increase in γ, and the possibility that a higher-order perturbation treatment would give us such a factor does seem remote.

Thus, because the major sources of error usually present in defect studies are of diminished importance in stacking-fault-energy calculations, it is difficult to identify any one uncertainty as being

most likely to cause disagreement with experiment. The best we can do at present is to simply note that there are still many approximations and idealizations present, both in the theory and in the derivation of stacking-fault energies from experimental observations and, for this reason, perhaps we should not expect much better agreement than that obtained here.

VI. SUMMARY AND CONCLUSIONS

We have applied the method of Blandin, Friedel, and Saada[5] to the calculation of stacking-fault energies in aluminum, magnesium, beryllium, copper, silver, and gold. Energy–wave-number characteristics representing various degrees of refinement of the theory were used in order that the sensitivity of the result to such refinements could be determined.

Our results for the polyvalent metals indicate that the stacking-fault energy is influenced by many-body and nonlocal effects, but not nearly so much as to invalidate the use of approximate model potentials. In fact, comparisons of results based on a simple local potential with those based on the more sophisticated nonlocal treatments suggest that, with certain semiempirical adjustments to account for the major effects of nonlocality, the simpler theory is entirely adequate for predicting trends and for obtaining rough estimates of the stacking-fault energy, as long as the use of such models is restricted to polyvalent metals. Calculations for copper, silver, and gold, on the other hand, show that the stacking-fault energies of these metals (and probably other monovalent metals as well) are quite sensitive to minor alterations in the energy–wave-number characteristic. The use of simplified semiempirical models for these metals could therefore lead to serious error.

The real-space formulation of Blandin *et al.* was found to have both its advantages and disadvantages. On the positive side, the fact that the method involves a sum of interplanar potentials over pairs of close-packed planes offers some interpretative advantages over the reciprocal-space treatment. It is very easy to see, for example, in terms of the amplitudes and oscillatory characteristics of the interplanar potentials, how interactions between various pairs of planes contribute to the stability or instability against faulting for a given close-packed structure.

The principal disadvantage of the method is that it presents some difficult computational problems, both in the sensitivity of the result to numerical-integration approximations and in the usual convergence problem associated with real-space lattice sums. Still, with the aid of the asymptotic approximations developed by Blandin *et al.*, the latter difficulty can be largely overcome, and the method therefore offers an instructive, though perhaps somewhat less accurate, [illegible]rnative to the more familiar reciprocal-sp[illegible]atment.

Comparisons of predicted stac[illegible]rgies with experimental results were disa[illegible] calculated values in most cases bei[illegible] substanti[illegible]ly lower than experimental values. [illegible] major uncertainties that one usually has [illegible] with in defect-energy calculations (the [illegible] perturbation theory, exchange and correlati[illegible] corrections, and the importance of nonloca[illegible]ts) are of minimal significance in the present application, it is difficult to explain why this disagreement exists. Although this is an unsettling situation, and one that we think deserves further study, we can draw some satisfaction from the fact that the calculations do correctly predict the stabilities of close-packed structures against faulting, and, at least roughly, the relative magnitudes of stacking-fault energies for different metals. The calculations also indicate that trends such as these can be predicted with reasonable success with a local-model potential, provided that the major effects of nonlocality, the suppression of the peak in the energy–wave-number characteristics at $q = 2k_F$, is approximately accounted for by an empirical adjustment. This may well be the most important result of the present work because it suggests that in spite of quantitative difficulties that seem to persist in even the most refined version of the theory, there is still much that can be learned from the simplest local approximation.

ACKNOWLEDGMENTS

The author is pleased to acknowledge several helpful discussions with C. G. Gardner, J. Lankford, and D. L. Davidson. H. G. Pennick deserves special thanks for his assistance with the computations.

[1]V. Heine and D. Weaire, Solid State Phys. 24, 249 (1970).
[2]W. Shyu, J. H. Wehling, H. R. Cordes, and G. Gaspari, Phys. Rev. B 4, 1802 (1971).
[3]R. W. Shaw, Jr. and V. Heine, Phys. Rev. B 5, 1646 (1972).
[4]R. W. Shaw, Jr., J. Phys. C 2, 2335 (1969).
[5]A. Blandin, J. Friedel, and G. Saada, J. Phys. Suppl. C 3, 128 (1966).
[6]R. W. Shaw, Jr., dissertation (Stanford University, 1968) (unpublished).
[7]R. W. Shaw, Jr. and R. Pynn, J. Phys. C 2, 2071 (1969).
[8]T. Yamamoto, J. Phys. Soc. Jap. 28, 938 (1970).
[9]W. A. Harrison, *Pseudopotentials in the Theory of Metals* (Benjamin, New York, 1966).
[10]G. A. Korn and T. M. Korn, *Mathematical Handbook for Scientists and Engineers* (McGraw-Hill, New York, 1968).
[11]M. L. Cohen and V. Heine, Solid State Phys. 24, 37 (1970).

[12]A. O. E. Animalu, Proc. R. Soc. A 294, 376 (1966).
[13]V. Heine and I. Abarenkov, Philos. Mag. 9, 451 (1964).
[14]A. O. E. Animalu and V. Heine, Philos. Mag. 12, 1249 (1965).
[15]I. Abarenkov and V. Heine, Philos. Mag. 12, 529 (1965).
[16]J. A. Moriarty, Phys. Rev. B 6, 1239 (1972).
[17]C. H. Hodges, Philos. Mag. 15, 371 (1967).
[18]P. Wilkes and C. M. Sargent, Met. Sci. J. 6, 216 (1972).
[19]A. R. Ducharme, Phys. Lett. A 31, 41 (1970).
[20]R. E. Smallman and P. S. Dobson, Met. Trans. 1, 2383 (1970).

APPENDIX B

Multi-Ion Interactions in Transition Metals

PHYSICAL REVIEW B VOLUME 9, NUMBER 12 15 JUNE 1974

Multi-ion interactions in transition metals

R. E. Beissner
Southwest Research Institute, San Antonio, Texas 78284
(Received 29 January 1974)

An energy-dependent t-matrix generalization of Harrison's theory of multi-ion interactions is developed. Explicit expressions are derived for two- and three-ion potentials in a system of ions having d-electron scattering resonances of the Breit-Wigner form. It is shown that although a simple pairwise interionic potential does not exist, one can define an effective potential such that the correct band-structure energy is obtained in the form of a pairwise sum. The effective pairwise potential is then computed through third order for an idealized transition-metal series. The results show that third- and possibly higher-order interactions must be included in the calculation to fully account for the effects of d-band splitting on interionic forces.

I. INTRODUCTION

The underlying assumption in the pseudopotential theory of nontransition metals is that conduction-electron–ion scattering is weak enough to be treated in the first Born approximation.[1,2] On the basis of this assumption, one then calculates electron densities and screening potentials that are self-consistent to first order in the electron-ion pseudopotential leading, via standard perturbation theory, to an expression for the total electronic energy that is correct to second order in the pseudopotential. By taking the Fourier transform of the second-order term in this expression, one then obtains a rather simple formula for the electronic part of the interionic potential. As it turns out, at this level of approximation the resulting potential is independent of the positions of neighboring ions; the only geometrical factor that enters is the separation distance of the ion pair.

The application of this simple model to transition metals is, however, clearly invalid. Here it is well known that the indirect interionic interaction is dominated by resonant scattering of d electrons and that a low-order perturbation treatment is therefore quite unrealistic. One might hope to improve the calculation, while still retaining the formal simplicity of the standard theory, by starting with an exact calculation for scattering by individual ions, while keeping the second-order approximation to the contributions of interionic scattering to the total energy. However, as Heine and Weaire have noted,[2] this leads to an interaction energy that is correct only for an isolated pair of ions; the convenient pairwise interaction form is thus obtained by simply ignoring the rest of the crystal. In view of the fact that scattering by neighboring ions is known to have a profound effect on even the atomiclike aspects of the electronic structures of transition metals (e.g., the splitting of a single-ion d resonance into subbands[3]), it would seem that the isolated-pair model could lead to serious error when applied to the calculation of interionic interactions in real crystals. What is needed, therefore, is a way of going beyond second order in interionic scattering in order to properly account for the effects of neighboring ions on interionic interactions.

Our main concern in the present work is the development of a formalism appropriate to such higher-order calculations for transition metals. The approach we use is similar to that used by Harrison in the development of his theory of multi-ion interactions in nontransition metals.[4] The basic idea is that one can write the perturbation expansion of the structure-dependent part of the electronic energy in a form such that the leading term is the sum of pairwise interionic potentials and successive terms are sums of three-ion and higher-order interactions. Each multi-ion interaction term in this expansion corresponds to a closed scattering path connecting a group of ions and the expansion is therefore conveniently represented as a sum of multi-ion interaction diagrams. Within this framework the higher-order correction terms we seek are therefore those corresponding to diagrams with three or more vertices.

There are, however, two generalizations of Harrison's formalism that are required before the multi-ion expansion idea can be applied to transition metals. The original development, because it was intended for applications to nontransition metals, was based on the assumption of weak, energy-independent scattering by individual ions. Both approximations are, of course, grossly inaccurate in transition metals where near-resonance conditions at energies of interest make scattering quite strong and highly energy dependent.

The extension to a partial wave treatment of scattering by individual ions, which permits one to avoid the weak scattering assumption, is actually quite straightforward. Such a development was reported first by Harrison in a note added to his original article,[4] and later by Lloyd and Oglesby,[5]

who based their development on a different expansion technique. An alternative treatment, which more closely resembles Harrison's original approach, is contained in Sec. II of this paper.

It is, however, the treatment of energy-dependent scattering that presents some difficulty and is, therefore, of more concern here. Actually, there are two parts to this problem, the first being encountered in the early stages of the formal development and the second in handling an integral over a product of resonant scattering amplitudes. If one starts with an expansion similar to Harrison's, the formal difficulty occurs when the energy-independent pseudopotential form factor used by Harrison is replaced by energy-dependent elements of the corresponding t matrix. In Sec. II we show that this can be handled by combining certain classes of scattering diagrams. With the Lloyd-Oglesby expansion, incidentally, this formal difficulty is avoided altogether, but at the expense, we think, of some loss of clarity as to which diagrams are to be included in the sum. Aside from this point, however, our formal result is in exact agreement with that of Lloyd and Oglesby.

In Sec. III we address the second part of the problem, that of performing an integral over energy-dependent scattering amplitudes. To do this we separate the resonant and nonresonant parts, assume the Breit-Wigner form for the resonant part, and make use of some of the approximations employed by Mezei and Grüner[6] in the treatment of a similar problem to perform the resulting integrals analytically. The end result is a general expression for the asymptotic form of the multi-ion interaction energy for cases where ion scattering amplitudes contain both resonant and nonresonant parts.

Next we turn to the problem posed earlier in this discussion, namely, an investigation of the role played by multiple interionic scattering in determining interionic interactions in a crystalline environment. First, we show that one can define an effective pairwise potential that includes multi-ion contributions. This effective interionic potential, which necessarily depends on crystal structure and on the orientation of the ion pair with respect to crystallographic axes, is shown to consist of the usual potential for an isolated pair plus correction terms corresponding to scattering by neighboring ions. It therefore forms a suitable basis for the study of interionic forces in real crystals.

Finally, in Sec. IV, we present some numerical computations of the effective interionic potential for nearest neighbors in a hypothetical face-centered-cubic transition-metal series. The results show that as the Fermi level is varied from the bottom to the top of the d band, the interaction energy for an isolated pair goes through a strong negative peak in the vicinity of the resonance energy followed by a weaker repulsive peak at higher energies. The interesting point, however, is that when third-order interactions with neighboring ions are added, the structure of the attractive peak is modified in such a way as to indicate the presence of an additional repulsive component at energies just above resonance. This is due, we suggest, to changes in the structures of bonding and antibonding subbands brought about by multi-ion scattering. Thus, as we indicated above, it would seem that third- and higher-order scattering among neighboring ions does indeed play a significant role in determining the nature of interionic interactions in transition-metal crystals.

II. FORMAL THEORY

Our starting point is Harrison's expression for the configuration-dependent part of the band-structure energy[4]

$$\tilde{U} = -\int_0^{E_F} \int_0^{E} \rho(E')\, dE'\, dE \,, \tag{1}$$

where $\rho(E)$ is the density of states,

$$\rho(E) = -(2/\pi)\mathrm{Im}\,\mathrm{Tr}G(E) \,.$$

Here Tr denotes the trace and $G(E)$ is the Green's operator for electrons. From the well-known relation

$$G(E) = G_0(E) + G_0(E)T(E)G_0(E) \,, \tag{2}$$

we see that $\tilde{U}$ contains, in addition to the configuration-dependent term containing the crystal t matrix $T(E)$, a free-electron contribution that is independent of the arrangement of ions (G_0 is the free-electron propagator). Since we are interested in structure-dependent properties, we will drop this term and calculate only the contribution of the second term in Eq. (2).

Next we use the t-matrix expansion[7]

$$T = \sum_{n=1}^{\infty} T_n \,, \tag{3}$$

with

$$T_n = \sum_{\vec{R}_1} \sum_{\vec{R}_2 \neq \vec{R}_1} \cdots \sum_{\vec{R}_n \neq \vec{R}_{n-1}} t(\vec{R}_1) G_0\, t(\vec{R}_2) \cdots G_0\, t(\vec{R}_n) \,, \tag{4}$$

where $t(\vec{R}_j)$ is the t operator for an ion at $\vec{R}_j$. But the first term in Eq. (3) is also independent of ion arrangement and can therefore be omitted. This leaves, for the structure-dependent energy,

$$U = -\frac{2}{\pi} \sum_{n=2}^{\infty} \int_0^{E_F} \int_0^{E} \mathrm{Im}\,\mathrm{Tr} G_0\, T_n\, G_0\, dE'\, dE \,. \tag{5}$$

By making use of the invariance of the trace under cyclic permutation of the operators, and from the identity

$$G_0^2 = -\frac{dG_0}{dE'}$$

n [with $t_j = t(\vec{R}_j)$]

$$G_0 T_n G_0 = \sum_{\vec{R}_1} \sum_{\vec{R}_1 \neq \vec{R}_2} \cdots \sum_{\vec{R}_n \neq \vec{R}_{n-1}} \mathrm{Tr} G_0 t_1 G_0 t_2 \cdots G_0 t_n G_0 = -\sum_{\vec{R}_1} \sum_{\vec{R}_2 \neq \vec{R}_1} \cdots \sum_{\substack{\vec{R}_n \neq \vec{R}_{n-1} \\ \vec{R}_n \neq \vec{R}_1}} \mathrm{Tr} \frac{dG_0}{dE'} t_1 G_0 t_2 \cdots G_0 t_n$$

$$-\sum_{\vec{R}_1} \sum_{\vec{R}_2 \neq \vec{R}_1} \cdots \sum_{\substack{\vec{R}_{n-1} \neq \vec{R}_{n-2} \\ \vec{R}_{n-1} \neq \vec{R}_1}} \mathrm{Tr} G_0 t_1 \frac{dG_0}{dE'} t_1 G_0 t_2 \cdots G_0 t_{n-1} . \tag{6}$$

t term on the right-hand side is the sum
n-ion scattering paths with the first and
s on different sites while the second term
onds to diagrams with the first and last ions
ame site. The next step is to show that this
class of diagrams can be combined with
rms to express the sum in Eq. (5) in a
onvenient form.

let v denote the energy-independent poten-
a particular ion, then the corresponding t
r satisfies

$$t(E') = v + v G_0(E') t(E') \tag{7}$$

from which we obtain

$$\frac{dt(E')}{dE'} = [1 - v G_0(E')]^{-1} v \frac{dG_0}{dE'} t(E') ; \tag{8}$$

but from Eq. (7) we have

$$[1 - v G_0(E')]^{-1} v = t(E')$$

and Eq. (8) can therefore be written

$$t(E') \frac{dG_0}{dE'} t(E') = \frac{dt}{dE'} . \tag{9}$$

Next we substitute Eq. (9) in Eq. (6) and perform cyclic permutations of indices and operators to show that

$$G_0 T_n G_0 = -\sum_{\vec{R}_1} \sum_{\vec{R}_2 \neq \vec{R}_1} \cdots \sum_{\substack{\vec{R}_n \neq \vec{R}_{n-1} \\ \vec{R}_n \neq \vec{R}_1}} \mathrm{Tr} G_0 t_1 G_0 \cdots \frac{dG_0}{dE'} t_k \cdots G_0 t_n$$

$$-\sum_{\vec{R}_1} \sum_{\vec{R}_2 \neq \vec{R}_1} \cdots \sum_{\substack{\vec{R}_{n-1} \neq \vec{R}_{n-2} \\ \vec{R}_{n-1} \neq \vec{R}_1}} \mathrm{Tr} G_0 t_1 G_0 \cdots G_0 \frac{dt_k}{dE'} \cdots G_0 t_{n-1} , \tag{10}$$

k is any index in the appropriate range. Since there are n such equal expressions for the first term - 1 expressions for the second term, we can add and divide by the numbers of expressions to obtain

$$G_0 T_n G_0 = \mathrm{Tr} G_0 (T_n^{(1)} + T_n^{(2)}) G_0 , \tag{11}$$

$$\mathrm{r} G_0 T_n^{(1)} G_0 = -\frac{1}{n} \sum_{\vec{R}_1} \sum_{\vec{R}_2 \neq \vec{R}_1} \cdots \sum_{\substack{\vec{R}_n \neq \vec{R}_{n-1} \\ \vec{R}_n \neq \vec{R}_1}} \mathrm{Tr} \left(\frac{dG_0}{dE'} t_1 G_0 \cdots t_n + G_0 t_1 \frac{dG_0}{dE'} t_2 \cdots t_n + \cdots + G_0 t_1 \cdots \frac{dG_0}{dE'} t_n \right) \tag{12}$$

$$^{(2)} G_0 = -\frac{1}{n-1} \sum_{\vec{R}_1} \sum_{\vec{R}_2 \neq \vec{R}_1} \cdots \sum_{\substack{\vec{R}_{n-1} \neq \vec{R}_{n-2} \\ \vec{R}_{n-1} \neq \vec{R}_1}} \mathrm{Tr} \left(G_0 \frac{dt_1}{dE'} G_0 \cdots t_{n-1} + G_0 t_1 G_0 \frac{dt_2}{dE'} \cdots t_{n-1} + \cdots + G_0 t_1 \cdots G_0 \frac{dt_{n-1}}{dE'} \right) . \tag{13}$$

olds for all $n > 2$. The pairwise interaction
$n = 2$) is

$$_2 G_0$$

$$-\frac{1}{2} \sum_{\vec{R}_1} \sum_{\vec{R}_2 \neq \vec{R}_1} \mathrm{Tr} \left(\frac{dG_0}{dE'} t_1 G_0 t_2 + G_0 t_1 \frac{dG_0}{dE'} t_2 \right) .$$

an be combined with Eq. (13) for $n = 3$ to give

$$_2 + T_3^{(2)}) G_0$$

$$= -\frac{1}{2} \sum_{\vec{R}_1} \sum_{\vec{R}_2 \neq \vec{R}_1} \mathrm{Tr} \frac{d}{dE'} (G_0 t_1 G_0 t_2) .$$

This process can be continued for all higher-order terms, with the result

$$\sum_{n=2}^{\infty} \mathrm{Tr} G_0 T_n G_0 = \sum_{n=2}^{\infty} \mathrm{Tr} G_0 (T_n^{(1)} + T_{n+1}^{(2)}) G_0$$

$$= -\sum_{n=2}^{\infty} \frac{1}{n} \sum_{\vec{R}_1} \sum_{\vec{R}_2 \neq \vec{R}_1} \cdots \sum_{\substack{\vec{R}_n \neq \vec{R}_{n-1} \\ \vec{R}_n \neq \vec{R}_1}} \mathrm{Tr} \frac{d}{dE'} (G_0 t_1 G_0 t_2 \cdots G_0 t_n) . \tag{14}$$

From this point on the development is, for the most part, the same as Harrison's treatment. We will, therefore, give only an abbreviated sketch, concentrating on those points where differences do occur.

To calculate the trace in Eq. (14) we express all operators in terms of their plane-wave matrix elements. Thus

$$\mathrm{Tr}(G_0 t_1 G_0 t_2 \cdots G_0 t_n) = \sum_{\vec{k}_1} \sum_{\vec{k}_2} \cdots \sum_{\vec{k}_n} \frac{\langle \vec{k}_1 \mid t_1 \mid \vec{k}_2 \rangle \langle \vec{k}_2 \mid t_2 \mid \vec{k}_3 \rangle \cdots \langle \vec{k}_n \mid t_n \mid \vec{k}_1 \rangle}{(E^+ - k_1^2)(E^+ - k_2^2) \cdots (E^+ - k_n^2)} , \tag{15}$$

where $E^+ = E' + i\delta$ and $\langle \vec{x} \mid \vec{k} \rangle = \Omega^{-1/2} e^{i\vec{k}\cdot\vec{x}}$ with Ω being the volume of the crystal. Since t_j is the t operator for an ion at $\vec{R}_j$ we have

$$\langle \vec{k}_j \mid t_j \mid \vec{k}_{j+1} \rangle = e^{i(\vec{k}_{j+1} - \vec{k}_j)\cdot\vec{R}_j} \langle \vec{k}_j \mid t_0 \mid \vec{k}_{j+1} \rangle$$
$$= -(4\pi/\Omega) e^{i(\vec{k}_{j+1} - \vec{k}_j)\cdot\vec{R}_j} f(E', \vec{k}_j, \vec{k}_{j+1}) , \tag{16}$$

where t_0 is the t operator for an ion at the origin and f, which is defined by Eq. (16), is a function that reduces to the scattering amplitude on the energy shell (i.e., when $k_j^2 = k_{j+1}^2 = E'$). If we substitute Eq. (16) in Eq. (15) and convert the sums to integrals, we obtain

$$\mathrm{Tr}(G_0 t_1 G_0 t_2 \cdots G_0 t_n)$$
$$= \left(-\frac{1}{2\pi^2}\right)^n \int d^3k_1 \cdots \int d^3k_n \frac{\exp[i(\vec{k}_1 \cdot \vec{R}_{n1} + \vec{k}_2 \cdot \vec{R}_{12} + \cdots + \vec{k}_n \cdot \vec{R}_{n-1,n})] f(E', \vec{k}_1, \vec{k}_2) \cdots f(E', \vec{k}_n, \vec{k}_1)}{(E^+ - k_1^2)(E^+ - k_2^2) \cdots (E^+ - k_n^2)} ,$$

where $\vec{R}_{j-1,j} = \vec{R}_{j-1} - \vec{R}_j$. In the asymptotic approximation, which amounts to evaluating each integral to the lowest order in $1/kR$, the partial-integration method described by Harrison gives

$$\mathrm{Tr} G_0 t_1 G_0 t_2 \cdots G_0 t_n = e^{iK's} \prod_{j=1}^{n} \frac{f(E', \theta_j)}{l_j} , \tag{17}$$

where $l_j = |\vec{R}_{j-1,j}|$, s is the sum of all l_j, θ_j is the scattering angle at the jth site, and $K'^2 = E'$. The function $f(E', \theta_j)$ is now evaluated on the energy shell and is, therefore, the scattering amplitude at energy E' and angle θ_j.

From Eqs. (5), (14), and (17) we find, for the n-ion contribution to v

$$v_n = -\frac{2}{\pi} \sum_{\substack{\text{paths and} \\ \text{directions}}} \mathrm{Im} \int_0^{E_F} e^{iKs} \prod_{j=1}^{n} \frac{f(E, \theta_j)}{l_j} \, dE . \tag{18}$$

In arriving at this expression, we have made use of Harrison's observation that in summing over all ion positions in an n-ion array, each diagram connecting the n ions occurs n times. The sum over paths and directions means that in an nth order sum one should include all n-vertex diagrams for which successive scatterers are on different sites, and, for $n > 2$, that the sum is to include both directions, clockwise and counterclockwise, in which the path can be traversed.

The only difference between this result and that obtained by Lloyd and Oglesby is that their sum includes only ring diagrams, i.e., diagrams in which all ions are distinct. For $n \geq 4$, however, it is possible to draw proper n-vertex diagrams (those for which successive scatterers are on different sites) that involve fewer than n ions, and for which all ions are therefore not distinct. The simplest example of this is the fourth-order diagram involving only two ions. In this case there are four scattering paths corresponding to propagation back and forth along the line joining the pair. Such a term is, of course, of fourth order and therefore asymptotically negligible compared to the second-order two-vertex diagram for same pair. It should not be dropped, however, in a calculation carried to fourth or higher order.

III. APPLICATION TO TRANSITION METALS

For nontransition metals, where the scattering amplitude is a slowly varying function of energy, one can integrate Eq. (18) by parts and, in the asymptotic approximation, drop the remaining integral which is of order $(1/k_F s)^2$ where k_F is the Fermi wave number. The result is[4,5]

$$v_n^{nr} = \frac{4k_F}{\pi} \sum_{\substack{\text{paths and} \\ \text{directions}}} \mathrm{Re} \frac{e^{ik_F s}}{s} \prod_{j=1}^{n} \frac{f^{nr}(E_F, \theta_j)}{l_j} , \tag{19}$$

where we have added the superscripts nr to indicate that Eq. (19) is valid for nonresonant scattering only. The reason one cannot use this result for resonant scatterers is that the term that was dropped to obtain Eq. (19) is an integral over the energy derivative of the scattering amplitude, a function with strong peaks near the resonance energy. Thus, for transition metals one must find another way of handling the integral in Eq. (18).

For our model of transition-metal scattering we assume a scattering amplitude consisting of resonant and nonresonant parts[6]

$$f(E, \theta) = f^{nr}(E, \theta) + f^{r}(E, \theta) ,$$

where the resonant part is of the Breit-Wigner form

$$f^r(E,\theta) \approx -\frac{2l+1}{K}\, e^{2i\delta_b}\, \frac{\Delta}{E-E_r+i\Delta}\, P_l(\cos\theta)\ . \tag{20}$$

Here δ_b is the so-called background phase shift,[9] and E_r and Δ are the energy and half-width of th resonance, respectively. The product of scattering amplitudes appearing in Eq. (18) is therefore

$$\prod_{j=1}^{n} f(E,\theta_j)$$

$$= f^{nr}(\theta_1) f^{nr}(\theta_2)\cdots f^{nr}(\theta_n) + f^r(\theta_1) f^{nr}(\theta_2)\cdots f^{nr}(\theta_n)$$

$$+\cdots + f^r(\theta_1) f^r(\theta_2)\cdots f^r(\theta_n)\ , \tag{21}$$

where the E dependence of all factors on the right-hand side is understood. The first term in this expansion contains nonresonant factors and can therefore be handled by the partial integration method described above. The last term, which corresponds to pure resonance scattering at each site, and the other terms, which correspond hybrid scattering, lead to integrals of the general form

$$U_{nm} = -\frac{2}{\pi}\,\mathrm{Im}\int_0^{E_F} e^{iKs} \times \frac{f^r(\theta_1) f^r(\theta_2)\cdots f^r(\theta_m) f^{nr}(\theta_{m+1})\cdots f^{nr}(\theta_n)}{l_1 l_2 \cdots l_n}\, dE. \tag{22}$$

We now assume that the resonance energy lies well above the bottom of the conduction band ($E_r \gg 0$), that the resonance region is narrow ($\Delta/E_r \ll 1$), and, as before, that the nonresonant factors are slowly varying functions of energy. This allows us to approximate the $f^{nr}(\theta)$ by their values at the resonance energy and replace the wave number in the exponential by the approximation

$$K \approx k_r\left(1+\frac{E-E_r}{2E_r}\right)\ .$$

Equation (20) then becomes

$$U_{nm} = -\frac{2}{\pi}\,(-1)^m \left(\frac{2l+1}{k_r}\right)^m \frac{\prod_{j=1}^{m} P_l(\cos\theta_j)}{\prod_{j=1}^{n} l_j} \times \mathrm{Im}\, f^{nr}(\theta_{m+1})\cdots f^{nr}(\theta_n)\, e^{i(k_r s + 2m\delta_b)}\, X_m(s)\ , \tag{23}$$

where

$$X_m(s) = \int_0^{E_F}\left(\frac{\Delta}{E-E_r+i\Delta}\right)^m e^{ik_r s(E-E_r)/2E_r}\, dE$$

$$= \Delta\, e^{\gamma s}\left[\left(\frac{\Delta}{-E_r+i\Delta}\right)^{m-1} E_m(z_1 s) - \left(\frac{\Delta}{E_F-E_r+i\Delta}\right)^{m-1} E_m(z_2 s)\right]\ . \tag{24}$$

Here $E_m(z)$ is the exponential integral,[10] $\gamma \approx \Delta/2k_r$, $z_1 = (\Delta + iE_r)/2k_r$, and $z_2 = [\Delta - i(E_F - E_r)]/2k_r$.

Explicit expressions for the two- and three-ion potentials are easily obtained by noting the combinations of factors involved in Eq. (21), relabeling indices as needed in Eq. (22), applying Eq. (23), and then adding the nonresonant part. The resulting potential for a single pair (with $l=2$) is

$$v_2(R) = \frac{2k_F}{\pi}\,\mathrm{Re}\,\frac{e^{i2k_F R}}{R^3}\,[f^{nr}(E_F,\pi)]^2 + \frac{10}{\pi k_r R^2}\,\mathrm{Im}\left(2e^{i(k_r R+2\delta_b)} f^{nr}(E_r,\pi) X_1(s) - \frac{5}{k_r}\, e^{i(2k_r R+4\delta_b)} X_2(s)\right), \tag{25}$$

where R is the interionic distance. For a single three-ion path, the potential, summed over both directions, is

$$v_3(\vec{R}_1,\vec{R}_2,\vec{R}_3) = \frac{8k_F}{\pi}\,\mathrm{Re}\,\frac{e^{ik_F s}}{s}\prod_{j=1}^{3}\frac{f(E_F,\theta_j)}{l_j} + \frac{10}{\pi k_r l_1 l_2 l_3}\,\mathrm{Im}\, e^{ik_r s}\left(2e^{2i\delta_b} X_1(s) F_1(\theta_1,\theta_2,\theta_3) - \frac{10}{k_r}\, e^{4i\delta_b} X_2(s) \times F_2(\theta_1,\theta_2,\theta_3) + \frac{50}{k_r^2}\, e^{6i\delta_b} X_3(s) F_3(\theta_1,\theta_2,\theta_3)\right), \tag{26}$$

where

$$F_1(\theta_1,\theta_2,\theta_3) = P_2(\cos\theta_1) f^{nr}(\theta_2) f^{nr}(\theta_3) + \text{c.p.}\ ,$$

$$F_2(\theta_1,\theta_2,\theta_3) = P_2(\cos\theta_1) P_2(\cos\theta_2) f^{nr}(\theta_3) + \text{c.p.}\ ,$$

$$F_3(\theta_1,\theta_2,\theta_3) = \prod_{j=1}^{3} P_2(\cos\theta_j)\ .$$

Here the l_j are interionic distances and the θ_j are scattering angles for the three-ion diagram, and c.p. stands for cyclic permutations of the angles θ_1, θ_2, θ_3. The total energies, corresponding to v_2 and v_3 of Eq. (18), are obtained by summing Eqs. (25) and (26) over all two- and three-ion paths.

Some simplification of these results should be possible if s, the round-trip path length, is large enough, for then one could retain only the leading term in the asymptotic expansions of the exponential integrals, $E_m(z_i s)$. However, in a related study involving the calculation of charge density oscillations around resonant scattering impurities, Mezei and Grüner[6] found that the use of a similar approximation can lead to serious errors in both the amplitude and phase of the oscillations at distances less than a few interatomic spacings. It is not difficult to see that such errors might result for interionic potentials as well. This is because in a transition metal the energy difference $E_F - E_r$

is of order Δ, making the absolute value of the argument of the second exponential integral in Eq. (24) roughly $(\Delta/E_r)k_r s$. Since $\Delta/E_r \ll 1$ this is likely to be a rather small number, at least for interactions involving the first few nearest-neighbor shells. Thus, for the computations described below, we used Eqs. (24)–(26) without further approximation.

IV. THIRD-ORDER CORRECTIONS IN TRANSITION METALS

In Sec. II we found that the configuration-dependent part of the band-structure energy is, from Eqs. (5) and (14),

$$U = -\frac{2}{\pi}\sum_{n=2}^{\infty}\frac{1}{n}\sum_{\vec{R}_1}\sum_{\vec{R}_2\neq\vec{R}_1}\cdots \times \sum_{\substack{\vec{R}_n\neq\vec{R}_{n-1}\\ \vec{R}_n\neq\vec{R}_1}} \mathrm{Im}\int_0^{E_F}\mathrm{Tr}(G_0 t_1 G_0 t_2\cdots G_0 t_n)\,dE\ . \tag{27}$$

By simply rearranging the order of summation we can rewrite this expression in the form of a sum over effective pairwise potentials. Thus

$$U = \frac{1}{2}\sum_{\vec{R}_1}\sum_{\vec{R}_2\neq\vec{R}_1} u(\vec{R}_1,\vec{R}_2)\ , \tag{28}$$

where

$$u(\vec{R}_1,\vec{R}_2) = -\frac{2}{\pi}\,\mathrm{Im}\int_0^{E_F}\mathrm{Tr}(G_0 t_1 G_0 t_2')\,dE\ , \tag{29}$$

with

$$t_2' = t_2 + t_2\sum_{n=3}^{\infty}\frac{2}{n}\sum_{\vec{R}_1\neq\vec{R}_2}\cdots\sum_{\substack{\vec{R}_n\neq\vec{R}_{n-1}\\ \vec{R}_n\neq\vec{R}_1}} G_0 t_3 G_0 t_4\cdots G_0 t_n\ . \tag{30}$$

Except in the lowest order approximation, $t_2'\approx t_2$, $u(\vec{R}_1,\vec{R}_2)$ is, of course, not a true pairwise potential in the usual sense, because it includes interactions with all other ions in the crystal. On the other hand, the effective potential formalism is useful for our present purpose because it shows how one should add multi-ion corrections to the isolated-pair approximation to obtain the correct result for the band-structure energy written as a sum of pairwise interactions. Thus, for example, we find that in the asymptotic approximation to third order

$$u(\vec{R}_1,\vec{R}_2) = u_2(|\vec{R}_2-\vec{R}_1|) + \frac{1}{3}\sum_{\substack{\vec{R}_3\neq\vec{R}_2\\ \vec{R}_3\neq\vec{R}_1}} u_3(\vec{R}_1,\vec{R}_2,\vec{R}_3)\ , \tag{31}$$

where u_2 and u_3 are given by Eqs. (25) and (26). We note once again that the correction term is dependent on the positions of ions 1 and 2 with respect to the other ions and is not, therefore, a simple function of separation distance.

For our initial numerical investigation of the role of multi-ion interactions in transition metals we applied Eq. (31) to the calculation of nearest-neighbor interactions in a face-centered-cubic crystal. The nearest-neighbor distance was taken to be 5 a.u., the resonance parameters were those used by Pettifor,[11] namely, $E_r = 0.5$ Ry and $\Delta = 0.03$ Ry, and pure s-wave scattering with a phase shift of 0.1 rad was assumed for the nonresonant part. To simulate, in a rough way, the behavior of the effective potential in a transition-metal series, we allowed the Fermi energy to vary from 0.4 to 0.6 Ry. The sum over neighboring ions included only the nearest neighbors of ions 1 and 2. While this cluster is too small for accurate quantitative predictions, density-of-states calculations by a similar cluster method[12,13] indicate that the nearest-neighbor model is adequate for qualitative studies of the effects of the splitting of the d resonance into subbands. Thus, our calculations should provide a reliable indication of at least one aspect of the effects of multi-ion interactions, i.e., the role of d-band splitting in the effective interionic interaction.

The results are plotted in Fig. 1 as a function of the position of the Fermi level with respect to the resonance energy. The main features in the isolated-pair potential, shown as a dashed curve in this figure, are the strong attractive peak that occurs as the Fermi level passes through the reso-

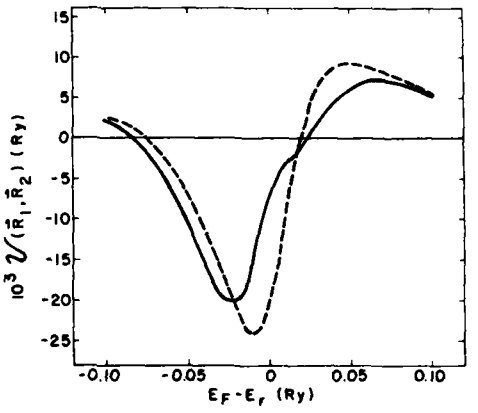

FIG. 1. Band-structure contributions to the interionic potential for nearest neighbors in a hypothetical face-centered-cubic transition-metal series. The dashed curve is the potential for an isolated pair, plotted as a function of the position of the Fermi level with respect to the resonance energy, while the solid curve was obtained by adding three-ion scattering corrections as described in the text. These results indicate that multi-ion interactions play an essential role in determining the effects of d-band splitting on interionic interactions in transition-metal crystals.

nance and the weaker repulsive peak at higher energies. However, the solid curve, which was obtained by adding third-order corrections, shows that the isolated-pair behavior is significantly altered by multi-ion interactions in a solid. It would appear from these results that multi-ion scattering tends to shift the attractive peak to a lower energy while introducing a new repulsive component at an energy slightly above resonance. This behavior corresponds, at least in a qualitative way, to the development of an additional peak in a cluster calculation of the d-band density of states.[12,13] According to the localized orbital model,[14] these peaks can be associated with bonding states at lower energies and antibonding states at higher energies. The predicted nature of the peak structure of the effective interionic potential, i.e., attractive at lower energies and repulsive at higher energies, is, of course, in agreement with the bonding-antibonding orbital picture.

While these results are encouraging, because they show that a relatively simple third-order correction gives an interionic potential in qualitative accord with what is known about the electronic structure of transition metals, it must be remembered that a number of approximations are involved. The very fact that third-order terms are important, for example, makes one wonder about the effects of fourth- and higher-order terms. The truncation of the cluster expansion at nearest-neighbor shells is also a matter of concern, particularly since such small cluster approximations are known to lead to poor results for the free-electron and hybridization contributions to the density of states.[13]

There are, in addition, some unanswered questions at a more fundamental level. The validity of the independent-electron self-consistent-potential model, which is implicit throughout the development, is itself subject to some criticism in the present context. For example, it is not clear that one can in fact find an approximate energy-independent exchange potential [such as is required by Eq. (8)] that will lead to an adequate description of nearest-neighbor interactions near the noble metal end of a transition-metal series.[11] [In a multi-ion treatment of the effective pairwise potential, nearest-neighbor interactions are involved, even in an asymptotic theory; see, for example, Eq. (31).] Furthermore, even if we ignore this matter by assuming that a suitable exchange approximation can be found, there remains the problem of removing half the electron-electron interaction energy, which is always counted twice in a calculation of the total energy in the independent-electron approximation. While it is rather easy to subtract this extra energy in a second-order pseudopotential treatment,[1] we know of no practical way to proceed within the framework of the t-matrix formalism. Thus, when treating transition metals, where resonance scattering demands a t-matrix (or equivalent) description of scattering by individual ions, it is common practice to simply ignore the double-counting of electron-electron energies,[2,5] as we did here. In the final analysis, what all of this really means is that in order to develop a tractable model, we have assumed that the approximations discussed above are of secondary importance, and that the major features of multi-ion interactions in transition metals are adequately accounted for by a simple multiple scattering calculation for a small cluster of ions.

There is, therefore, ample reason to question the quantitative accuracy of such features as the positions, heights and widths of the peaks shown in Fig. 1. On the other hand, the results of other calculations and comparisons with experiment[11–13] indicate that our calculational model should provide a reasonable description of resonant scattering effects, and that one should expect the main result, the existence of attractive and repulsive structures in the effective interionic potential, to persist in more accurate calculations.

ACKNOWLEDGMENTS

The author wishes to thank C. G. Gardner for several helpful discussions. This work was performed under contract with the U. S. Army Research Office.

[1] W. A. Harrison, *Pseudopotentials in the Theory of Metals* (Benjamin, New York, 1966).
[2] V. Heine and D. Weaire, Solid State Phys. 24, 249 (1970).
[3] P. W. Anderson and W. L. Macmillan, in *Proceedings of the International School of Physics, Enrico Fermi*, edited by W. Marshall (Academic, New York, 1967).
[4] W. A. Harrison, Phys. Rev. B 7, 2408 (1973).
[5] P. Lloyd and J. Oglesby, J. Phys. F 3, 1683 (1973).
[6] F. Mezei and G. Grüner, Phys. Rev. Lett. 29, 1465 (1972).
[7] S. F. Edwards, Philos. Mag. 6, 617 (1961).
[8] E. Merzbacher, *Quantum Mechanics* (Wiley, New York, 1970).
[9] J. R. Taylor, *Scattering Theory* (Wiley, New York, 1972).
[10] M. Abramowitz and I. A. Stegun, *Handbook of Mathematical Functions* (U. S. GPO, Washington, D.C., 1964).
[11] D. G. Pettifor, J. Phys. C 3, 367 (1970).
[12] J. Keller and R. Jones, J. Phys. F 1, L33 (1971).
[13] D. House and P. V. Smith, J. Phys. F 3, 753 (1973).
[14] J. Friedel, in *The Physics of Metals*, edited by J. M. Ziman (Cambridge U. P., Cambridge, England, 1969).

APPENDIX C

Role of Multi-Ion Interactions in the Stacking-Fault Energies of Transition Metals

PHYSICAL REVIEW B VOLUME 13, NUMBER 12 15 JUNE 1976

Role of multi-ion interactions in the stacking-fault energies of transition metals

R. E. Beissner
Southwest Research Institute, San Antonio, Texas 78284
(Received 2 March 1976)

The theory of multi-ion interactions is applied to calculations of the stacking-fault energies of transition metals. It is found that observed trends in the stabilities of close-packed transition metals can be explained on the basis of a simple model in which resonant scattering, three-ion interactions dominate.

I. INTRODUCTION

The results of recent calculations of stacking-fault energies and comparisons with experimental data indicate that a pseudopotential expansion carried to second order in the energy is adequate for the treatment of nontransition metals.[1,2] As Heine and Weaire[3] had noted earlier, it was to be expected that a second-order theory would be successful in this particular application because the pseudopotential matrix elements involved in the perturbation expansion are small.

For transition metals, on the other hand, it is unlikely that such a simple theory will suffice because the resonant scattering of d electrons by transition-metal ions leads to large matrix elements and, hence, to slower convergence of the perturbation expansion. Indeed, even for the noble metals, where one might hope that the effects of resonant scattering are not too pronounced, calculated stacking-fault energies based on a second-order approximation are in poor agreement with experimental results.[1,2] It seems clear, therefore, that a successful theory of stacking-fault energies in transition metals, and perhaps the noble metals as well, must include the effects of higher-order terms in the perturbation expansion.[4] The purpose of the work reported here was to see if an extension to third order will adequately account for observed trends in the stacking-fault energies and relative stabilities of close-packed transition metals.

In analogy with Harrison's formulation of the second-order theory[5] of stacking-fault energies, one might attempt a third-order calculation by making use of the formal expression[6] for the third-order energy in terms of the plane-wave matrix elements of the pseudopotential and the structure factors for the perfect and faulted crystal. It is well known, however, that calculations of third-order energies by this method are extremely complex, even for perfect nontransition-metal crystals.[7,8] Since the prospect of extending such a calculation to stacking faults with the additional complication of resonant scattering is indeed formidable, for the investigation reported here we choose an alternative, approximate approach based on the theory of multi-ion interactions.[9,10]

In short, our approach is based on Harrison's observation that the third-order term in the perturbation expansion of the total energy can be written as a sum of three-ion interaction energies.[9] The third-order term in the expression for the stacking-fault energy is therefore the difference between the three-ion sum for the faulted crystal and the corresponding sum for the perfect crystal. By truncating these sums, i.e., by keeping only those three-ion interactions judged to be dominant in the determination of the stacking-fault energy, we obtain an approximation to the third-order energy.

In the text of this paper we will first describe in more detail the method for calculating the third-order energy. An approximate method for estimating the second-order energy will then be derived, followed by a discussion of the electron-ion scattering model used in numerical computations. The results of our study, which are presented in the concluding section, show that for most transition metals it is the three-ion terms, not pairwise interactions, that comprise the dominant contribution to the stacking-fault energy. Although quantitative agreement with experimental data on stacking-fault energies is only fair, the calculations do adequately explain observed trends in the relative stabilities of close-packed structures for the first three transition-metal series.

II. CALCULATION OF THE THREE ION ENERGY

Our starting point is the following general expression for the three-ion contribution to the stacking-fault energy:

$$\gamma_3=\frac{1}{2A}\sum_i\sum_{j\neq i}\sum_{\substack{k\neq i\\ k\neq j}}\left[v_3(\vec{R}_i^F,\vec{R}_j^F,\vec{R}_k^F)-v_3(\vec{R}_i^P,\vec{R}_j^P,\vec{R}_k^P)\right], \tag{1}$$

where $\vec{R}_i^F$ and $\vec{R}_i^P$ are ion positions in the faulted (F) and perfect (P) crystals, A is the fault area, and v_3 is the three-ion interaction energy defined in Ref. 10. Since v_3 already includes a sum over

cyclic permutations of ion positions (i.e., a sum of identical three-ion diagrams) only distinct diagrams are to be included in the sums on i, j, and k. Also, terms in which all three ion positions lie on the same side of the fault plane do not contribute because in such cases the three-ion energies are the same in the faulted and perfect crystals. Thus the only diagrams that need be considered are those distinct diagrams where two of the position vectors terminate on opposite sides of the fault plane. We therefore choose $\vec{R}_i$ to be the position of an ion on one side of the fault plane and $\vec{R}_k$ a position on the opposite side, with $\vec{R}_j$ on either side.

Figure 1 is an example of a pair of three ion configurations that give a nonvanishing contribution in the calculation of the intrinsic fault energy in an fcc crystal. Here $\vec{R}_i$ and $\vec{R}_j$ are the same in the perfect and faulted structures while $\vec{R}_k$ terminates at the positions indicated by $\vec{R}_k^P$ and $\vec{R}_k^F$ in the perfect and faulted crystals, respectively.

For this particular geometrical arrangement, it is easily seen that for each ion position $\vec{R}_j$ below the fault plane there are three equivalent diagrams corresponding to the three nearest-neighbor positions of $\vec{R}_i$. Also, there are three more equivalent diagrams in the mirror-image configuration in which $\vec{R}_k$ and $\vec{R}_j$ terminate above the plane while $\vec{R}_i$ lies below. Thus, assuming that the energy difference in Eq. (1) is the same for all $\vec{R}_j$ below the fault plane, we obtain, for that part of the stacking fault energy due to the interactions illustrated in Fig. 1,

$$\Delta\gamma_3 = (1/2\omega)(6\upsilon_3^{ABA} - 6\upsilon_3^{ABC}) ,$$

where ω is the area per ion and υ^{ABA} and υ^{ABC} are the energies corresponding to the particular diagrams considered here. Similar arguments can,

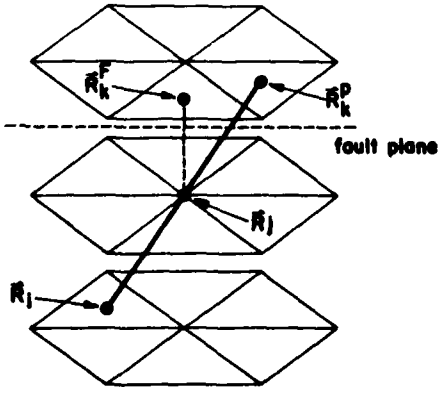

FIG. 1. Typical pair of three-ion interactions that contribute to the intrinsic stacking-fault energy for face-centered-cubic crystals. Here $\vec{R}_k^P$ and $\vec{R}_k^F$ are ion positions in the perfect (P) and faulted (F) crystals, while $\vec{R}_i$ and $\vec{R}_j$ are the same in both cases.

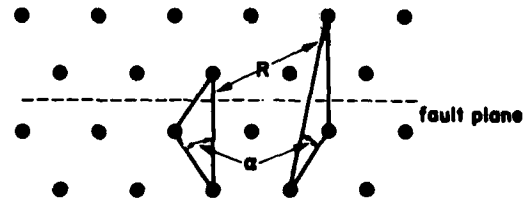

FIG. 2. Schematic illustration of three-ion interactions. Terms included in the truncated stacking-fault energy sum were those for which either $\alpha \leq 30°$ or $R \leq 20$ a.u.

of course, be applied to other three-ion configurations thus leading to the formula

$$\gamma_3 = \frac{1}{2\omega}\left(\sum_i N_i^F \upsilon_3^F(i) - \sum_i N_i^P \upsilon_3^P(i)\right) , \qquad (2)$$

where N_i^F is the number of equivalent diagrams of the ith geometry in the faulted crystal. $\upsilon_3^F(i)$ is the corresponding energy, the N_i^P and $\upsilon_3^P(i)$ are the diagram weights and energies for the perfect fcc structure, and the sum is over all nonequivalent three-ion diagrams.

In the applications discussed in Sec. V, the only diagrams considered were those for which at least two of the three ions were nearest neighbors and for which the third ion was in either the adjacent or next-nearest plane, as illustrated in Fig. 2. In addition, the sums over diagrams were limited to terms for which either $\alpha \leq 30°$ or $R \leq 20$ a.u. (see Fig. 2). While the truncation of the sums at these particular values of α and R is somewhat arbitrary, it can be seen from the expression for υ_3 given in Ref. 10 that the three-ion energy is inversely proportional to the product of the three interior path lengths times the roundtrip distance, thus causing υ_3 to fall off rather rapidly with increasing R. Also, because the resonant scattering terms in υ_3 contain products of the Legendre polynomials $P_2(\cos\Theta_i)$, where Θ_i is the scattering angle at the ith ion site, the energy tends to be larger for diagrams with $\alpha \approx 0$ than for diagrams with larger α. Actual computations of υ_3 confirmed these expected trends, in that they showed that energies corresponding to the larger values of α and R are small, usually about 10% of the dominant terms. Still, it should be noted that in some cases the larger terms tend to cancel and, when this happens, the truncation error can be significant. We will return to this point when discussing the results of our computations in Sec. V.

III. CALCULATION OF THE PAIRWISE INTERACTION ENERGY

To calculate that part of the stacking fault energy due to pairwise interactions we used the for-

malism of Blandin *et al.*[11] They showed that the pairwise contribution to γ can be written

$$\gamma_2 = \sum_{n=2}^{\infty} N(n)\Delta\phi(nh) ,$$

where h is the distance between close-packed planes, $N(n)$ is an integral weight corresponding to a particular fault configuration, and $\Delta\phi(nh)$ is an interplanar potential difference.[1,3] Blandin *et al.*, also showed that the potential difference is related to the energy-wave number characteristic $\Phi(q)$ as follows:

$$\Delta\phi(nh) \approx \frac{9h}{\pi\omega}\int_{-\infty}^{\infty} \Phi[(q_z^2+g^2)^{1/2}]\, e^{iq_z nh}\, dq_z , \qquad (3)$$

where g is the magnitude of the smallest nonvanishing reciprocal-lattice vector.

From the Fourier transform relationship[3] between $\Phi(q)$ and the pairwise interaction energy v_2, we find, using the asymptotic approximation,[10]

$$v_2(R) \sim -\frac{2}{\pi}\int_0^{E_F} \mathrm{Im}\, e^{2i\kappa R}\frac{f^2(E,\pi)}{R^2}\, dE$$

that for $q > 2\kappa_F$, where κ_F is the Fermi wave number,

$$\Phi(q) \approx -\frac{4}{q\Omega_0}\int_0^{E_F} |f(E,\pi)|^2 \left(\tfrac{1}{2}\cos 2\eta \ln\left|\frac{q+2\kappa}{q-2\kappa}\right| + \frac{\pi}{2}\sin 2\eta\right) dE \qquad (4)$$

where Ω_0 is the volume per ion, $f(E,\pi)$ is the scattering amplitude at energy E and scattering angle π, and $\kappa = \sqrt{E}$. The angle η is defined in terms of the scattering phase shifts δ_l by $\tan\eta = \alpha/\beta$, where

$$\alpha = \sum_l (-1)^l (2l+1)\cos\delta_l \sin\delta_l ,$$

$$\beta = \sum_l (-1)^l (2l+1)\sin^2\delta_l .$$

The condition $q > 2\kappa_F$ is satisfied here because, from Eq. (3), $q \geq g$ and $g > 2\kappa_F$ for all transition metals. Substitution of Eq. (4) in Eq. (3) gives, to first order in $1/nh$ and neglecting terms of order $\exp(-gnh)$

$$\Delta\phi(nh) \approx \frac{18}{nh\omega^2}\int_0^{E_F} |f(E,\pi)|^2 \cos 2\eta \frac{e^{-2\lambda_g nh}}{\sqrt{E}}\, dE ,$$

where

$$\lambda_g = [(\tfrac{1}{2}g)^2 - E]^{1/2} .$$

In applying this result in the computations described below the final integration was numerically evaluated, and only the term corresponding to next-nearest-neighbor plane interactions ($n = 2$) was retained in the stacking fault energy sum.

IV. CALCULATION OF PHASE SHIFTS

Our choice of a model for the calculation of scattering phase shifts for transition metal ions is based largely on the work of Pettifor.[12] He showed that one can reproduce, with reasonable accuracy, the results of more detailed calculations of the densities of states of transition metals, by basing a simpler calculation on the assumption that the d-electron resonance energy E_r and width Δ are constants for the first three transition-metal series. In the calculation reported here we made the additional approximations that the nonresonant scattering phase shifts can be derived from a pseudopotential which, again, is the same for all elements, and that the nearest-neighbor distance is the same (5.0 a.u.) for all elements. This leaves us with a rather simple calculational model in which the only parameter that distinguishes one element from the next is the Fermi energy. However, except for the approximation concerning phase shifts for nonresonant scattering, this is the same model used by Pettifor in his calculations of the relative energies of the hcp, fcc, and bcc structures. The fact that Pettifor's results are in accord with the observed structures of transition metals suggests that the model, through obviously an idealization, forms a reasonable basis for the study of stacking fault energies as well.

For the resonance parameters we used Moriarty's values for copper[13] ($E_r = 0.33$ Ry and $\Delta = 0.014$ Ry). Fermi energies as a function of valence Z were determined by adding an average of Pettifor's calculated values of $E_F - E_r$ for the fcc and hcp structures to the value chosen for E_r. The value of the resonant part of the d electron phase shift was determined from the formula

$$\tan(\delta_2 - \delta_b) = \Delta/(E_r - E) ,$$

where δ_2 and δ_b are the resonant and nonresonant parts of the $l = 2$ phase shift.

To calculate the nonresonant scattering phase shifts we used the empty core potential, the core radius being that given by Ashcroft and Langreth[14] for copper. The phase shifts were calculated in the first Born approximation and were based on the uniform screening charge assumption.[15] Because there is considerable uncertainty as to the validity of such a simple model, we performed two sets of calculations using effective valences (Z_s) of one and two in the nonresonant scattering pseudopotential.

V. RESULTS AND DISCUSSION

The results of our calculations are shown in Fig. 3. These plots show the stacking fault energy for intrinsic faults in fcc crystals as a function of Z,

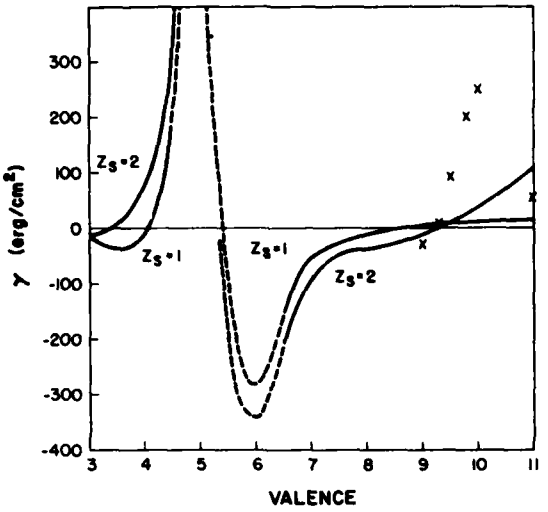

FIG. 3. Calculated intrinsic stacking-fault energies for face-centered-cubic crystals. The parameter Z_s is the valence assumed in the calculation of nonresonant scattering phase shifts. The dashed parts of the curves correspond to values of the total valence (including d electrons) where neither close-packed structure is stable. Experimental data, shown here by the symbol ×, are taken from Ref. 16 for copper ($Z = 11$) and nickel-cobalt alloys ($9 < Z < 10$), and from Ref. 17 for cobalt ($Z = 9$).

the total valence, for both values of Z_s. The dashed part of the curve corresponds to those values of Z where neither close-packed structure is stable and where, therefore, no comparisons with observed stable structures or stacking fault energies are possible. Also shown are experimental data for cobalt ($Z = 9$), nickel ($Z = 10$), copper ($Z = 11$), and cobalt-nickel alloys. The stacking fault energy for hcp cobalt is shown as a negative number because the theoretical expression for the energy of an intrinsic fault in an hcp crystal is approximately equal to minus the expression for the intrinsic fcc energy. As can be seen from the stacking sequences for the perfect and faulted crystals, this relationship is exact if one ignores all interactions involving third and more distant neighbors planes.

The first point to be noted here is that the two calculated curves are in reasonably good agreement for most values of Z. Since these two curves are based on nonresonant scattering phase shifts that differ by about a factor of 2, this must mean that the details of nonresonant scattering are relatively unimportant, and that the general trend of stacking fault energy versus valence is determined largely by resonant scattering properties. It should be noted, however, that the resonance width Δ, which we have taken from Moriarty's calculation, is related to nonresonant scattering properties through hybridization. One would therefore expect that a first-principles calculation would show a stronger dependence on nonresonant scattering properties than is indicated here.

Another point to be noted regarding Fig. 3 is that the stability of the fcc phase against faulting is correctly predicted for most values of Z. Thus, for $Z > 9$ we obtain positive values, which indicates stability against faulting in fcc crystals, while for $6 < Z < 9$ and $Z < 4$, where the stable close-packed structure is hcp, we obtain negative fault energies. The only notable exception is the $Z_s = 2$ curve at $Z = 4$ (titanium, zirconium, and hafnium), where the calculation indicates that the fcc structure is stable. This failure may well be due to the approximate treatment of nonresonant scattering, since the energy for $Z_s = 1$ has the correct sign. On the other hand, the fact that the absolute value stacking fault energy is much smaller at $Z = 4$ than at other values of Z indicates that there is considerable cancellation in the sum of two- and three-ion interaction energies, and that the truncation error mentioned above may therefore be significant. It should also be noted that a similar situation exists at $Z = 9$ (cobalt, rhodium, and iridium). Here, however, one of the elements (cobalt) is in fact stable in the hcp phase, while the other two form stable fcc crystals.

It is of interest to compare these results with Pettifor's calculations of the relative energies of close-packed phases.[12] As was noted previously, our assumptions of constant resonance parameters and nearest-neighbor distance are consistent with Pettifor's model although he used different numerical values for the resonance parameters. However, the principal difference between his model and ours lies in the treatment of nonresonant scattering. In spite of these differences our results for the relative stabilities of the fcc and hcp structures as a function of Z are in reasonably good agreement with Pettifor's. Thus he finds that there is a region of hcp stability near $Z = 4$ followed by an fcc stable region near $Z = 5$, an fcc to hcp transition near $Z = 7$ and finally, an hcp to fcc transition near $Z = 9$. We take this, and the fact that the results agree with observed trends in crystal structure, as indications that our simple scattering model is adequate as a first approximation, and that we have included the most significant terms in our approximate summation of the multi-ion expansion.

Regarding the calculated values of the stacking-fault energies, as can be seen in Fig. 3, agreement with experimental data is satisfactory for copper and cobalt, but poor for nickel and cobalt-nickel alloys. In view of the very simple model that was used in calculating electron-ion scattering

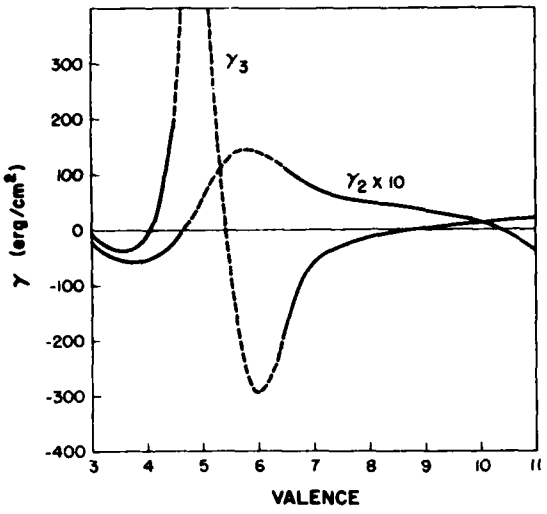

FIG. 4. Pairwise (γ_2) and three-ion (γ_3) contributions to the stacking fault energy for $Z_s = 1$. At almost all values of the valence the three-ion energy is much greater than the pairwise contribution, which is multiplied by 10 in this plot.

phase shifts, we do not consider these comparisons particularly significant, except, perhaps, as an indication that a more careful treatment is needed for quantitative comparisons with experiment.

Finally, in Fig. 4 we show the two- and three-ion contributions to the stacking fault energy for $Z_s = 1$ (the results for $Z_s = 2$ are similar). The important point to be noted here is that three-ion interactions dominate at almost all values of Z. Although one might expect, on the basis of our earlier calculation for the noble metals,[1] that a more-accurate nonasymptotic calculation would yield larger values for the pairwise contribution, we still believe that the dominance of three-ion terms exhibited here is at least qualitatively correct. One reason for this is that the pairwise energies are so small compared to three-ion energies that the errors introduced through the asymptotic approximation, being roughly of the same order of magnitude as the pairwise predictions themselves,[1] are expected to be insignificant compared to the three-ion energies.

Another reason is that from Pettifor's calculation, and from the observed stability of close-packed phases as a function of Z, one would expect three hcp-fcc transitions in a transition metal series. The three-ion energy does, in fact, show three such transitions while the pairwise energy has only two. Thus assuming only that the shapes of the two- and three-ion curves shown in Fig. 4 are correct, one would expect three-ion contributions to dominate.

In conclusion, therefore, we have demonstrated that observed trends in the stabilities of close-packed transition metals can be explained on the basis of a third-order calculation involving a simple resonant scattering model of electron-ion interactions. The calculations indicate that such trends are governed largely by three-ion interactions at most values of the valence. Comparisons with experimentally measured stacking-fault energies show, as expected, that a more careful treatment is needed for quantitative predictions of stacking-fault energies. Still, the degree of success realized in the prediction of structural trends and, at least, the correct sign and order of magnitude of stacking-fault energies, supports our principal conclusions regarding the dominant roles of resonant scattering and three-ion interactions.

ACKNOWLEDGMENT

This work was supported in part by the U. S. Army Research Office.

[1] R. E. Beissner, Phys. Rev. B 8, 5432 (1973).
[2] J. F. Devlin, J. Phys. F 4, 1865 (1974).
[3] V. Heine and D. Weaire, Solid State Phys. 24, 249 (1970).
[4] An alternative approach based on the tight-binding approximation but ignoring s-d hybridization is suggested by F. Ducastelle and F. Cyrot-Lackmann, J. Phys. Chem. Solids 32, 285 (1971). See also, T. C. Tisone, Acta Met. 21, 229 (1973).
[5] W. A. Harrison, *Pseudopotentials in the Theory of Metals* (Benjamin, New York, 1966).
[6] P. Lloyd and A. Sholl, J. Phys. C 1, 1620 (1968).
[7] E. G. Brovman, Yu. Kagan, and A. Holas, Zh. Eksp. Teor. Fiz 61, 737 (1971) [Sov. Phys.-JETP 34, 394 (1972)].
[8] C. M. Bertoni, V. Bortolani, C. Calandra, and F. Nizzoli, J. Phys. F 3, L244 (1973).
[9] W. A. Harris, Phys. Rev. B 7, 2408 (1973).
[10] R. E. Beissner, Phys. Rev. B 9, 5108 (1974).
[11] A. Blandin, J. Friedel, and G. Saada, J. Phys. C Suppl. 3, 128 (1966).
[12] D. G. Pettifor, J. Phys. C 3, 367 (1970).
[13] J. A. Moriarty, Phys. Rev. B 6, 1239 (1972).
[14] N. W. Ashcroft and D. C. Langreth, Phys. Rev. 159, 500 (1967).
[15] R. W. Shaw, Jr., Phys. Rev. B 5, 4742 (1972).
[16] P. C. J. Gallagher, Met. Trans. 1, 2429 (1970).
[17] T. Ericsson, Acta Metallogr. 14, 853 (1966).

APPENDIX D

Self-Consistency in the Third-Order Perturbation Theory of Simple Metals

SELF CONSISTENCY IN THE THIRD ORDER PERTURBATION THEORY OF SIMPLE METALS

R.E. BEISSNER
Southwest Research Institute, San Antonio, TX 78284, USA

Received 4 April 1978

It is pointed out that the Lloyd–Sholl expression for the total energy is self consistent through third order in the electron–ion pseudopotential.

Several years ago Lloyd and Sholl [1] and later Brovman et al. [2] independently developed an expression for the third order term in the expansion of the total energy of a metal. Although self-consistency of the electron–ion pseudopotential is not discussed in these works, proper consideration of nonlinear screening to second order in the pseudopotential, which is required in a self-consistent third order theory of the total energy, is implicit in the calculations. An explicit expression for the second order, self-consistent pseudopotential was presented later by Bertoni et al. [3], but they did not show how the second order screening term enters the total energy expression. The purpose of this letter is to clarify the role of nonlinear screening in the third order energy. We show that the third order terms associated with nonlinear screening cancel in the total energy calculation and that the Lloyd–Sholl result is therefore self-consistent to third order.

The total energy of a crystal can be written as the sum of a free electron energy, a direct interionic interaction energy, and the band structure energy, which is the structure dependent part of the electron–ion interaction energy. Because screening effects enter only in the band structure energy, we need not consider the other terms. According to Lloyd and Sholl the band structure energy per ion is

$$E_b = \frac{\Omega_0}{2}\sum_{p\neq 0}\frac{1-\epsilon(p)}{\Omega_0 V(p)}|W_p|^2 - \frac{\Omega_0}{2}\sum_{p\neq 0}\frac{|W_p^v|^2}{\Omega_0 V(p)} + \Omega_0\sum_{p_1}\sum_{p_2} g(p_1,p_2,p_3)W_{p_1}W_{p_2}W_{p_3} + \text{higher order terms}, \tag{1}$$

where W_p is the self-consistent pseudopotential, $\epsilon(p)$ is the dielectric function, and $\Omega_0 V(p)$ is the Coulomb interaction corrected for exchange and correlation energies. It is related to the corrected dielectric function $\epsilon(p)$ and the Hartree dielectric function $\epsilon_0(p)$, as follows:

$$\Omega_0 V(p) = \frac{8\pi}{p^2}\,\frac{1-\epsilon(p)}{1-\epsilon_0(p)}.$$

The potential W_p^v is that due to valence electrons and $g(p_1,p_2,p_3)$ is the function defined by Lloyd and Sholl, with $p_3 = -(p_1 + p_2)$. The second term in eq. (1) is the correction for double counting of electron–electron interactions in a self-consistent field treatment.

In the linear screening approximation the self-consistent pseudopotential is given by

$$W_p \sim W_p^{(1)} = W_p^{\text{ion}}/\epsilon(p),$$

where W_p^{ion} is the ionic pseudopotential. To account for higher order, nonlinear screening, we take

$$W_p = W_p^{(1)} + \Delta W_p, \tag{2}$$

where ΔW_p is a correction for second and higher order terms in the screening charge density expansion. The valence electron potential is therefore

$$W_p^v = W_p^{(1)} - W_p^{ion} + \Delta W_p = \frac{1-\epsilon(p)}{\epsilon(p)} W_p^{ion} + \Delta W_p . \quad (3)$$

If we substitute eqs. (2) and (3) in the first two terms in eq. (1) we find that the terms linear in ΔW_p cancel exactly. This leaves only a term in $|\Delta W_p|^2$, which is of fourth order, plus higher order corrections from the other terms in eq. (1). Therefore, to third order in $W_p^{(1)}$, we have

$$E_b = \frac{\Omega_0}{2} \sum_{p \neq 0} \frac{1-\epsilon(p)}{\Omega_0 V(p)} \epsilon(p) |W_p^{(1)}|^2 + \Omega_0 \sum_{p_1} \sum_{p_2} g(p_1, p_2, p_3) W_{p_1}^{(1)} W_{p_2}^{(1)} W_{p_3}^{(1)} .$$

This is exactly the Lloyd–Sholl result, and is exactly the same as the third order energy based on a linear screening approximation of the self-consistent pseudopotential. Our calculation demonstrates, however, that it is self-consistent to third order in the pseudopotential.

This work was supported by the U.S. Army Research Office.

References

[1] P. Lloyd and C.A. Sholl, J. Phys. C2 (1968) 1620.
[2] E.G. Brovman, Yu. Kagan and A. Kholas, Zh. Eksp. Teor. Fiz. 61 (1971) 737; Engl. transl. Sov. Phys. JETP 34 (1972) 394.
[3] C.M. Bertoni, V. Bortolani, C. Calandra and F. Nizzoli, J. Phys. F4 (1974) 19.

APPENDIX E

An Anisotropic Screening Effect in the Theory of Electric Field Gradients in Dilute Alloys of Simple Metals

AN ANISOTROPIC SCREENING EFFECT IN THE THEORY OF ELECTRIC FIELD GRADIENTS IN DILUTE ALLOYS OF SIMPLE METALS

R.E. BEISSNER
Southwest Research Institute, San Antonio, TX 78284, USA

Received 1 June 1978
Revised manuscript received 8 February 1979

The Kohn–Vosko formula for electric field gradients associated with point defects is modified to account for the effect of anisotropic screening charge density on the core enhancement factor.

Within the past several years, very powerful techniques have been developed that allow one to determine, from nuclear magnetic resonance experiments with dilute alloys, the magnitude of the electric field gradient (EFG) at each of the first few neighbor shells around a solute ion [1–5]. These EFG data, because they relate directly to the screening charge distribution induced by the solute ion, provide an important test of theories of defect screening in metals.

The relationship between the screening charge density and the EFG at host ion sites was explored several years ago by Kohn and Vosko [6] and Blandin and Friedel [7], who independently derived an approximate expression for the EFG. Their theory is a first-order perturbation calculation of the screening charge density and involves certain additional approximations based on the assumption that the impurity–host ion distance is large. Comparison of several calculations, based on various versions of this theory, with experimental EFG data reveal certain consistent points of disagreement [8–11]. The best known of these is that calculated EFG's are almost always too small, particularly at the nearest-neighbor shell where the experimental values are usually larger by a factor of two or more. This has generally been attributed to the expected failure of the theory at short distances [12]. Another possibility is that additional contributions to the EFG from nonvanishing net charge densities in neighbouring ion cells may be appreciable [13].

Recently, however, a new point of disagreement has emerged that is more difficult to explain. According to the experimental results for aluminum reviewed by Minier and Ho Dung [10], the EFG at the second neighbor shell is consistently much smaller than that at the first, third, and in some cases, even the fourth and fifth shells for a large number of different impurity ions. As Holtham and Jena [12] point out, this depression of the second-neighbour EFG must be a property of the host crystal, and not the solute ion, because it happens in the same way for solutes with positive, negative and vanishing valence differences. However, their attempt to explain this trend by refinement of the first-order theory was not successful.

This failure of the first-order theory led Minier and Ho Dung [10] to suggest that the screening charge density in aluminum is anisotropic. If this is the case, then higher-order terms in the host crystal potential are needed, because all other terms in the perturbation expansion lead to an isotropic density. In other words, one should use Bloch functions as the unperturbed states, rather than plane waves, as is done in the first-order theory.

In this communication we examine one of the consequences of extending the theory of the EFG beyond a first-order, plane-wave treatment. We will show that when this is done, the formal expression for the EFG is similar to the Kohn–Vosko result, but with a generalized definition of the core enhancement factor that appears in their formula [6].

Our starting point is the general expression for the

Table 1
Core enhancement correction factors for various host ion directions.

Direction	[110]	[100]	[211]	[111]
	1.10	0.80	0.92	0.98

EFG at a host ion site $\boldsymbol{R}_n$ in terms of the screening charge density $\delta\rho(\boldsymbol{x})$,

$$q(\boldsymbol{R}_n) = -2\int \frac{\delta\rho(\boldsymbol{R}_n + \boldsymbol{r}')P_2(\mu')}{r'^3}\,d^3r' , \qquad (1)$$

where μ' is the cosine of the angle between $\boldsymbol{R}_n$ and $\boldsymbol{r}'$, and $P_2(\mu')$ is a Legendre polynomial. This can be written in terms of an approximate charge density $\delta\rho_s(\boldsymbol{x}')$ as follows:

$$q(\boldsymbol{R}_n) = -2\tilde{\alpha}(\boldsymbol{R}_n, k_F)\int \frac{\delta\rho_s(\boldsymbol{R}_n + \boldsymbol{r}')P_2(\mu')}{r'^3}\,d^3r' , \qquad (2)$$

where $\tilde{\alpha}$ is a ratio of integrals defined by eqs. (1) and (2). At this point, if no approximations are introduced, the choice of $\delta\rho_s$ obviously has no effect on the final result, although it does determine the consistent definitions of the core enhancement factor $\tilde{\alpha}$ and the approximate screening charge density. Now, however, following Kohn and Vosko, we will introduce an approximation that eliminates the dependence of $\tilde{\alpha}$ on host ion distance R_n, and another approximation in the evaluation of the remaining integral in eq. (2). Because of these approximations the final result will depend on our choice of $\delta\rho_s$.

We choose to let $\delta\rho_s$ be the smooth part of the screening charge density as defined in the theory of pseudopotentials [14]. If we let $\phi^0_{\boldsymbol{k}}(\boldsymbol{x})$ be the pseudo wave function for the perfect crystal, $\phi_{\boldsymbol{k}}(\boldsymbol{x})$ the perturbed pseudo wave function, and $\psi^0_{\boldsymbol{k}}(\boldsymbol{x})$, $\psi_{\boldsymbol{k}}(\boldsymbol{x})$ the corresponding true wave functions, then, to first order in the defect pseudopotential W, the true screening charge density is

$$\delta\rho(\boldsymbol{x}) = 2\sum_{k\le k_F}\sum_{k'\ne k}\left[\frac{\langle\phi^0_{\boldsymbol{k}}|W|\phi^0_{\boldsymbol{k}'}\rangle}{k^2 - k'^2}\psi^{0*}_{\boldsymbol{k}}\psi^0_{\boldsymbol{k}'} + \text{c.c.}\right],$$

while the smooth part, $\delta\rho_s$, is given by a similar expression with $\phi^0_{\boldsymbol{k}}$ in place of $\psi^0_{\boldsymbol{k}}$. Next, following Kohn and Vosko, we write the Bloch functions $\phi^0_{\boldsymbol{k}}$ and $\psi^0_{\boldsymbol{k}}$ in the form

$$\psi^0_{\boldsymbol{k}}(\boldsymbol{x}) = e^{i\boldsymbol{k}\cdot\boldsymbol{x}}u_{\boldsymbol{k}}(\boldsymbol{x}) ,$$

where $u_{\boldsymbol{k}}$ is periodic, and evaluate $\delta\rho$ and $\delta\rho_s$ to lowest order in $1/|\boldsymbol{x}|$. The result is

$$\delta\rho(\boldsymbol{x}) \sim \frac{\pi k_F\Omega^2}{(2\pi)^4|\boldsymbol{x}|^3}\left[W_{\boldsymbol{k}_F,-\boldsymbol{k}_F}\psi^{0*}_{-\boldsymbol{k}_F}(\boldsymbol{x})\psi^0_{\boldsymbol{k}_F}(\boldsymbol{x}) + \text{c.c.}\right],$$

where Ω is the crystal volume, $\boldsymbol{k}_F\boldsymbol{x} = k_F\boldsymbol{x}/|\boldsymbol{x}|$, and

$$W_{\boldsymbol{k}_F,-\boldsymbol{k}_F} = \langle\phi^0_{\boldsymbol{k}_F}|W|\phi^0_{-\boldsymbol{k}_F}\rangle .$$

Again, the expression for $\delta\rho_s$ is similar. Substitution in the expression for $\tilde{\alpha}$ leads to the approximate result

$$\tilde{\alpha}(\boldsymbol{k}_F) = \frac{\int[\psi^0_{\boldsymbol{k}_F}(\boldsymbol{r}')]^2P_2(\mu')\,d^3r'/r'^3}{\int[\phi^0_{\boldsymbol{k}_F}(\boldsymbol{r}')]^2P_2(\mu')\,d^3r'/r'^3} . \qquad (3)$$

To evaluate the remaining integral in eq. (2) we expand $\delta\rho_s(\boldsymbol{x})$ in plane waves and integrate to obtain

$$\int\delta\rho_s(\boldsymbol{R}_n + \boldsymbol{r}')P_2(\mu')\,d^3r'/r'^3$$

$$= -\tfrac{4}{3}\pi\sum_{\boldsymbol{q}}\delta\rho_s(\boldsymbol{q})P_2(\hat{\boldsymbol{q}}\cdot\hat{\boldsymbol{R}}_n)e^{i\boldsymbol{q}\cdot\boldsymbol{R}_n} \sim -\tfrac{4}{3}\pi\delta\rho_s(\boldsymbol{R}_n) ,$$

where $\hat{\boldsymbol{q}}$ and $\hat{\boldsymbol{R}}_n$ are unit vectors. In the last step we assume that, because R_n is large, the only significant values of $\boldsymbol{q}$ are those parallel and antiparallel to $\boldsymbol{R}_n$, in which case $P_2(\hat{\boldsymbol{q}}\cdot\hat{\boldsymbol{R}}_n) = 1$.

The final expression for the EFG is therefore similar to the Kohn–Vosko formula

$$q(\boldsymbol{R}_n) = \tfrac{8}{3}\pi\tilde{\alpha}(\boldsymbol{k}_F)\delta\rho_s(\boldsymbol{R}_n) , \qquad (4)$$

where $\tilde{\alpha}$ is given by eq. (3) and $\delta\rho_s$ is the smooth part of the screening charge density as determined to first order in W using $\phi^0_{\boldsymbol{k}}$ as the unperturbed wave functions. It is easily seen that if one uses the plane-wave approximation to $\phi^0_{\boldsymbol{k}}$ and the asymptotic approximation to $\delta\rho_s$, then eqs. (3) and (4) reduce to the Kohn–Vosko formula.

To investigate the numerical significance of our modification of the core enhancement factor we used the aluminum form factor data of Bertoni et al. [15], in a first-order perturbation approximation to $\phi^0_{\boldsymbol{k}}$, to calculate the ratio $\tilde{\alpha}/\alpha$, where α is the enhancement factor in the plane-wave approximation. The resulting expression is

$$\tilde{\alpha}/\alpha = \left[1 + 2\sum_{K\ne 0}\frac{\omega_K}{k_F^2 - |\boldsymbol{k}_F - \boldsymbol{K}|^2}P_2(\cos\psi_{\boldsymbol{K}})\right]^{-1} ,$$

where $\boldsymbol{K}$ is a reciprocal lattice vector, ω_K is the host crystal form factor, and $\psi_{\boldsymbol{K}}$ is the angle between $\boldsymbol{k}_F$ and $2\boldsymbol{k}_F - \boldsymbol{K}$. Numerical results are given in table 1.

These data suggest that the modification of α required by a Bloch wave treatment of defect scattering can be significant. In the particular approximation used here the principal effects are a depression of the enhancement factor in the [100] direction and a slight enhancement in the [110] direction. These effects are, however, much too small to account for all of the experimentally observed depression of the EFG at the second neighbor shell in aluminum. *Hopefully, this* will be explained by a second-order calculation of the anisotropic screening charge density, the second factor in eq. (4), which is now in progress.

This work was supported by the U.S. Army Research Office.

References

[1] A.G. Redfield, Phys. Rev. 130 (1963) 589.
[2] M. Minier, Phys. Rev. 182 (1969) 437.
[3] L.E. Drain, Phys. Rev. B8 (1973) 3628.
[4] R. Nevald, B.L. Jensen and P.B. Fynbo, J. Phys. F4 (1974) 1320.
[5] J.A.R. Stiles and D Ll. Williams, J. Phys. F4 (1974) 2297.
[6] W. Kohn and S.H. Vosko, Phys. Rev. 119 (1960) 912.
[7] A. Blandin and J. Friedel, J. Phys. Radium 21 (1960) 689.
[8] M. Minier and S. Ho Dung, J. Phys. F1 (1977) 503.
[9] G. Grumer and M. Minier, Adv. Phys. 26 (1977) 231.
[10] P.M. Holtham and P. Jena, J. Phys. F5 (1975) 1649.
[11] P.L. Sagalyn and M.N. Alexander, Phys. Rev. B15 (1977) 5581.
[12] W.A. Harrison, Pseudopotentials in the theory of metals (Benjamin, New York, 1966).
[13] C.M. Bertoni, V. Bortolani, C. Calandra and F. Nizzoli, J. Phys. F3 (1973) L244.

APPENDIX F

Self-Consistent, Second-Order Screening of Point Defects in Aluminum

(Submitted to Physical Review B)

Self-Consistent, Second-Order Screening of Point Defects in Aluminum

R. E. Beissner
Southwest Research Institute, San Antonio, Texas 78284

ABSTRACT

Numerical computations of self-consistent, second-order screening charge densities are presented for a proton, an aluminum ion, and substitutional zinc and magnesium in jellium with the electron density of aluminum. Comparisons with more accurate density functional calculations show that a second-order treatment fails, as expected, for the proton, but gives reasonable results for the aluminum ion. Second-order corrections to the linear screening charge densities are found to be small for the weaker-scattering substitutional defects. It is concluded that a second-order theory is adequate for substitutional defects with small valence differences, and may find limited use even for strong-scattering defects, such as the vacancy, provided high accuracy is not required.

I. INTRODUCTION

The success of the linear screening approximation in the theory of perfect, non-transition metals crystals has been attributed to the small values of the pseudopotential or model potential matrix elements that enter such calculations[1]. For a perfect crystal, matrix elements are evaluated only at the rather large wavenumbers corresponding to reciprocal lattice vectors, where their values are indeed usually much less than the Fermi energy of the metal. This justifies the use of first-order perturbation theory in the calculation of screening charge densities which, in its self-consistent form, comprises the linear screening approximation.

This argument cannot be applied to an imperfect crystal, because a defect screening calculation involves matrix elements evaluated at small wavenumnbers, where values can be of the order of the Fermi energy. The linear screening approximation is therefore of questionable validity in such problems, and one must look to a higher order theory. In general, this presents a formidable mathematical difficulty because the problem of self-consistency is then non-linear.

In recent years, this nonlinear screening problem for point defects has been the subject of several numerical studies. Most such calculations have been based on density functional theory[2-7], though a few investigations using the Korringa-Kohn-Rostoker (KKR) Green's-function method[8-10] and the supercell model[11-13] have also been reported. While each of these methods can claim high accuracy in the treatment of nonlinear screening effects, all suffer from computational complexities which tend to restrict the class of defect problems that can be treated. In particular, it seems to be impractical, at the present time, to apply such methods to anything more complex than the isolated point defect, or, in the case of the supercell method, a periodic array of point defects.

For certain strong-scattering cases, such as the screening of interstitial hydrogen, a fully self-consistent numerical treatment is probably essential for most purposes. On the other hand, there are many other defect problems where the perturbing potential is not so strong and where an approximate treatment might suffice. These include substitutional point defects, stacking faults and similar planar defects, and perhaps even vacancies and interstitials in applications where high accuracy is not required.

We are led, therefore, to consider simpler, alternate methods for obtaining approximate solutions to the nonlinear screening problem. In particular, in this article we examine the use of second-order perturbation theory in the calculation of screening charge densities. Though the theory is, in principle, applicable to an arbitrary arrangement of scattering centers, our numerical results are limited to point defects in the jellium model. Our aim is to provide some insight as to the magnitude of second-order terms in both strong- and weak-scattering cases, the role of self-consistency, and, in general, the validity of an approximate, second-order theory of defect screening.

The next section is essentially a restatement of the second-order screening theory of Lloyd and Sholl[14] and Brovman, et al.,[15] in terms of defect and host crystal potentials. It serves mostly as background for the discussion of numerical results, which are presented in Sec. III. The calculations include approximate and self-consistent screening charge densities for a proton, an isolated aluminum ion (to simulate the vacancy potential) and substitutional magnesium and zinc. We conclude that an approximate second-order theory, in which the defect potentials are screened to first order, is adequate for weak-scattering, substitutional defects, and may prove useful even for stronger scatterers such as vacancies.

II. THEORY

The development that follows is based on the model potential theory of screening by valence electrons, in which the ionic model potential is nonlocal[16]. However, following Bertoni, et al.,[17] we assume at the outset that the nonlocal potential can be replaced by the local potential that leads to the same screening charge density as a fully nonlocal calculation in the linear screening approximation. The Fourier transform of the smooth part of the electron density, i.e., that part derived from the model wave function, is then[14]

$$\rho_s(\vec{q}) = \frac{q^2}{8\pi} \frac{1-\varepsilon(q)}{1-G(q)} W(\vec{q}) + 3\sum_{\vec{p}_1 \neq 0} g(p_1,p_2,q) W^*(\vec{p}_1) W^*(\vec{p}_2) \qquad (1)$$

where $\vec{p}_2 = -(\vec{p}_1 + \vec{q})$, $\varepsilon(q)$ is the dielectric function, $G(q)$ is the exchange-correlation correction[1], $g(p_1,p_2,q)$ is the function defined by Lloyd and Sholl[14], and $W(\vec{q})$ is the Fourier transform of the self-consistent potential in Rydbergs.

The electron potential energy due to valence electrons is related to the electron density through Poisson's equation, modified to account for exchange and correlation energies. Thus we have[1]

$$W(\vec{q}) - W_{ion}(\vec{q}) = \frac{8\pi}{q^2} (1-G(q))(\rho_s(\vec{q}) + \rho_d(\vec{q})) \qquad (2)$$

where $W_{ion}(\vec{q})$ is the ionic model potential, and $\rho_d(q)$ is the transform of the depletion charge density.

To derive the second order self-consistency condition on $W(\vec{q})$ we eliminate $\rho_s(\vec{q})$ from Eqs. (1) and (2) to obtain

$$W(\vec{q}) = W_\ell(\vec{q}) + \frac{24\pi}{q^2}\,\frac{1-G(q)}{\varepsilon(q)} \sum_{\vec{p}_1 \neq 0} g(p_1, p_2, q) W^*(\vec{p}_1) W^*(\vec{p}_2) \tag{3}$$

where $W_\ell(\vec{q})$ is the linear screening approximation to $W(\vec{q})$, i.e.,

$$W_\ell(\vec{q}) = \tilde{W}_{ion}(\vec{q})/\varepsilon(q) \tag{4}$$

with

$$\tilde{W}_{ion}(\vec{q}) = W_{ion}(\vec{q}) + \frac{8\pi}{q^2}\,[1-G(q)]\rho_d(\vec{q}) \tag{5}$$

Finally, from Eqs. (1) and (3) we rewrite the density equation in the more convenient form,

$$\rho_s(\vec{q}) = \frac{q^2}{8\pi}\,\frac{1-\varepsilon(q)}{1-G(q)}\left[W_\ell(\vec{q}) + \frac{W(\vec{q}) - W_\ell(\vec{q})}{1-\varepsilon(q)}\right] \tag{6}$$

in which the first term is the linear screening approximation and the second term is the second-order, nonlinear correction.

Equations (3) and (6) comprise a statement of the general second-order, self-consistent screening problem for local potentials. An approximate solution, valid to third order in $W_\ell(\vec{q})$, is obtained by a single iteration of Eq. (3), i.e. by substituting $W_\ell(\vec{q})$ in the sum on the right side[18]. This

leads to a relatively simple, closed form approximation to the screening charge density which can be applied to an arbitrary arrangement of ions. The accuracy of this approximate treatment of self-consistant screening is one of the points we study here.

In calculations of the defect screening charge density we are concerned with the change in electron density caused by the creation of a defect in a host crystal. We therefore take

$$W(\vec{q}) = W^{h}(\vec{q}) + W^{d}(\vec{q}) \tag{7}$$

where $W^{h}(\vec{q})$ is given by Eq. (3) for the host crystal, and $W^{d}(\vec{q})$ is the change in potential due to the defect. Similar expressions hold for the first order potential $W_{\ell}(\vec{q})$ and for the bare ion potential.

Substitution of Eq. (7) in Eq. (6) gives, for the change in $\rho_{s}(\vec{q})$ due to the defect

$$\delta\rho_{s}(\vec{q}) = \frac{q^2}{8\pi}\,\frac{1-\varepsilon(q)}{1-G(q)}\left[W_{\ell}^{d}(\vec{q}) + \frac{W^{d}(\vec{q}) - W_{\ell}^{d}(\vec{q})}{1-\varepsilon(q)}\right] \tag{8}$$

while substitution in Eq. (3) leads to

$$W^{d}(\vec{q}) = W_{\ell}^{d}(\vec{q}) + \frac{24\pi}{q^2}\cdot\frac{1-G(q)}{\varepsilon(q)}\sum_{\vec{p}_1\neq 0} g(p_1,p_2,q)W^{d^*}(\vec{p}_1)W^{d^*}(\vec{p}_2)$$

$$+ \frac{48\pi}{q^2}\,\frac{1-G(q)}{\varepsilon(q)}\sum_{\vec{p}_1\neq 0} g(p_1,p_2,q)W^{h^*}(\vec{p}_1)W^{d^*}(\vec{p}_2) \tag{9}$$

The last term in Eq. (9), which contains $W^h(\vec{q})$ as well as $W^d(\vec{q})$, demonstrates the dependence of the self-consistent defect potential, and thus the screening charge density, on the arrangement of neighboring ions.

Because the host crystal potential is weak, the accuracy of this approximate theory is determined largely by the relative magnitudes of the first and second terms on the right side of Eqs. (8) and (9). In general, one would expect the theory is useful only if the second-order term in Eq. (8) is small compared to the linear screening term, as this may be taken to imply that third- and higher-order terms are smaller still, and can therefore be neglected. For the computations described in the next section, we therefore drop the host crystal term in Eq. (9) and examine the changes in screening charge density caused by second-order defect terms. This amounts to the jellium approximation, in which case Eqs. (8) and (9) reduce to

$$\delta\rho_s(q) = \frac{q^2}{8\pi N}\ \frac{1-\varepsilon(q)}{1-G(q)}\ \left[\omega_\ell(q) + \frac{\omega(q) - \omega_\ell(q)}{1-\varepsilon(q)}\right] \qquad (10)$$

and

$$\omega(q)=\omega_\ell(q) + \frac{24\pi}{q^2}\ \frac{1-G(q)}{\varepsilon(q)}\ \frac{\Omega_o}{(2\pi)^3}\ \int g(p_1,p_2,q)\,\omega(p_1)\,\omega(p_2)\,d\vec{p}_1 \qquad (11)$$

where $\omega(q)$ is the defect form factor, Ω_0 is the average volume per ion and N is the number of ions in the crystal.

III. NUMERICAL RESULTS

Computations were performed for a proton, an isolated aluminum ion using the Rasolt-Taylor[3], Shaw[16] and Heine-Abarenkov[19] model potentials, and for substitutional zinc and magnesium in an aluminum host using the Shaw potential. In all cases, the averaged local potential defined by Bertoni, et al[17], was used in computing the linear screening form factor $\omega_\ell(q)$. For substitutional zinc and magnesium $\omega_\ell(q)$ was taken as the difference between the impurity and host form factors, using the impurity model potential parameters and depletion charges calculated by Taut and Paasch[20] for an aluminum host crystal. Unless otherwise noted, the exchange and correlation function G(q) was taken from Toigo and Woodruff[21].

The nonlinear integral equation for the self-consistent form factor, Eq. (11), was solved by successive approximations using $\omega_\ell(q)$ as the initial approximation. Computations were performed in a 71 point mesh with spacing $\Delta\chi = 0.05$ where $\chi = q/2k_f$, k_f being the Fermi wavenumber. Convergence of the iterative process is illustrated in Figure 1 where we show the linear screening approximation, which includes the depletion charge term in Eq. (5), and approximations to $\omega(q)$ after one, two and three iterations. For the weaker difference potentials used for substitutional defects only one iteration was required, while convergence of the process for the proton potential required five iterations.

In all cases, the principal effect of nonlinear screening is the addition of a repulsive potential at small values of q. This causes a decrease in the absolute magnitude of $\omega(q)$ for the proton and aluminum ion, as shown in Figure 1, and a slight increase in the repulsive difference potentials for zinc and magnesium. The difference between the self-consistent form factor

and the form factor obtained after one iteration was found to be small for aluminum, somewhat greater for the proton, and negligible for substitutional zinc and magnesium.

The fact that the form factor is altered only at smaller values of q deserves comment. From Eq. (10) we see that the second-order correction term is divided by $1-\varepsilon(q)$ which diverges in the long wavelength limit. The corresponding limit of $\delta\rho_s(q)$, which is proportional to the integrated screening charge, is therefore unaffected by the addition of the second order term, as is required by charge conservation. Also, because the difference $\omega(q) - \omega_\ell(q)$ is nonvanishing only at small q, where $\varepsilon(q)$ is large, Eq. (10) tells us that the Fourier transform of the screening charge density is not as sensitive to nonlinear effects as is the form factor itself. This may explain the observation that nonlinear corrections to the screening charge density are less pronounced than corrections to other functions derived from the form factor, such as the interionic potential and phonon spectra[4]. It should also serve as a warning that the conclusions drawn from comparisons of charge densities may not apply to the calculation of other properties.

Calculated screening charge densities are shown in Figures 2 through 6. For the proton and aluminum ion we show the linear screening result, the approximate second order density and the self-consistent second order density. For substitutional zinc and magnesium the differences between the approximate and self-consistent distributions are negligible.

The results for the proton, which are presented in Figure 2, show a strong nonlinear effect and a significant difference between the approximate and self-consistent solutions. At large distances the principal effects are a large shift in phase and an increase in the amplitude of the Friedel oscillations, while at small distances there is a pronounced increase in electron

y. Although these trends are in qualitative agreement with the results
e accurate calculations, quantitative agreement is not obtained.
ations based on the density functional approach[2] show a somewhat
r shift in phase and a smaller amplitude in the long range oscillations,
greater increase in density near the proton. At the proton site, for
e, the value shown in Figure 2 is about one-third the correct value.
Results obtained with the Shaw potential for an aluminum ion are shown
ure 3. Here again we find that second order effects are significant,
at changes in the screening charge density are not as dramatic as was
se for a proton. The principal effects are a slight shift in the phase
increase in amplitude of the Friedel oscillations with some distortion
density inside the core. In this case, the difference between the
consistent and approximate treatments of second order screening is
gible at most distances.

We also performed self-consistent calculations using the
t-Taylor[3] and Heine-Abarenkov[19] potentials for the aluminum ion. The
ts are presented in Figure 4, which also includes the self-consistent
data. Another calculation based on the Rasolt-Taylor potential with the
ctric function used by Dagens, et al[4] is not shown here because the
t does not differ significantly from the Rasolt-Taylor curve in Figure 4.
nclude, from a comparison of Figures 3 and 4, that, except at short dis-
s, the changes produced by second-order screening are of roughly the same
tude as those associated with the use of different model potentials.

It is perhaps more useful to compare our second-order approximation for
luminum ion with the more accurate density functional calculations re-
d by Manninen, et al[7]. From their Figure 1 and our Figures 3 and 4

we see that, at distances greater than 2.0 a.u., our results lie roughly in between their curves for the jellium model and the jellium vacancy model (jellium with the positive background removed from the ion cell), though the amplitude of our Friedel oscillations is slightly greater. While this does not prove that a second-order treatment is adequate, it does at least show that screening charge densities calculated in this approximation are reasonable, even for strong scattering centers like isolated ions and vacancies.

Finally, in Figures 5 and 6 we show the first- and second-order charge densities for two weak-scattering centers, substitutional zinc and magnesium. Here again the principal nonlinear effects are a shift in phase and an increase in amplitude of the Friedel oscillations, and a rearrangement of charge in the core. These effects are, however, quite small compared to the nonlinear effects obtained for the proton and aluminum ion, presumably because the potentials used here were derived from differences in ion potentials and are therefore weaker than potentials for isolated ions. If this is so, then calculations for substitutional impurities with greater valence differences should show stronger nonlinear effects.

IV. CONCLUSION

Self-consistent, second-order screening charge densities have been calculated in the jellium approximation for a proton, an isolated aluminum ion and substitutional magnesium and zinc in aluminum. As one would expect, the results do not agree with more accurate density functional calculations for the strongest scattering center, the proton, although the changes produced by the addition of second-order terms are qualitatively correct. For the substitutional defects, numerical results indicate that a simpler theory, in which

form factors are calculated in the linear screening approximation, is suitable provided the valence difference is small. In the case of somewhat stronger perturbations, such as the isolated ion or vacancy, the accuracy of a second-order treatment is subject to question. Still, the changes in the screening charge distribution produced by the self-consistent addition of second-order terms are reasonable, and the theory might therefore find limited application even in such strong scattering situations.

ACKNOWLEDGEMENT

This work was supported by the U.S. Army Research Office.

REFERENCES

1. V. Heine and D. Weaire, Solid State Phys. 24. 249 (1970).

2. Z. D. Popovic, M. J. Stott, J. P. Carbotte, and G. R. Piercy, Phys. Rev. B 13, 590 (1976).

3. M. Rasolt and R. Taylor, Phys. Rev. B 11, 2717 (1975).

4. L. Dagens, M. Rasolt, and R. Taylor, Phys. Rev. B 11, 2726 (1975).

5. A. K. Gupta, P. Jena, and K. S. Singwi, Phys. Rev. B 18, 2712 (1978).

6. P. Jena, A. K. Gupta, and K. S. Singwi, Phys. Rev. B 18, 2723 (1978).

7. M. Manninen, P. Jena, R. M. Nieminen, and J. K. Lee, Phys. Rev. B 24, 7057 (1981).

8. T. H. Dupree, Ann. Phys., NY 15, 63 (1961).

9. R. Zeller and P. H. Dedericks, Phys. Rev. Lett. 42, 1713 (1979).

10. J. Deutz, P. H. Dedericks, and R. Zeller, J. Phys. F 11, 1787 (1981).

11. S. G. Louie, M. Schluter, J. R. Chelikowsky, and M. L. Cohen, Phys. Rev. B 13, 1654 (1976).

12. R. P. Gupta and R. W. Siegel, Phys. Rev. B 22, 4572 (1980).

13. B. Chakraborty, R. W. Siegel, and W. E. Pickett, Phys. Rev. B 24, 5445 (1981).

14. P. Lloyd and A. C. Sholl, J. Phys. C 1, 1620 (1968).

15. E. G. Brovman, Yu. Kagan, and A. Kholas, Zh. Eksp. Teor. Fiz. 61, 737 (1971); Eng. transl. Sov. Phys. JETP 34, 394 (1972).

16. R. W. Shaw, J. Phys. C 2, 2350 (1969).

17. C. M. Bertoni, V. Bortolani, C. Calandra, and F. Nizzoli, J. Phys. F 4, 19 (1974).

18. R. E. Beissner, Phys. Lett. 67A, 155 (1978).

19. V. Heine and I. V. Abarenkov, Phil. Mag. 9, 451 (1964); A.O.E. Animalu and V. Heine, Phil. Mag 12, 1249 (1965).

20. M. Taut and G. Paasch, Phys. Stat. Sol. B 51, 295 (1972).

21. F. Toigo and T. O. Woodruff, Phys. Rev. B 2, 3958 (1970).

FIGURE CAPTIONS

Figure 1. Self-consistent form factor for aluminum. The lower solid curve is the linear screening approximation including depletion charge effects, while the upper solid curve is the second-order self-consistent form factor. The dotted and dashed curves were obtained after one and two iterations, respectively, of Eq. 11.

Figure 2. Second-order screening charge density for the proton. The dotted curve is the linear screening approximation, the dashed curve corresponds to the approximate second-order form factor obtained after one iteration and the solid curve is the self-consistent result.

Figure 3. Second-order screening charge density for the aluminum ion. The legend is the same as in Figure 2.

Figure 4. Self-consistent, second-order screening charge densities for the aluminum ion. The dotted curve corresponds to a damped Heine-Abarenkov potential[19], the dashed curve to the Rasolt-Taylor potential[3] and the solid curve to the optimized model potential[16].

Figure 5. Screening charge density for substitutional magnesium in an aluminum host. The dotted curve is the linear screening result while the solid curve is the self-consistent, second-order density.

Figure 6. Screening charge density for substitutional zinc in an aluminum host. The legend is the same as in Figure 5.

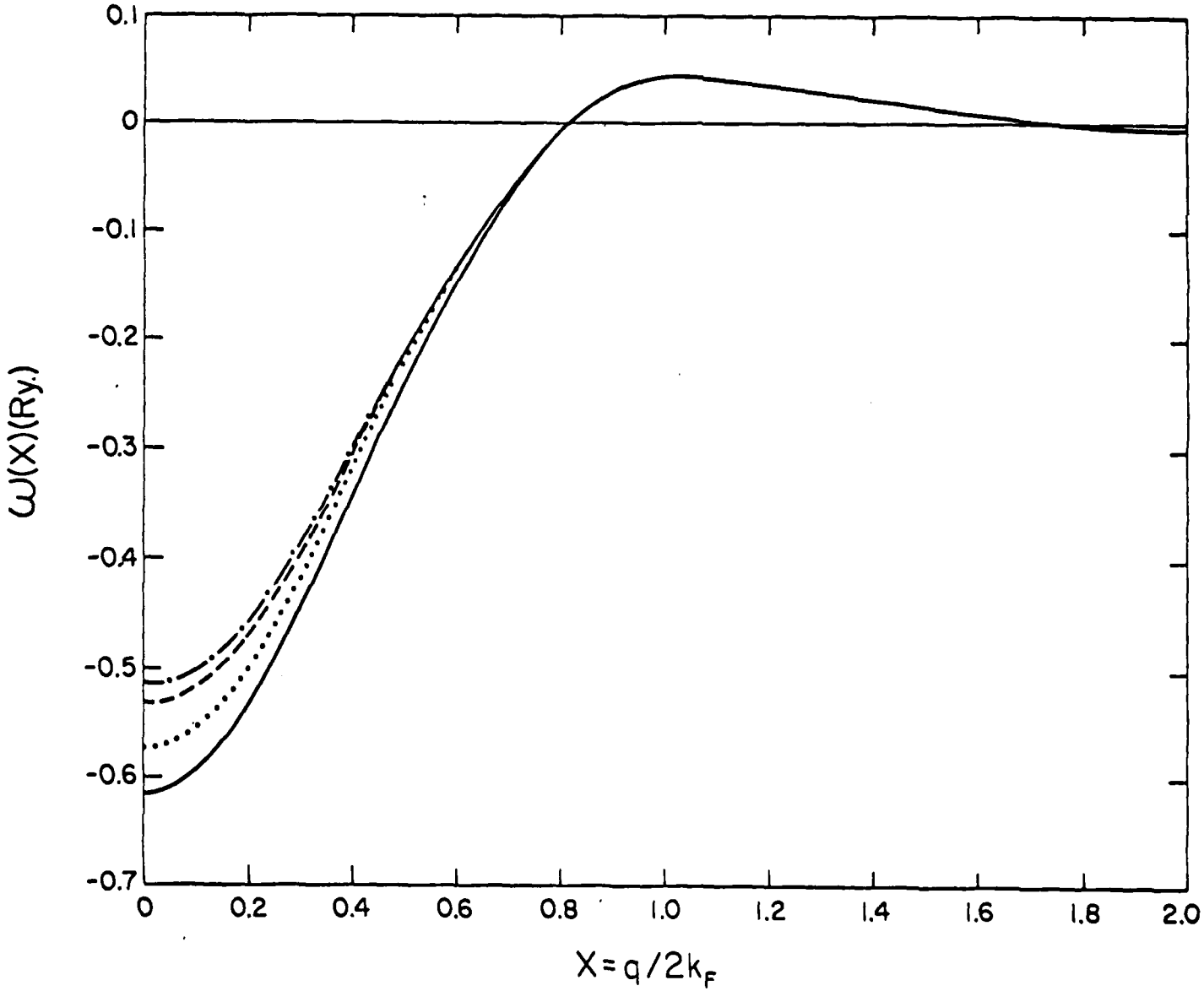

FIGURE 1

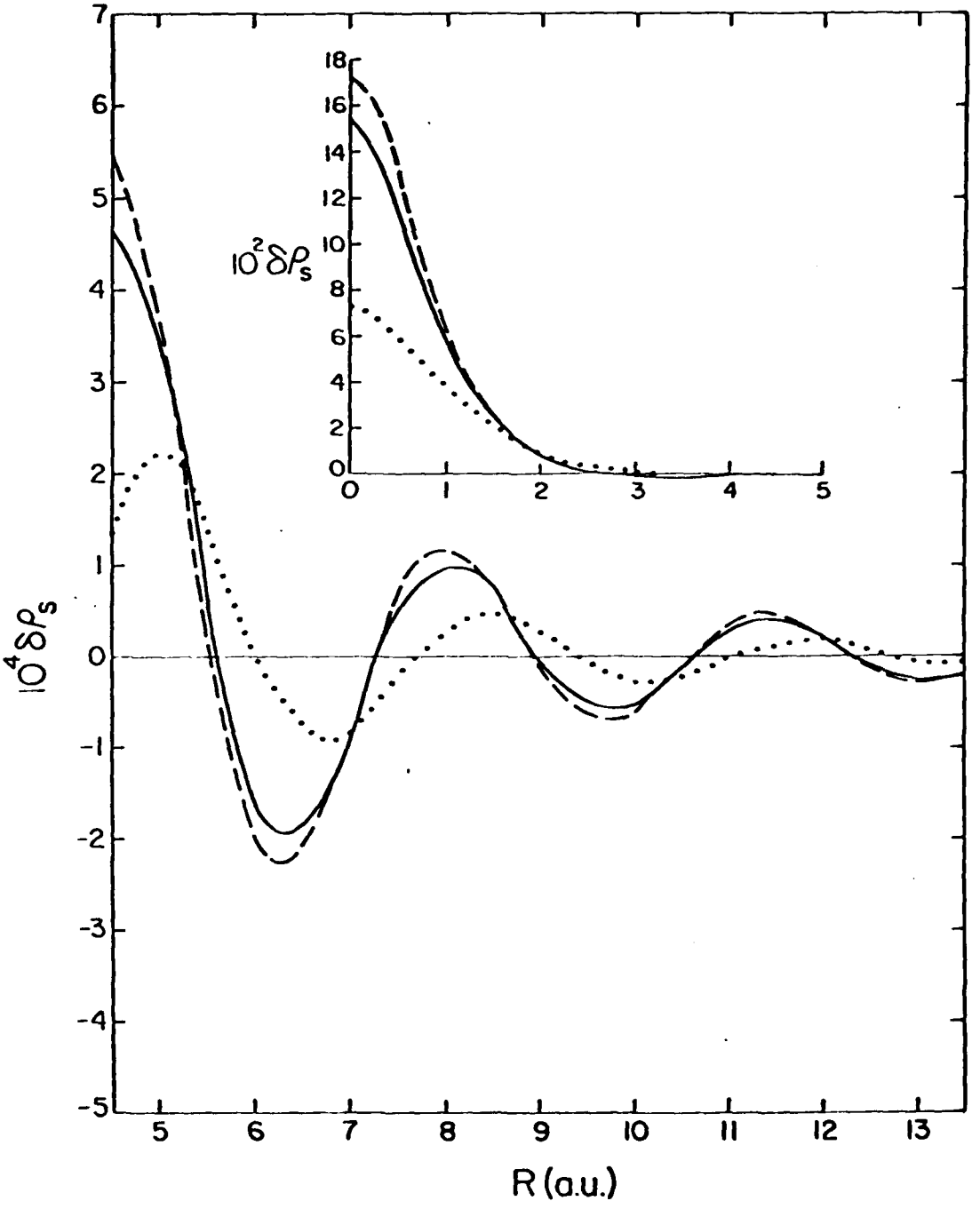

FIGURE 2

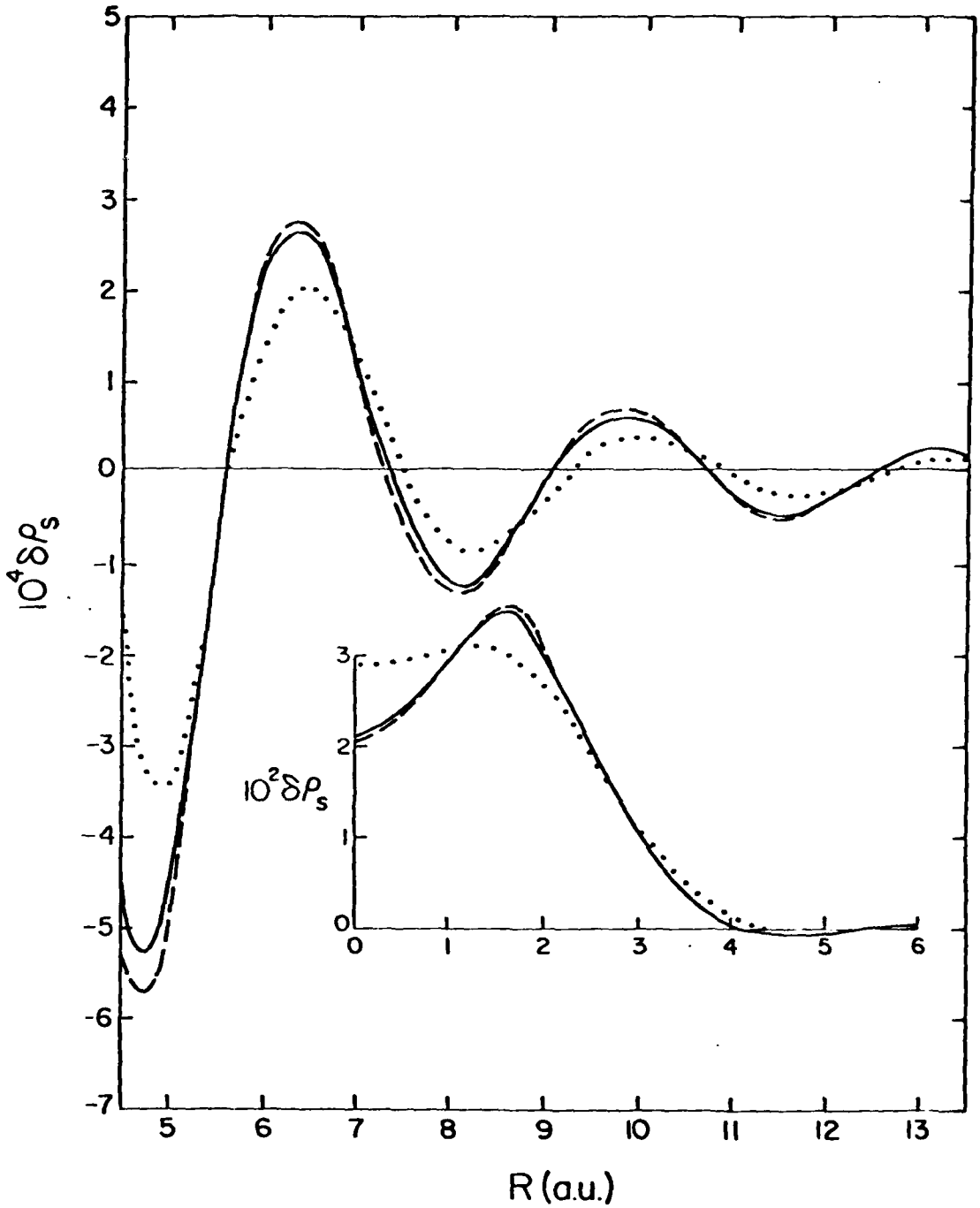

FIGURE 3

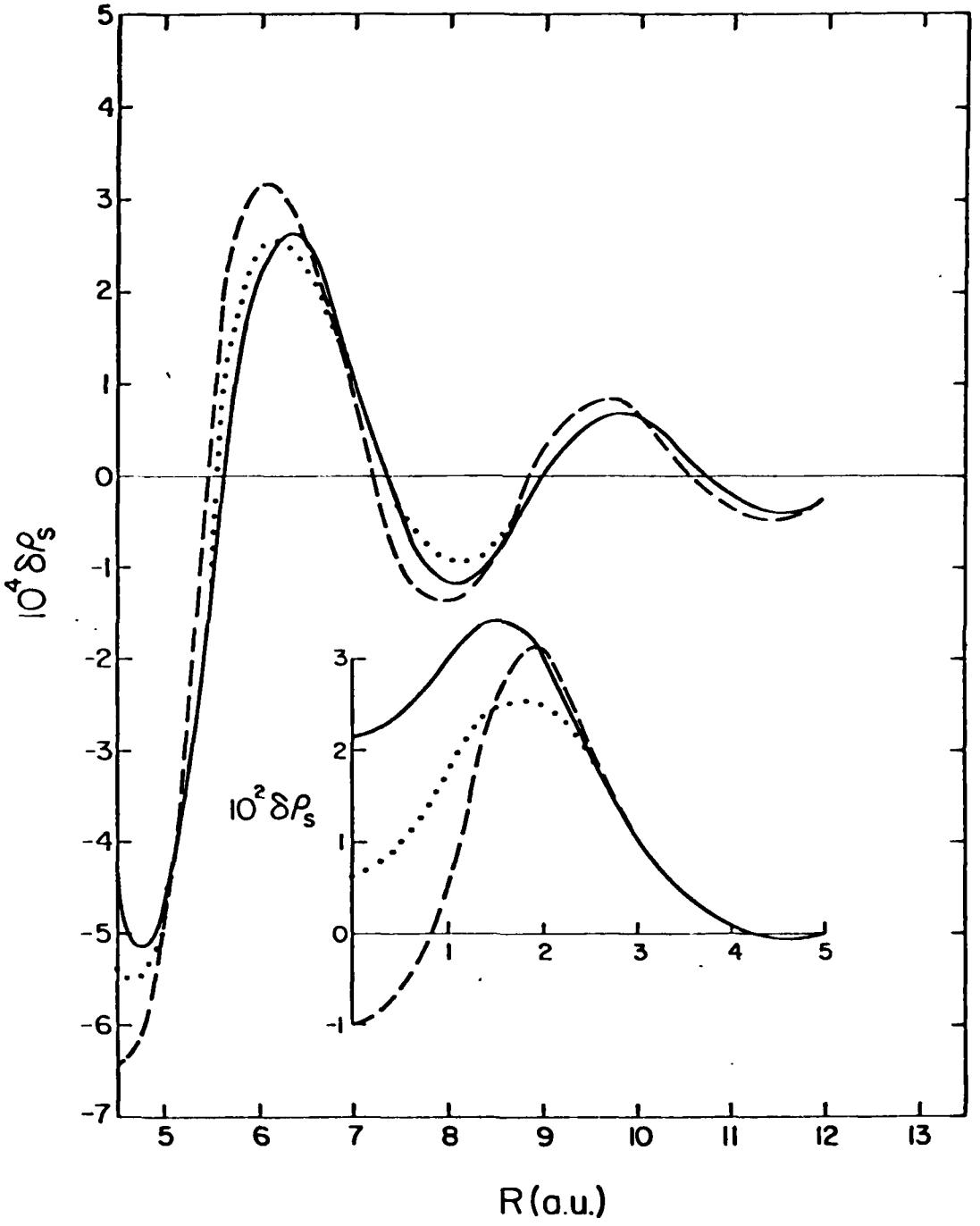

FIGURE 4

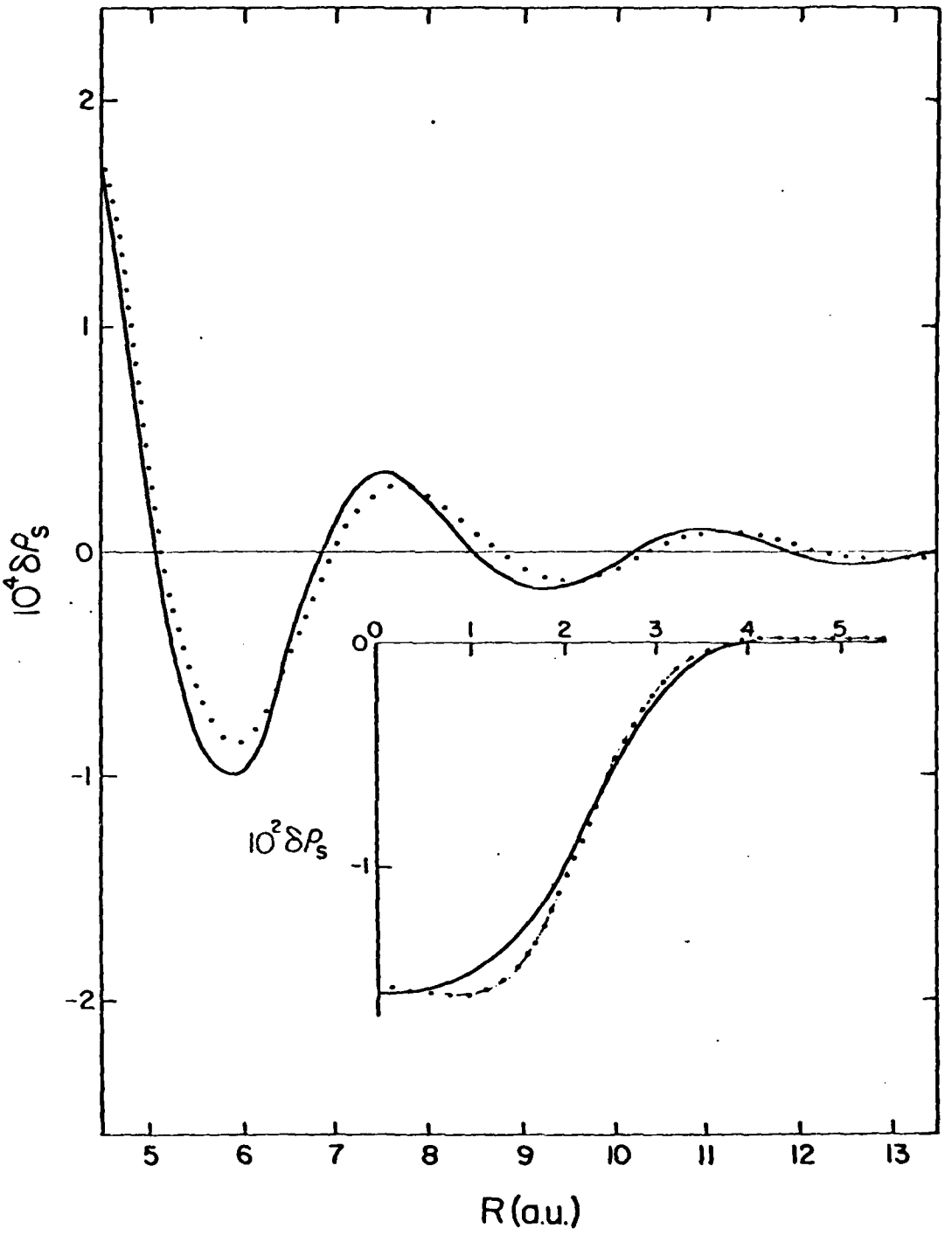
2
1
0
-1
-2
$10^4 \delta\rho_s$
5
6
7
8
9
10
11
12
13
R(a.u.)
0
1
2
3
4
5
$10^2 \delta\rho_s$
-1

FIGURE 5

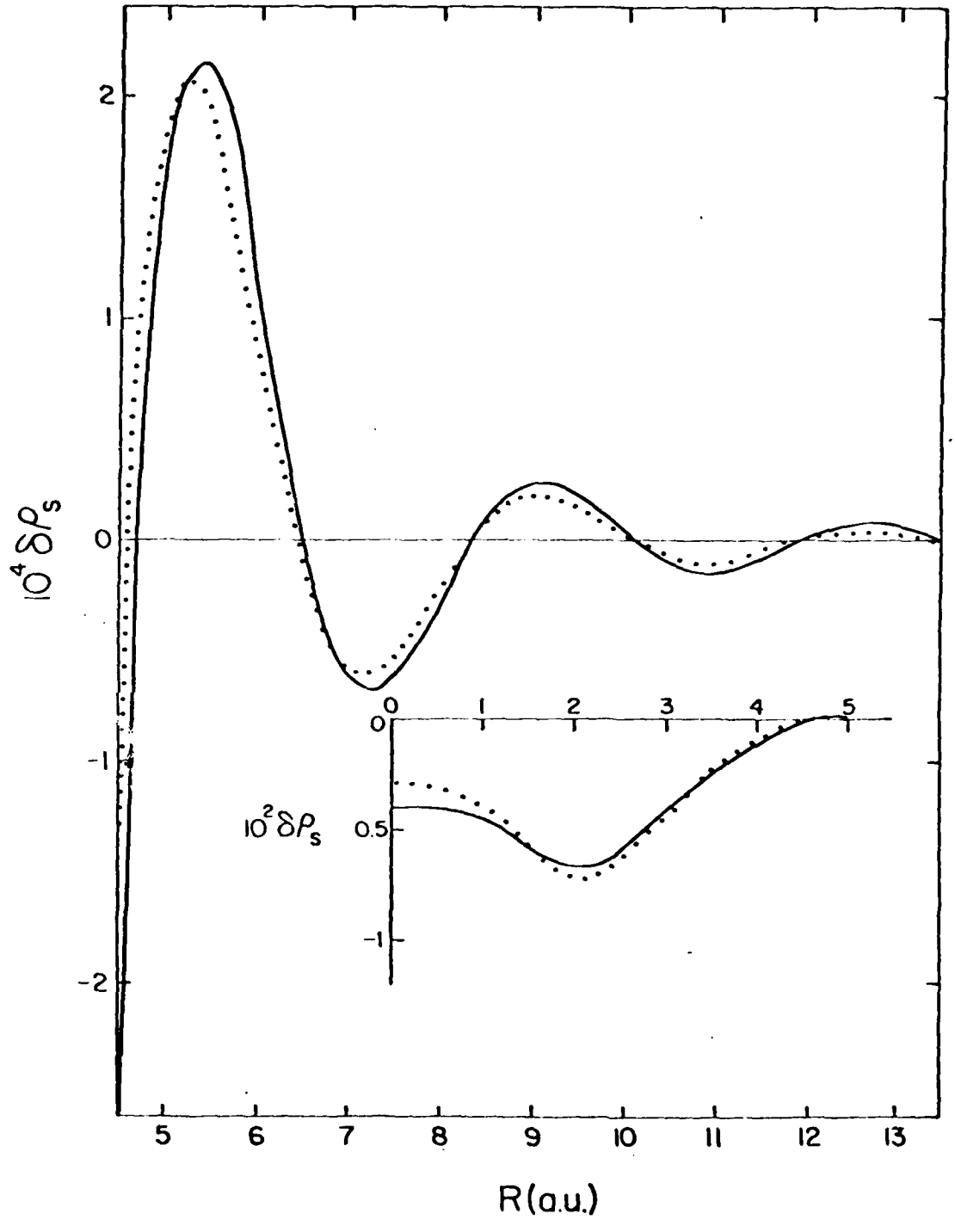
$10^4 \delta\rho_s$
2
1
0
-1
-2
5
6
7
8
9
10
11
12
13
R(a.u.)
$10^2 \delta\rho_s$
0
1
2
3
4
5
0
0.5
-1

FIGURE 6

APPENDIX G

New Contributions to the Valence Effect Electric Field Gradient in Simple Metal Alloys

(Submitted to Physical Review B)

New Contribution to the Valence Effect Electric Field Gradient in Simple Metal Alloys

R. E. Beissner
Southwest Research Institute, San Antonio, Texas 78284

ABSTRACT

Electric field gradient (EFG) calculations for metal alloys are usually based on an asymptotic theory in which the valence effect EFG is proportional to the screening charge density. We show, by means of second order computations that avoid the usual asymptotic approximation, that this proportionality does not hold for hetrovalent alloys of aluminum. In such cases, the charge density is oscillatory and is significantly affected by the addition of anisotropic second-order terms, while the EFG is dominated by the isotropic first order term and is non-oscillatory. This failure of the usual asymptotic EFG theory is attributed to the inadequacy of the asymptotic approximation in the long wavelength limit. An approximate correction term is derived and found to be proportional to the difference in valence between impurity and host ions. Additional first-order computations show that the corrected EFG formula gives good agreement with results obtained by direct numerical evaluation of the exact expression for the EFG.

I. INTRODUCTION

When a point defect is created at a host ion site in a cubic metal, the resulting disturbance produces electric field gradients (EFG), which are measurable by nuclear magnetic resonance methods,[1,2] at neighboring host ion sites. As is well known, the EFG has two components, the so-called valence-effect EFG, caused by the redistribution of conduction electrons, and the size-effect EFG, caused by lattice distortion.[3,4] The valence-effect EFG is generally assumed to be given by the Kohn-Vosko formula[5] (also derived independently by Blandin and Friedel[6]) which states that the EFG at a given host ion site is directly proportional to the screening charge density at that site. Calculations of the size-effect component are based on the theory of Sagalyn, et al,[3] which assumes that the EFG tensor is proportional to the local strain tensor.

As was demonstrated by Sagalyn and Alexander[4] and others,[7-9] both the valence- and size-effect contributions must be included to obtain satisfactory agreement with experimental EFG data. Realizing this, we nevertheless chose to concentrate on the valence-effect EFG in the work reported here. The reason we made this choice is that our original intent was to investigate anisotropic screening effects in the hope of explaining the anomalously small values of the EFG observed at the second neighbor site in most aluminum alloys.[10] This we sought to do through a nonlinear, second-order calculation of the screening charge density, as explained in Section II.

The result of our calculation, which is also presented in Section II, shows a pronounced anisotropy in the screening charge distribution. In Section III, however, we show that if we avoid an asymptotic approximation in the evaluation of the valence-effect EFG integral, then second-order screening terms, which include the anisotropic part, are insignificant compared to the

rder, linear screening term in cases where the impurity and host
s differ. As a corollary to this result we find, contrary to the
sko formula, that the EFG is not proportional to the screening charge
in such hetrovalent alloys.

is leads to the main point of the article, which we present in Section
re we reexamine the approximations involved in the Kohn-Vosko treatment
ive a correction term, proportional to the valence difference, to their
tic formula. Through numerical computations, we then show that the
ted asymptotic formula gives good agreement with results obtained by
numerical integration. We conclude, therefore, that when host and
ty valences differ, the correction term derived here is essential to the
te prediction of the valence-effect EFG in simple metal alloys.

II. ANISOTROPIC SCREENING CALCULATIONS

n the preceding article[11] we reported numerical studies of the
onsistent, second-order screening charge density for various point
s in aluminum. The calculations, which were performed in the jellium
imation, indicate that a second-order treatment should suffice for
cattering substitutional defects for which the difference between the
nd solute valences is not too large. In this section we extend the
ations to include second-order scattering events involving the host
l.

s before, we define the defect potential as the difference in model
ials between the impurity and host ions. When the model potential for
st crystal is added to the jellium model, the screening charge density
s anisotropic and the self-consistent defect potential is therefore also
ropic. However, based on recent self-consistent supercell calculations
vacancy in aluminum,[12] the anisotropy in the defect potential is expected

to be weak. We therefore average the potential over direction and thus obtain the following integral equation for the self-consistent defect form factor $\omega(q)$:

$$\omega(q) = \omega_0(q) + \frac{48\pi}{q^2}\left[\frac{1-G(q)}{\varepsilon(q)}\right]\sum_{\vec{K}\neq 0} \omega_K^h \frac{1}{4\pi}\int g(q,K,p)\,\omega(p)\,d\Omega_p \qquad (1)$$

with

$$\omega_0(q) = \omega_\ell(q) + \frac{24\pi}{q^2}\left[\frac{1-G(q)}{\varepsilon(q)}\right]\frac{1}{N}\sum_{\vec{p}} g(q,p,r)\,\omega(p)\,\omega(r) \qquad (2)$$

In these expressions $\varepsilon(q)$ is the Hartree dielectric function, $G(q)$ is the exchange-correlation correction, ω_K^h is the host crystal form factor at reciprocal lattice vector $\vec{K}$, $g(q,K,p)$ is the function defined by Lloyd and Sholl,[13] and $\omega_\ell(q)$ is the defect form factor in the linear screening approximation. The integral in Eq. (1) is over the direction of the vector $\vec{p} = -(\vec{q}+\vec{K})$, and $r = |\vec{q}+\vec{p}|$ in Eq. (2).

The Fourier transform of the smooth part of the screening charge density is

$$\delta\rho_s(\vec{q}) = \delta\rho_s^o(q) + \frac{6}{\varepsilon(q)}\sum_{\vec{K}\neq 0} g(q,K,p)\,\omega_K^h\omega(p) \qquad (3)$$

where

$$\delta\rho_s^o(q) = \frac{q^2}{8\pi}\left[\frac{1-\varepsilon(q)}{1-G(q)}\right]\left[\omega_\ell(q) + \frac{\omega_o(q)-\omega_\ell(q)}{1-\varepsilon(q)}\right] \qquad (4)$$

The isotropic part of the screening charge density, $\delta\rho_s^o(q)$, has the same form as in the jellium model. However, it does not equal the density obtained in the jellium approximation because the potential $\omega_b(q)$ that appears in Eq. (4) is coupled to the spherical average host crystal potential through Eqs. (1) and (2).

For numerical computation of the screening charge density, we derived local form factors from the exponentially-damped, nonlocal potentials of Heine and Abarenkov[14] by the averaging method of Bertoni, et al,[15] and used data from Toigo and Woodruff[16] for the exchange-correlation function G(q). The self-consistency condition, Eq. (1), was solved by an iterative method described elsewhere,[11] and the resulting self-consistent defect potential was then used to compute the transform of the screening charge density according to Eqs. (3) and (4). The inverse transform is shown in Figure 1 for two crystallographic directions, along with the isotropic term $\delta\rho_s^o$.

These results indicate that the addition of the host crystal potential to the jellium model produces a significant, anisotropic distortion of the screening charge at large distances from the defect, and, as shown in the inset in Figure 1, an isotropic shift in the smooth part of the charge density at the impurity site. This rather large change at the impurity site is consistent with the calculations of Manninen and Nieminen,[17] who found that the addition of a spherical average crystal potential to their density functional model of a vacancy also produced a large shift in density at the vacancy site. Our principal interest at present, however, is in the anisotropic screening charge density at neighboring ion sites. If indeed the EFG at these sites is proportional to the smooth part of the screening charge distribution, then the results displayed in Figure 1 say that the addition of

the host crystal potential should produce anisotropic shifts in the EFG distribution over neighboring ion shells. This is the point we address in the next section.

III. SECOND-ORDER CONTRIBUTIONS TO THE EFG

If we let $\delta\rho(\vec{r})$ be the <u>total</u> change in valence electron density, which includes changes in the oscillatory part inside host ion cores, then the valence-effect EFG at host ion position $\vec{R}$ is given by[4,5,9]

$$q_V(\vec{R}) = -\frac{2e\Delta Z}{R^3} + \frac{4}{3}\pi e\delta\rho(\vec{R}) + 2e\int P_2(\hat{r}\cdot\hat{R})\delta\rho(\vec{R}+\vec{r})\frac{d^3r}{r^3}$$

$$= -\frac{2e\Delta Z}{R^3} + \frac{4}{3}\pi e\delta\rho(\vec{R}) - \frac{8\pi e}{3N}\sum_{\vec{q}}\delta\rho(\vec{q})P_2(\hat{q}\cdot\hat{R})e^{i\vec{q}\cdot\vec{R}} \qquad (5)$$

where $\hat{r}$, $\hat{R}$ and $\hat{q}$ are unit vectors, P_2 $(\cos\Theta)$ is a Legendre polynomial, and ΔZ is the impurity valence minus the host valence. This is the principal component of the traceless valence effect EFG tensor as defined by Sagalyn and Alexander;[4] in their notation the quantity we calculate is $-eq_{||}^{V}$. Our analysis differs from that of Ponnambalam and Jena[9] because our charge density is not spherically symmetric with respect to the impurity ion, which requires that we use the general form given by Eq. (5), rather than the spherically symmetric form derived by Ponnambalam and Jena.

Next, following Kohn and Vosko,[5] we assume that $\delta\rho(\vec{q})$ can be replaced by $\alpha\delta\rho_s(\vec{q})$ where α is the core enhancement factor that provides an approximate correction for the effects of charge density oscillations in the core and $\delta\rho_s$ is the smooth part of the valence electron density. From the original

development,[5] it can be seen that the core enhancement approximation rests on the assumption that R is large, i.e. it is an asymptotic approximation. We might, therefore, also assume that the only important $\vec{q}$ directions in the integral in Eq. (5) are those that are nearly parallel to $\vec{R}$, in which case $P_2(q.R) \sim 1$. In this case the integral becomes proportional to $\delta\rho_s(\vec{R})$ and we recover the Kohn-Vosko formula. (This will be demonstrated in a slightly different way in the next section.) However, in the calculations reported below we chose to avoid this particular approximation because it was a rather simple matter to insert the factor $P_2(\hat{q}\cdot\hat{R})$ in the numerical integration routine already developed for our charge density calculations, and thus provide a test of at least one aspect of the large R approximation.

Typical results are shown in Table I. The entries are EFG contributions in units of 10^{13} cgs-esu for a core enhancement factor $\alpha = 10.0$. The major column headings, Term 1, etc., correspond to the first, second and third terms in Eq. (5). The subheadings 1, 2 and 3 correspond, respectively, to the linear screening, second-order isotropic, and second-order anisotropic components of the charge density $\delta\rho_s(\vec{q})$.

The most important point to be noted here is that the integral term (Term 3) is <u>not</u> proportional to $\delta\rho_s(\vec{R})$. In fact, the linear screening contribution to this term (Column 1), which dominates at all R, is non-oscillatory, while $\delta\rho_s(\vec{R})$ itself exhibits the familiar Friedel oscillations at large R. The immediate conclusions are that (1) the approximation $P_2(\hat{q}.\hat{R})\sim 1$ leads to serious error, and (2) nonlinear screening to the EFG are not as important as one might expect from calculations of the charge density alone.

We are led, therefore, to a reexamination of the asymptotic approximation as it affects the integral term in Eq. (5), and also as it affects the core enhancement approximation, which is also based on the assumption that R is large. In the development that follows we will drop nonlinear terms because, as can be seen from Table I, the linear screening part of the integral term is the dominant component of the EFG at all R.

IV. A NEW ASYMPTOTIC APPROXIMATION

We return to Eq. (5) and focus, for the moment, on the total change in charge density, $\delta\rho(\vec{r})$. To avoid the core enhancement approximation we must determine the impurity-induced change in the total valence electron wave function, including the oscillatory part in the cores of host ions. To do this we use linear screening theory and the core state projection operator[18] in a straightforward, first-order perturbation calculation. The resulting expression for the charge density is

$$\delta\rho(\vec{R}+\vec{r}) = \frac{1}{N}\sum_{\vec{q}} \frac{q^2}{8\pi}\left[\frac{1-\varepsilon(q)}{1-G(q)}\right]\omega(q)e^{i\vec{q}\cdot\vec{R}}\left[e^{i\vec{q}\cdot\vec{r}}+f(\vec{q},\vec{r})\right] \tag{6}$$

where $f(\vec{q},\vec{r})$, which determines the shift in orthogonalization charge density, is given by

$$\frac{q^2}{8\pi}\left[\frac{1-\varepsilon(q)}{1-G(q)}\right]f(\vec{q},\vec{r}) = \sum_{\vec{k}} \frac{f_o(k)}{k^2-|\vec{k}+\vec{q}|^2}\left[\langle\vec{k}|1-p|\vec{r}\rangle\langle\vec{r}|1-p|\vec{k}+\vec{q}\rangle\right.$$

$$\left. - \langle\vec{k}|\vec{r}\rangle\langle\vec{r}|\vec{k}+\vec{q}\rangle\right] \tag{7}$$

where $f_o(k)$ is the electron occupation number for electron state $|\vec{k}\rangle$, and p is the core state projection operator for a host ion at the origin. In the Appendix we show that substitution of Eq. (6) in the integral term in Eq. (5) leads to

$$q_{int}(R) = \frac{4e\Omega_o}{3\pi}\int_0^\infty \frac{q^2}{8\pi}\left[\frac{1-\varepsilon(q)}{1-G(q)}\right]\omega(q)\left[1+F(q)\right]j_2(qR)q^2dq \tag{8}$$

where Ω_o is the volume per ion, $j_2(qR)$ is a spherical Bessel function, and F(q) is the function defined in the Appendix and plotted Figure 2.

The approximation $P_2(\hat{q}\cdot\hat{R})\sim 1$ in Eq. (5) is equivalent to using the asymptotic approximation

$$j_2(qR)\sim - j_o(qR) \tag{9}$$

in Eq. (8). If we do this, and, in addition, replace F(q) by its value at the singular point $q = 2k_f$, then Eq. (8) reduces to the Kohn-Vosko form

$$q_{int}(R) \sim - \frac{8\pi e}{3}\alpha\delta\rho_s(R) \tag{10}$$

with $\alpha = 1+F(2k_f)$. As we show in the Appendix, the second term in Eq. (5) can also be written in this form. Thus, by combining the second and third terms in Eq. (5), we find that the electronic part of the EFG is given by Eq. (10) with $\alpha = 1+F(2k_f)-\beta$, where β is the quantity defined in the Appendix. The numerical value of α based on Herman-Skillman[19] core functions for aluminum and the on-the-Fermi-sphere (OFS) approximation[20] to nonlocal terms is 6.8, which compares favorably with other calculations of the core enhancement factor for aluminum.[21]

The difficulty with this development is that Eq. (9) becomes a poor approximation as $q \to 0$, and leads to a serious inaccuracy in the estimation of $q_{int}(R)$. This is illustrated in Figure 3, which is a plot of the function

$$\psi(q) = \frac{q^4}{8\pi}\left[\frac{1-\varepsilon(q)}{1-G(q)}\right]\omega(q)j_2(qR)$$

$$= q^2\delta\rho_s(q)j_2(qR) \qquad (11)$$

and the approximation to $\psi(q)$ obtained from Eq. (9). In this illustration, R is the nearest neighbor distance in aluminum, and $\omega(q)$ is the average defect form factor for a magnesium impurity in aluminum. We note that, because $\delta\rho_s(q)$ is the screening charge density for a hetrovalent impurity, charge conservation requires that $\delta\rho_s(q)$ be nonvanishing as $q \to 0$.[20] For a homovalent impurity, however, $\delta\rho_s(q) \to 0$ as $q \to 0$, and the error introduced by the asymptotic approximation is not as large as that shown in Figure 3. This, we shall see, is reflected in the correction term derived below.

To obtain a better approximation to $q_{int}(R)$ we add the term

$$\Delta q(R) = \frac{4e\Omega_o}{\pi R}\int_o^\infty \frac{q^2}{8\pi}\left[\frac{1-\varepsilon(q)}{1-G(q)}\right]\omega(q)\left[1+F(q)\right]j_1(qR)qdq \qquad (12)$$

where we have used the identity $j_o(Z) + j_2(Z) = 3j_1(Z)/Z$. A very simple form results if we assume that the integrand in this expression is negligible for large q, take the long wavelength limits of $q^2\varepsilon(q)$ and F(q), and cut the integration off at q_0, the first zero of $\omega(q)$. With M(q) defined by

$$\omega(q) = -\frac{8\pi\Delta Z}{\Omega_o q^2}M(q) \qquad (13)$$

we obtain

$$\Delta q(R) \sim \frac{4e\Delta Z[1+F(o)]}{\pi R}\int_o^{q_o} qM(q)j_1(qR)dq \qquad (14)$$

We now assume that $\Delta q(r)$ is insensitive to the form of $M(q)$ as long as $M(0) = 1$ and $M(q_0) = 0$. To obtain an integrable form we therefore take

$$M(q) \sim j_o(\pi q/q_o) \tag{15}$$

which gives, to lowest order in 1/R,

$$\Delta q(R) \sim 2e\Delta Z\left[1+F(o)\right]/R^3 \tag{16}$$

A new asymptotic formula for the EFG is obtained by combining $\Delta q(R)$ with our estimates of the other terms in Eq. (5). The result is

$$q(R) \sim \frac{2e\Delta ZF(o)}{R^3} - \frac{8\pi e}{3}\left[1+F(2k_F)-\beta\right]\delta\rho_s(R) \tag{17}$$

Figure 4 shows the two components of q as well as the total EFG according to Eq. (17), along with data obtained by direct numerical integration of Eq. (5), again for magnesium in aluminum. Similar results were obtained for substitutional zinc, silicon and germanium in aluminum. For gallium, with $\Delta Z=0$, the familiar oscillatory form was obtained in both calculations with agreement between the two being somewhat poorer than that shown here. Thus, it appears that the asymptotic approximation leading to the first term in Eq. (17) is adequate, and that the result is reasonably accurate when $\Delta Z \neq 0$ and the first term dominates.

V. CONCLUSION

Equation (17) is the principal result of the present work. It is a corrected asymptotic formula for the valence effect EFG caused by an impurity ion with valence difference ΔZ. The correction to the Kohn-Vosko formula, the first term on the right side of Eq. (17), is the sum of the EFG due to the bare impurity ion and the EFG associated with the long wavelength behavior of the screening charge density. For large impurity-host ion distance, which is assumed here, the ionic term cancels exactly with the plane wave part of the screening term. This leaves, as the only contribution from the long wavelength term, the EFG caused by the shift in orthogonalization charge associated with a completely screened impurity ion. The result is proportional to ΔZ and is the dominant contribution to the EFG unless the valence difference vanishes.

The development leading to Eq. (17) shows why nonlinear screening does not contribute significantly to the valence effect EFG even though nonlinear effects are important in calculations of the charge density itself. This is because when $\Delta Z \neq 0$ the dominant contribution to the EFG comes from the long wavelength limit of the charge density or, equivalently, from an integral of the charge density over all space, and, as is well known, this limit is given exactly by linear screening theory.[20] In other words, nonlinear corrections vanish as $q \to 0$ and therefore do not affect the first term in Eq. (17).

Although our numerical results pertain only to alloys of aluminum, we believe the principal conclusion to be valid for all simple metal alloys. The heart of the matter is the failure of the usual asymptotic approximation in the long wavelength limit, as illustrated in Figure 3. Regardless of how one corrects for this deficiency, the result must reflect the behavior of the charge density at small values of the wavenumber and must, therefore, be at

least approximately proportional to the valence difference.

ACKNOWLEDGEMENT

This work was supported by the U.S. Army Research Office.

APPENDIX

To calculate $f(\vec{q},\vec{r})$ we expand the plane wave and core functions in Eq. (7) in spherical harmonics in a coordinate system with the polar axis in the $\vec{q}$ direction. Then, with the help of the addition theorem for spherical harmonics and the recursion relation for Legendre polynomials to simplify terms involving 2p core states, we find that f(q,r) is a function of the magnitudes of $\vec{q}$ and $\vec{r}$ and μ, the cosine of the angle between $\vec{q}$ and $\vec{r}$. This allows us to write $f(\vec{q},\vec{r})$ as a sum of Legendre polynomials in μ. Then, after substitution in Eqs. (6) and (5) and integration over $\vec{r}$ we obtain the following result for the integral term in Eq. (5):

$$q_{int}(R) = -\frac{8\pi e}{3N}\int_{\vec{q}} \frac{q^2}{8\pi}\left[\frac{1-\varepsilon(q)}{1-G(q)}\right]\omega(q)P_2(\hat{q}\cdot\hat{R})e^{i\vec{q}\cdot\vec{R}}\left[1+F(q)\right]$$

where $\hat{q}$ and $\hat{R}$ are unit vectors and F(q) is given by

$$F(q) = -\frac{3}{2}\int_0^\infty \frac{1}{r}\int_{-1}^{1} f(q,r,\mu)P_2(\mu)d\mu dr$$

If we use the on-the-Fermi-spheri (OFS) approximation[20] to the matrix elements in Eq. (7) then the $\vec{k}$ integral is easily evaluated and the resulting expression for F(q) is

$$F(q) = \sum_{NL}\sum(2L+1)\left[f_{NL}(k_F,q) + f_{NL}(k_q,q)\right] + \gamma$$

where

$$f_{NL}(k,q) = 3(-1)^L F_{NL}(k) \sum_{\ell\ell'} i^{\ell'-\ell}(2\ell+1)(2\ell'+1)\begin{pmatrix} 2 & \ell & \ell' \\ 0 & 0 & 0 \end{pmatrix}^2 P_\ell(\xi_q)$$

$$x\int_0^\infty \frac{P_{NL}(r)}{r^2} j_{\ell'}(qr)\frac{d^L}{d(kr)^L} j_\ell(kr)dr$$

$$\gamma = \frac{9}{5}F_{21}(k_F)F_{21}(k_q)(1+\xi_q^2)\int_0^\infty \frac{P_{21}(r)}{r^3}dr$$

$$F_{NL}(k) = \int_0^\infty P_{NL}(r) j_\ell(kr) r dr$$

For $q < 2k_f$, $k_q = |\vec{k}+\vec{q}| = k_f$ and $\xi_q = q/2k_f$, while for $q > 2k_f$, $k_q = q - k_f$ and $\xi_q = 1$ (OFS approximation). The numbers N and L are core state quantum numbers and $P_{NL}(r)$ is the corresponding radial wave function. To calculate the function shown in Figure 2, we used the core functions tabulated by Herman and Skillman.[19]

The quantity β that appears in Eq. (17) is determined by the function $f(q,r)$ evaluated $r = 0$. From Eq. (7) it is easily shown that, in the OFS approximation

$$f(q,o) = -\sum_{N=1}^{2}\left[F_{N0}(k_F) + (F_{N0}(k_q) - F_{N0}(k_F)\sum_{N'=1}^{2} F_{N'0}(k_q)R_{N'0}\right]R_{N0}$$

where

$$R_{NL} = \lim_{r\to 0} P_{NL}(r)/r$$

If we approximate $f(q,0)$ by its value at $q = 2k_f$ then we find, from Eq. (6),

$$\delta\rho(R) \sim 2\beta\delta\rho_s(R)$$

where

$$\beta = \frac{1}{2}\left[1 + f(2k_F,0)\right]$$

REFERENCES

1. N. Bloembergen and T. J. Rowland, Acta Metall. 1, 731 (1953).
2. G. Grüner and M. Minier, Adv. Phys. 26, 231.
3. P. L. Sagalyn, A. Paskin, and R. J. Harrison, Phys. Rev. 124, 428 (1961).
4. P. L. Sagalyn and M. N. Alexander, Phys. Rev. B 15, 5581 (1977).
5. W. Kohn and S. H. Vosko, Phys. Rev. 119, 912 (1960).
6. A. Blandin and J. Friedel, J. Phys. Radium (Paris) 21, 689 (1960).
7. K. K. Prasad Rao and N. C. Mohapatra, Phys. Rev. B 22, 3767 (1980).
8. K. K. Prasad Rao, N. C. Mohapatra, and S. Hafizuddin, Phys. Rev. B 24, 1941 (1981).
9. M. J. Ponnambalam and P. Jena, Phys. Rev. Lett. 46, 610 (1981).
10. M. Minier and S. Ho Dung, J. Phys. F 7, 503 (1977).
11. R. E. Beissner, *preceding article.*
12. B. Chakraborty, R. W. Siegel, and W. E. Pickett, Phys. Rev. B 24, 5445 (1981).
13. P. Lloyd and A. C. Sholl, J. Phys. C 1, 1620 (1968).
14. V. Heine and I. V. Abarenkov, Phil. Mag. 9, 451 (1964).
15. C. M. Bertoni, V. Bortolani, C. Calandra, and F. Nizzoli, J. Phys. F 4, 19 (1974).
16. F. Toigo and T. O. Woodruff, Phys. Rev. B 2, 3958 (1970).
17. M. Manninen and R. M. Nieminen, J. Phys. F 8, 2243 (1978).
18. W. A. Harrison, "Pseudopotentials in the Theory of Metals", W. A. Benjamin, Inc., New York (1966).
19. F. Herman and S. Skillman, "Atomic Structure Calculations", Prentice-Hall, Englewood Cliffs (1963).
20. V. Heine and D. Weaire, Solid State Phys. 24, 249 (1970).
21. P. M. Holtham and P. Jena, J. Phys. F 5, 1649 (1975).

TABLE I. Electric field gradient (in units of 10^{15} cgs-esu) in the 100 direction for a magnesium ion in dilute [illegible]. Terms 1, 2 and 3 refer to the first, second and third terms in Eq. (5), while subheadings 1, 2, and 3 correspond, respectively, to linear screening, second-order isotropic and second-order anisotropic components of the charge density. The letter a denotes the lattice constant.

R/a	Term 1	Term 2			Term 3			q TOTAL
		1	2	3	1	2	3	
.2	181.9	-185.9	14.06	12.37	- 34.28	-2.51	66.14	51.8
.3	53.88	-112.7	3.75	.05	-102.1	12.43	36.16	-108.5
.4	22.73	- 34.51	-2.42	4.75	-147.6	12.60	1.63	-142.8
.5	11.64	3.16	-1.24	- .52	-127.3	4.55	- .38	-110.1
.6	6.74	4.45	- .50	-1.66	- 74.21	1.57	.12	- 63.5
.7	4.24	- 1.12	- .35	- .70	- 38.00	.76	.36	- 34.8
.8	2.84	- 1.57	- .03	.32	- 24.94	- .03	- .65	- 24.1
.9	2.00	- .35	.17	.65	- 19.55	- .35	-1.27	- 18.7
1.0	1.46	.29	.05	- .04	- 15.34	- .04	- .30	- 13.9
1.1	1.09	.42	- .10	- .64	- 11.72	.23	.56	- 10.2
1.2	.84	- .03	- .06	- .39	- 8.22	.10	.18	- 7.6
1.3	.66	- .03	.05	.09	- 5.96	- .12	- .46	- 5.8

AD-A117 451 SOUTHWEST RESEARCH INST SAN ANTONIO TX F/G 11/6
RESEARCH ON MULTI-ION INTERACTIONS AND DEFECTS IN METALS.(U)
JUL 82 R E BEISSNER DAAG29-79-C-0099
UNCLASSIFIED ARO-16387.4-PH ARO-10993.3-PH NL

2 OF 2

END
DATE FILMED
08-82
DTIC

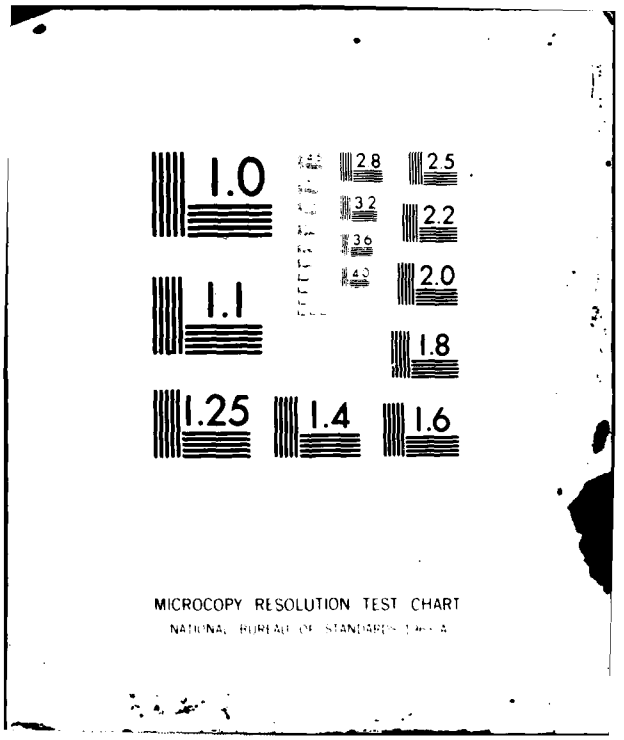
1.0
1.1
1.25
2.8
3.2
3.6
4.0
2.5
2.2
2.0
1.8
1.4
1.6
MICROCOPY RESOLUTION TEST CHART
NATIONAL BUREAU OF STANDARDS 1963-A

FIGURE CAPTIONS

Figure 1. Anisotropic screening charge density in the 110 and 112 directions for a magnesium ion in aluminum. The isotropic term $\delta\rho_s^o$ is defined by Eq. (4).

Figure 2. The function F(q) that governs the orthogonalization charge contribution to the electric field gradient as in Eq. (8).

Figure 3. The solid curve is the function $\psi(q)$ defined by Eq. (11); the dashed curve is the approximation obtained by using Eq. (9). The extra node in the approximate curve leads to a large error in the electric field gradient integral unless solute and solvent valences are equal.

Figure 4. Contributions to the electric field gradient for a magnesium impurity in aluminum. The lower dotted curve is the first term in Eq. (17), the upper dotted curve is the second term and the dashed curve is their sum. The solid curve is the result obtained by numerical integration of Eq. (8).

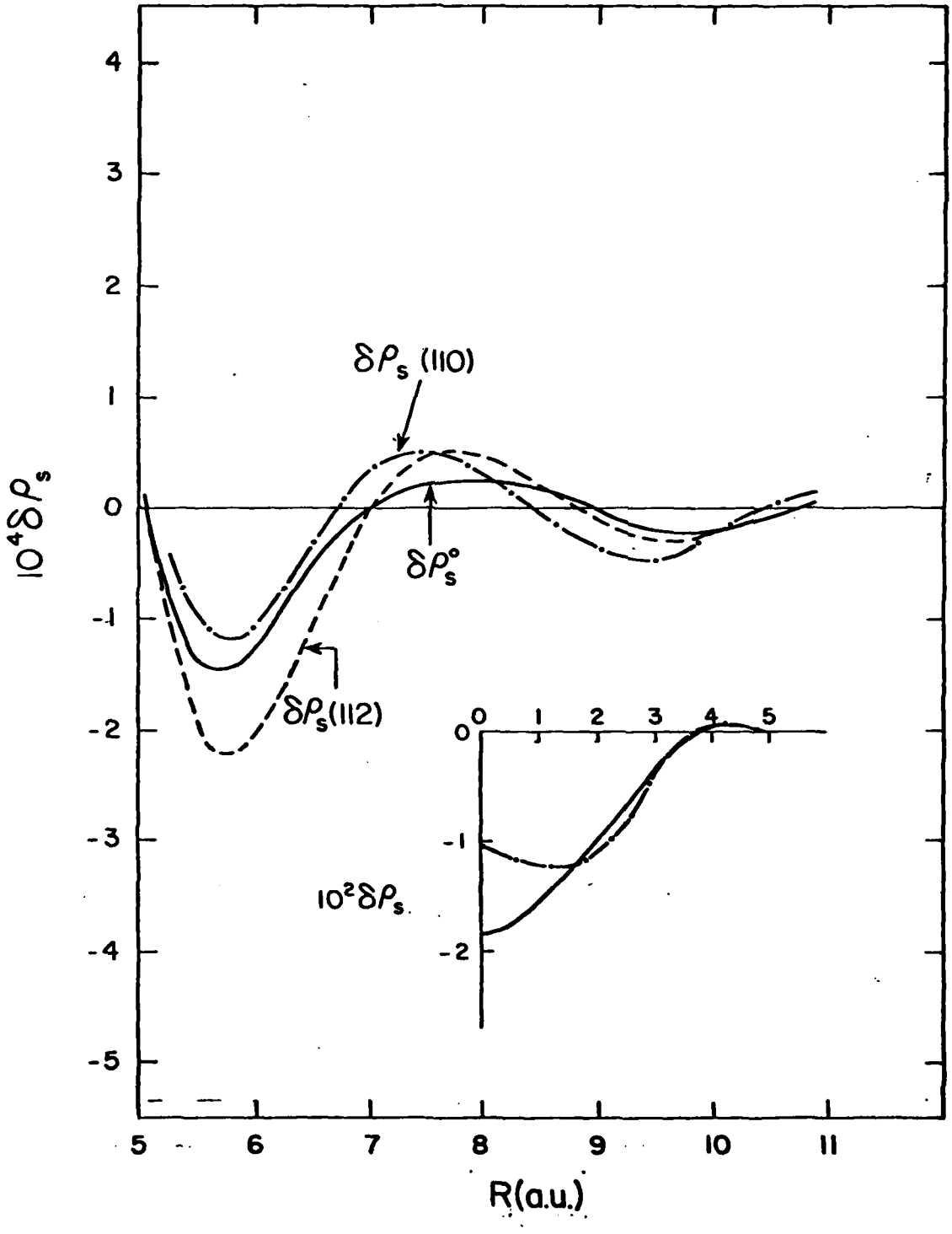
4
3
2
1
0
-1
-2
-3
-4
-5
$10^4\delta\rho_s$
$\delta\rho_s$ (110)
$\delta\rho_s^\circ$
$\delta\rho_s$(112)
0
1
2
3
4
5
0
-1
-2
$10^2\delta\rho_s$
5
6
7
8
9
10
11
R(a.u.)

FIGURE 1

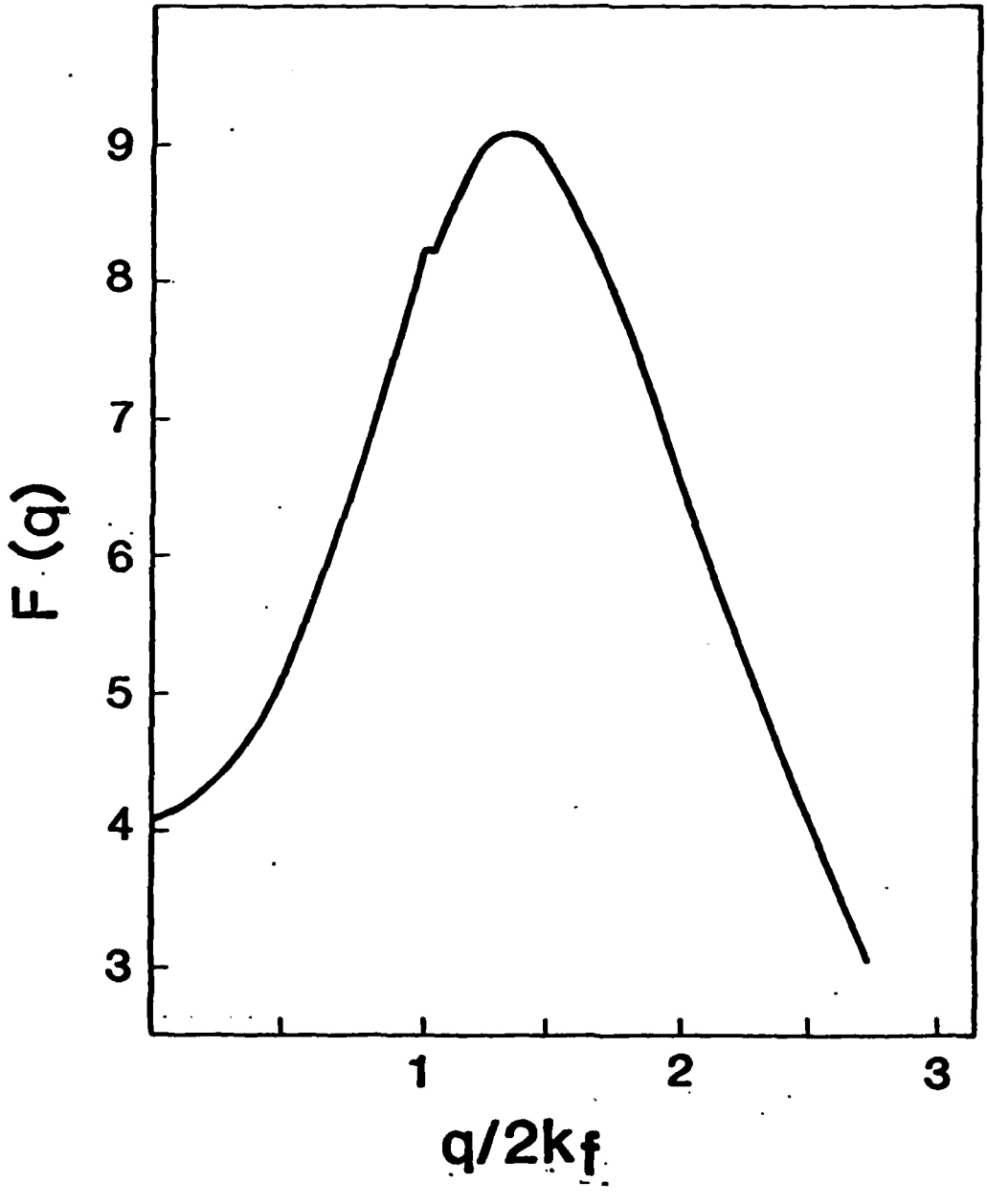

FIGURE 2

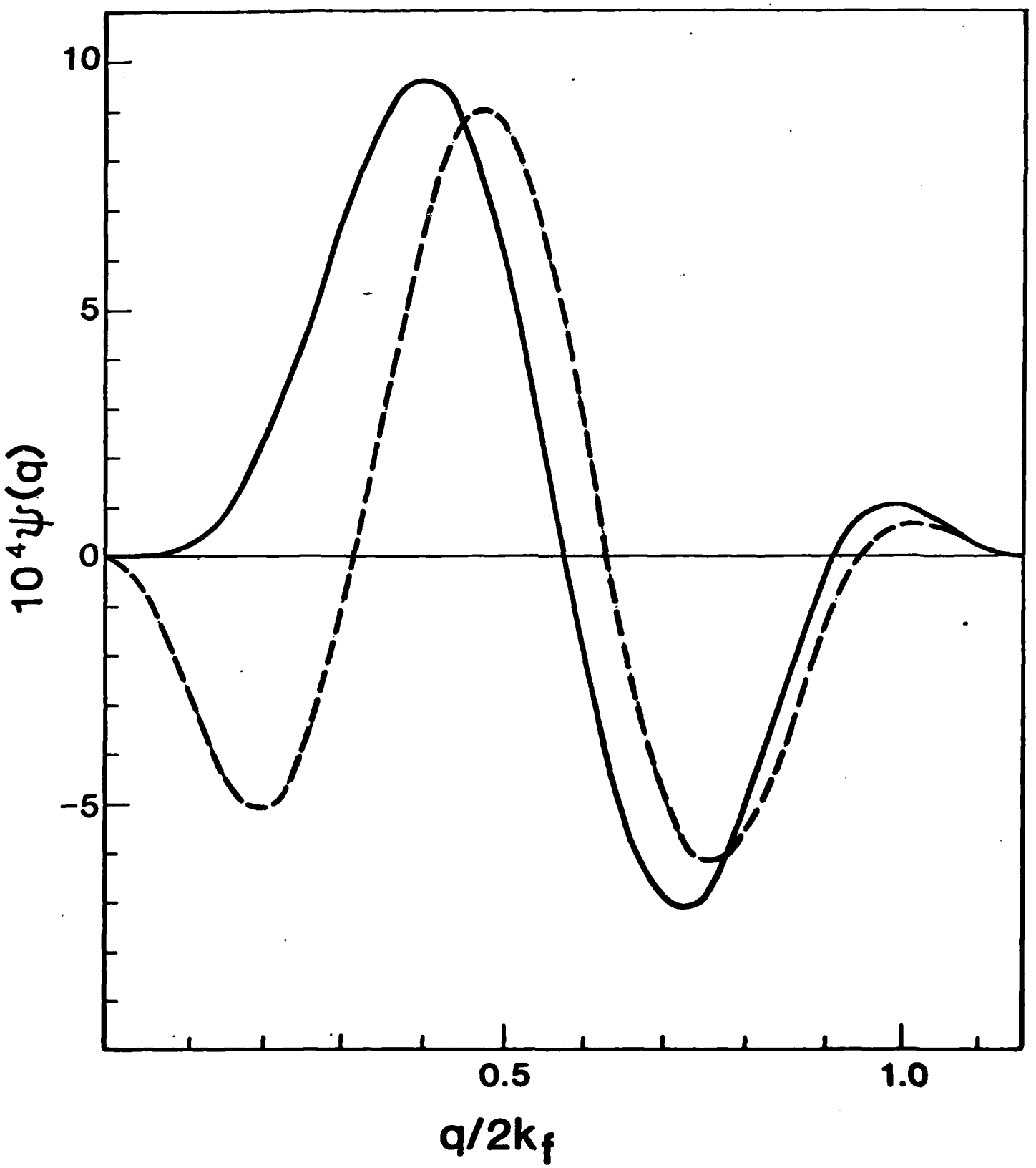

FIGURE 3

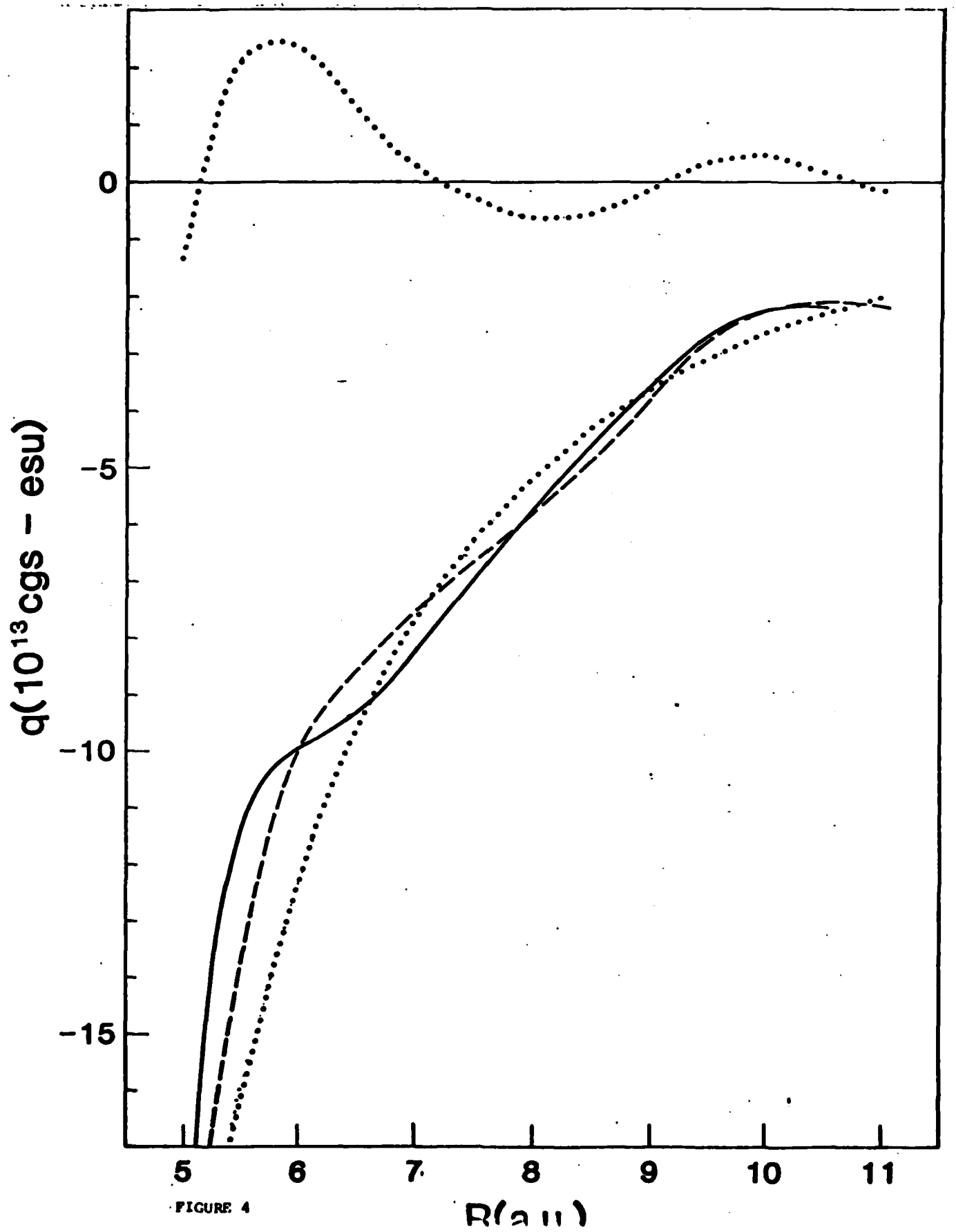

FIGURE 4

APPENDIX H

Third-Order Calculation of Lattice Distortion for a Vacancy in Aluminum

(Draft of a paper to be submitted to Physical Review B)

In this report we examine the influence of third-order forces on the lattice distortion field for a vacancy in aluminum. We chose to do this particular calculation because our earlier study of second-order corrections to the screening charge density, which give rise to third order forces, produced results in reasonable agreement with more accurate density functional calculations. There was, therefore, some reason to expect that a third-order force approximation would suffice, at least as an indicator of the relative magnitudes of second- and third-order terms.

For our calculation we used the method of lattice statics with the second- and third-order force expression given by Solt and Werner for a hetrovalent alloy with potential difference Δv. For the vacancy we took Δv to be the negative of the aluminum ion potential in the linear screening approximation. The potential used for this purpose, and for calculating the dynamical matrix, was that developed by Sen, et al., with screening given by Taylor's dielectric function. This potential is a two-parameter model potential of the Heine-Abarenkov form, with parameters adjusted so as to obtain the best overall agreement with a number of experimentally determined properties of aluminum, including the phonon spectrum. Because the potential of Sen, et al, gives good agreement with the phonon spectrum in a second-order calculation, we did not include third-order terms in our calculation of the dynamical matrix and its inverse, the lattice Green's function.

With the lattice statics method, the calculation of lattice displacement vectors involves an integration over the first Brillouin zone. For this purpose we used the special-direction method with a 64 point gaussian integration along each of 21 directions in 1/48th of the zone. In second-order, the displacements obtained from this integration differed by less than 2% from those obtained with 32 point integrals in 10 directions.

Second- and third-order displacements, in units of one-half the lattice constant, are given in Table I. Our second-order displacements are much smaller than those reported by Singhal, particularly in the first four neighbor shells. This we attributed to the use of different pseudopotentials. The addition of third-order forces makes most of the displacements smaller still, and even produces sign changes for the second and fifth neighbors. This indicates that third-order ion-vacancy forces are generally repulsive, tending to decrease the inward relaxation of ions around the vacancy, in agreement with Hasegawa's finding that third-order interionic forces are generally attractive.

The disturbing point illustrated by these data is the magnitude of third-order effects, particularly at the first and second neighbor sites. If we are to believe that third-order terms are actually as large as indicated here, then we must be concerned about the magnitudes of fourth- and higher order terms that were not included in our calculation. In other words, we must then question the usefulness of a third-order theory of interionic forces involving defects. On the other hand, our calculation is a local approximation, and this could have led to significant error in the calculation of forces. We tend to believe that the second-order part of the calculation, including the determination of the dynamical matrix, is reasonably accurate because it is based on an empirical potential fitted to experimental data through second-order theory. However, the success of this local potential in second-order calculations does not justify its use in third-order terms where nonlocal effects may be quite different.

Had third-order effects been smaller, we might be justified in ignoring higher-order terms and the uncertainties introduced through a local approximation for the third-order term. It is clear, however, that this

cannot be done. We must conclude, therefore, that the local, third-order theory of interionic forces involving defects is subject to serious question.

This work was supported by the U.S. Army Research Office.

TABLE I. Second- and Third-Order Lattice Displacement Vectors in Units of One-Half the Lattice Constant a at Lattice Sites $a\vec{\ell}/2$

	Second Order			Third Order		
$\vec{\ell}$	$2u_1/a$	$2u_2/a$	$2u_3/a$	$2u_1/a$	$2u_2/a$	$2u_3/a$
110	-0.0102	-0.0102	0.0	-0.0051	-0.0051	0.0
200	-0.0042	0.0	0.0	0.0029	0.0	0.0
211	-0.0021	-0.0013	-0.0013	-0.0021	-0.0016	-0.0016
220	-0.0048	-0.0048	0.0	-0.0035	-0.0035	0.0
310	-0.0006	-0.0009	0.0	0.0006	-0.0001	0.0
222	-0.0008	-0.0008	-0.0008	-0.0005	-0.0005	-0.0005
321	-0.0018	-0.0013	-0.0009	-0.0011	-0.0003	-0.0005
400	0.0001	0.0	0.0	.0001	0.0	0.0
411	-0.0003	-0.0002	-0.0002	-0.0003	-0.0003	-0.0003
330	-0.0017	-0.0017	0.0	-0.0010	-0.0010	0.0

REFERENCES

1. W. A. Harrison, "Pseudopotentials in the Theory of Metals," W. A. Benjamin, Inc., New York (1966).

2. V. Heine and D. Weaire, Solid State Phys. 24, 249 (1970).

3. W. A. Harrison, Phys. Rev. B 7, 2408 (1973).

4. R. E. Beissner, Phys. Rev. B 9, 5108 (1974).

5. C. M. Bertoni, V. Bortolani, C. Calandra, and F. Nizzoli, J. Phys. F 4, 19 (1974).

6. P. Lloyd and A. C. Sholl, J. Phys. C 1, 1620 (1968).

7. E. G. Brovman and Yu. Kagan, Sov. Phys. JETP 30, 721 (1970).

8. A. R. Williams, J. Phys. F 3, 781 (1973).

9. M. Hasegawa, J. Phys. F 6, 649 (1976).

10. C. B. So and C. H. Woo, J. Phys. F 11, 325 (1981).

11. G. Jacucci, R. Taylor, A. Tenenbaum and N. van Doan, J. Phys, F 11, 793 (1981).

12. M. Rasolt and R. Taylor, Phys. Rev. B 11, 2717 (1975).

13. R. E. Beissner, Phys. Rev. B 8, 5432 (1973).

14. G. Solt and K. Werner, Phys. Rev. B 24, 817 (1981).

15. R. E. Beissner, Phys. Rev. B 13, 5131 (1976).

16. E. G. Brovman and Yu. Kagan, Sov. Phys. JETP 25, 365 (1967).

17. W. Kohn and S. H. Vosko, Phys. Rev. 119, 912 (1960).

18. A. Blandin and J. Friedel, J. Phys. Radium 21, 689 (1960).

19. M. Minier and S. Ho Dung, J. Phys. F 1, 503 (1977).

20. N. W. Ashcroft, Phys. Letters 23, 48 (1966).

21. M. Appapillai and A. R. Williams, J. Phys. F 3, 759 (1973).

22. Z. D. Popovic, M. J. Stott, J. P. Carbotte, and G. R. Piercy, Phys. Rev. B 13, 590 (1976).

23. L. Dagens, M. Rasolt and R. Taylor, Phys. Rev. B 11, 2726 (1975).

24. M. Manninen, P. Jena, R. M. Nieminen, and J. K. Lee, Phys. Rev. B 24, 7057 (1981).

25. P. L. Sagalyn and M. N. Alexander, Phys. Rev. B 15, 5581 (1977). In the notation of these authors the quantity we calculate is $-eq_{\parallel}^{V}$, the principal component of the traceless valence effect EFG tensor.

26. R. E. Beissner, Phys. Lett. 71A, 109 (1979).

27. P. M. Holtham and P. Jena, J. Phys. F 5, 1649 (1975).

28. G. Solt, Phys. Rev. B 18, 720 (1978).

29. R. Benedek and P. S. Ho, J. Phys. F 3, 1285 (1973).

30. V. K. Tewary, Adv. Phys. 22, 758 (1973).

31. D. Sen, S. K. Sarkar, D. Roy, and S. Sengupta, Phys. Rev. B 24, 876 (1981).

32. S. P. Singhal, Phys. Rev. B 8, 3641 (1973).


MED
8